University of Louisville
ThinkIR: The University of Louisville's Institutional Repository

Electronic Theses and Dissertations

5-2022

Utilizing shockwave theory and deep learning to estimate intersection traffic flow and queue length based on connected vehicle data.

Abdulmaged Algomaiah
University of Louisville

Follow this and additional works at: https://ir.library.louisville.edu/etd

 Part of the Transportation Engineering Commons

Recommended Citation

Algomaiah, Abdulmaged, "Utilizing shockwave theory and deep learning to estimate intersection traffic flow and queue length based on connected vehicle data." (2022). *Electronic Theses and Dissertations.* Paper 3813.
https://doi.org/10.18297/etd/3813

This Doctoral Dissertation is brought to you for free and open access by ThinkIR: The University of Louisville's Institutional Repository. It has been accepted for inclusion in Electronic Theses and Dissertations by an authorized administrator of ThinkIR: The University of Louisville's Institutional Repository. This title appears here courtesy of the author, who has retained all other copyrights. For more information, please contact thinkir@louisville.edu.

UTILIZING SHOCKWAVE THEORY AND DEEP LEARNING TO ESTIMATE INTERSECTION TRAFFIC FLOW AND QUEUE LENGTH BASED ON CONNECTED VEHICLE DATA

By
Abdulmaged Algomaiah
B.S., Queensland University of Technology, 2014
M.S., University of Louisville, 2017

A Dissertation
Submitted to the Faculty of
J.B. Speed School of Engineering at the University of Louisville
in Partial Fulfillment of the Requirements
for the Degree of

Doctor of Philosophy
in Civil Engineering

Department of Civil & Environmental Engineering
University of Louisville
Louisville, Kentucky

May 2022

Copyright 2022 by Abdulmaged Algomaiah

All rights reserved

UTILIZING SHOCKWAVE THEORY AND DEEP LEARNING TO ESTIMATE INTERSECTION TRAFFIC FLOW AND QUEUE LENGTH BASED ON CONNECTED VEHICLE DATA

By

Abdulmaged Algomaiah
B.S., Queensland University of Technology, 2014
M.S., University of Louisville, 2017

A Dissertation Approved on

April 25, 2022

by the following Thesis Committee:

_____
Dr. Zhixia (Richard) Li

_____
Dr. Zhihui Sun

_____
Dr. Thomas Rockaway

_____
Dr. Hongxiang Li

DEDICATION

To all those who appreciate, support and love Majeed.

ACKNOWLEDGMENTS

I would like to thank my supervisor Dr. Zhixia (Richard) Li for his constant support and motivation since early stage of my journey in research. I am deeply thankful for the time he spent on sharing his knowledge and experience. He has always been a source of encouragement and profound guidance. Dr. Li's support and guidance is a significant factor behind my achievements in terms of journal publications, conferences, and awards. I am sure that Ph.D. candidates are lucky to be supervised by Dr. Li, and they have the potentiality to achieve high levels of success with his support and guidance.

I am sincerely grateful to Dr. Zhihui Sun for her support as a chair of the department and for her comments as a as committee member. My gratitude is expressed to Dr. Thomas Rockaway and Dr. Hongxiang Li for their participation in the committee and their valuable feedback. I also would like to deeply thank Dr. J.P. Mohsen for his advice and his ultimate support.

I would like to thank my former fellow graduate researcher Dr. Song Wang for the five years we spent at the Center for Transportation Innovation. We shared the space in the lab, and we also shared thoughts, support, and encouragement. I am grateful to his fellowship, and I appreciate his cooperation.

My words cannot be enough to thank all my friends whom I got to know here in Louisville, Kentucky. They were the fuel of my social life, and without them, my personal life would be unbearable. I shared a great deal of joyful time, and they were there for me when I needed them. It is hard to name them all, but they certainly know themselves.

I would like to thank Quills Coffee for the great cup of coffee they make me almost every morning. Since the pandemic, they provide me the space and atmosphere with a perfect dose of caffeine to brainstorm and write efficiently. My thanks extend to all the baristas, especially Nick in the Highlands and Justin in Nulu.

My gratitude extends to the person who taught me academic English about 12 years ago, Marlyn McKennnariey. She was not only a teacher, but Marlyn was a mentor and a close friend. I am thankful to her support and care that she has been showing during my life in Australia, and I appreciate that we are still in touch.

Last but not least, there are not enough words to express my gratitude to my parents Mohammad and Jawaher Algomaiah for their ultimate love. They do not know what exactly I am doing, but all they know that I am working hard to achieve my dreams. My thanks extend to my siblings who have always been proud of me, and they always express their support. Special thanks to my siblings Abdulelah, Arwa, Abdullah, and Ghalia for being close to me whenever I need them.

ABSTRACT

UTILIZING SHOCKWAVE THEORY AND DEEP LEARNING TO ESTIMATE INTERSECTION TRAFFIC FLOW AND QUEUE LENGTH BASED ON CONNECTED VEHICLE DATA

Abdulmaged Algomaiah

April 25, 2022

The development of Connected Vehicles (CV) facilitates the use of trajectory data to estimate queue length and traffic volume at signalized intersections. The previously proposed models involved additional information that may require conducting different types of data collection. Also, most models need higher market penetration rate or more than a vehicle per cycle to provide adequate estimation. This is mainly because a significant number of the estimation models utilized only queued vehicles. However, the state of motion in non-queued vehicles, particularly slowed-down vehicles, provides much information about the traffic characteristics. There is a lack of exploiting the information from slowed-down vehicles in identifying the last queued vehicle to improve the estimation models. The importance of this work is to propose a cycle-by-cycle queue length and traffic volume estimation models by utilizing the slowed-down vehicles. It proposes a sophisticated model to estimate the queue length and traffic volume from

connected vehicles with low market penetration rate (MPR) by utilizing shockwave theory and deep learning technique (artificial neural network). The work starts with establishing a relationship between the slowed-down vehicles and last queued vehicles based on shockwave theory and traffic flow dynamics. Then, the queue estimation algorithm is modeled based on the capacity state and deep learning technique. The traffic volume algorithm modeled is based on the queue length information. Four experiments were conducted to investigate the performance of the queue length and traffic volume estimation models on dataset from simulation environment and real-world data. The queue length results of the simulation experiment demonstrated an adequate mean absolute percentage error (MAPE) of 13.44%, which means an accuracy of 86.56%. The highest MAPE was 19.16% (80.84% accuracy) and the lowest was 7.36% (92.64%). The results of the queue length algorithm applied on real-world data demonstrated an MAPE of 21.97% (78.03% accuracy). The performance of the traffic volume algorithm on simulation data demonstrated an excellent MAPE of 11.8% (88.2% accuracy). The performance of the algorithm based on real-world data from demonstrated an MAPE of 23.57% (76.43% accuracy). Although the previous models can provide similar accuracy rates, they require higher MPR. With the low MPR of 10%, the proposed models revealed an adequate estimation accuracy of the cycle-by-cycle queue length and traffic volume.

TABLE OF CONTENTS

LIST OF TABLES

LIST OF FIGURES

CHAPTER I: INTRODUCTION

The estimation of queue length and traffic volume are essential inputs for optimizing the traffic signal timing and evaluating other traffic signal measurements. The conventional methods of estimating queue length and traffic volume mainly require other traffic flow characteristics such as previous traffic volumes and speed acquired from physical sensors such as loop detectors, radar, and video cameras (Liu et al., 2009; Sharma et al., 2007; Skabardonis & Geroliminis, 2008; Vigos et al., 2008). The information from devices with global positioning system (GPS) devices provides the chance to use the data in terms of time and location in the estimation of many traffic characteristics. Some smartphone applications record vehicle positions every 0.1 second, which improves the accuracy of the estimation models (Zhang et al., 2020). The recent advancements in communication in terms of Vehicle-to-Vehicle (V2V) and Vehicle-to-Infrastructure (V2I) has provided a great opportunity to utilize the trajectory data of connected vehicles (CVs) as probe vehicles. In other words, trajectory data of CVs is represented in time and distance, and it can be used to recognize the spatial-temporal characteristics of the traffic. This new method is a promising solution as it provides a cost-effective advantage of queue length and traffic volume estimation without the need of installing additional devices at the signalized intersections.

Some of the proposed models provide adequate queue length and traffic volume estimations when there is a sufficient market penetration rate (Cheng et al., 2012; Tiaprasert et al., 2015; Zhang et al., 2019). However, when the market penetration rate is realistically low, the models show instability and inaccuracy, which makes the implementation of the models in the near future potentially unattainable. Other models demonstrate a good queue length or traffic volume accuracy with lower market penetration rate (Hao et al., 2013; Tan et al., 2021). Nevertheless, the main limitation of the models is the requirement of market penetration rate as an input in the models along with the information from the adjacent intersections, which requires more data collections. Some other models can estimate the queue length or traffic volume with a low market penetration rate yielding an improved accuracy (Tan et al., 2021; Wang et al., 2020; Zheng et al., 2019). Yet, the models lack independency as they require additional information of some intersection parameters such as shockwave speed and free-flow speed, which limits the estimation model to intersections where data collection has been previously conducted. Furthermore, all other previous studies rarely utilize the information from non-queued vehicles in their models (Tan et al., 2021), which limits the state of motion in non-queued vehicles includes slowed-down vehicles that provide much information about the traffic characteristics. A major advantage of the slowed-down vehicle is the proximity of the last queued vehicle, which is a key element as it states the boundary of the queue length and the traffic flow during red time. Therefore, estimating the last queued vehicle through the slowed-down vehicles can improve the accuracy of the queue length and traffic volume estimation.

There is a lack of research that establishes the relationship between the slowed-down vehicles and the last queued vehicles and integrates it in traffic volume estimation model. Based on the traffic flow dynamics, vehicles slow down approaching the signalized intersection when the shockwave is still dissipating. The slowed-down vehicles join the moving queue in the capacity state where the queued vehicles are increasing their speed in a particular pattern. The spatiotemporal speed distribution of the queued vehicles in the capacity state can be modeled to identify the last queued vehicle from the time, distance, and speed of the slowed-down vehicles. Based on a prior sampled trajectory data with the traffic signal information only, a deep learning technique (artificial neural network) is utilized to obtain queue length and traffic volume estimation model. After that, the real-time trajectory data of each cycle can be implemented in the trained algorithm to estimate the traffic volume.

1.1. Research Gap and Motivation

Based on the shortcomings in current models, the research gaps in queue length and traffic volume estimation from connected vehicle data are highlighted as the following:

- The requirement of additional information attained by conducting different types of data collection,
- The need of higher market penetration rate or more than a vehicle per cycle to provide adequate estimation, and

- The lack of exploiting the information from non-queued vehicles, particularly slowed-down vehicles, in identifying the last queued vehicle and estimating the queue length and traffic volume.

The motivation of this work is to fill the research gap by proposing sophisticated queue length and traffic volume estimation algorithms that utilize slowed-down vehicles. The algorithm relies on previous trajectory data as a training dataset without the need of different types of data collection. In this novel technique, one slowed-down vehicle per cycle can be enough to provide adequate queue length and traffic volume estimation by utilizing shockwave theory and deep learning technique without the need of external traffic parameters.

1.2. Contribution and Objectives

The contribution of this paper focuses on filling the research gap by proposing a novel model that leverages slowed-down vehicles in identifying the position of the last queued vehicle to eventually estimate the queue length and traffic volume. The proposed model avoids external dependencies and relies on learning about the macroscopic parameters (for the signalized intersections) and microscopic parameters (for the vehicles) from a prior day of CV trajectory data. Thus, shockwave theory and deep learning technique are utilized to incorporate macroscopic and microscopic parameters in the estimation model. This method is adopted because the speed distribution of the queue dissipation process in the capacity state can facilitate identifying the speed of the last queued vehicle, therefore, demonstrating the position the last queued vehicle.

The training of data to learn from the prior dataset aims to predict the microscopic and macroscopic characteristics of the traffic at the signalized intersection without the need of interpretation. The learning in artificial neural network (ANN) meets the prediction requirement in this work beside the fact that its learning curve might include different local minima and might converge to different non-nested sequential architectures (Ripley, 1996). These advantages make ANN more flexible than other deep learning techniques and encourage applying it in the training, testing, and validating in the estimation process.

By considering the research gap and the unique contribution of this work, the objectives of this paper are summarized as the following:

- **Objective 1:** Establishing a relationship between the slowed-down vehicle and last queued vehicle based on shockwave theory and the capacity state,
- **Objective 2:** Utilizing only a prior dataset and a deep learning technique to identify the last queued vehicle information based on the slowed-down vehicle,
- **Objective 3:** Proposing a queue length estimation algorithm based on lower market penetration rates., and
- **Objective 4:** Developing a traffic volume estimation algorithm considering the queue length estimation model.

1.3. Dissertation Organization

To address the research gaps and achieve the objectives of this dissertation, the rest of the manuscript is organized as the following:

- Chapter II: highlights the literature review of the research related to queue length and traffic volume estimation from trajectory data,
- Chapter III: establishes the theoretical relationship between the slowed-down vehicle and last queued vehicle based on shockwave theory and the capacity state,
- Chapter IV: enhances the relationship between the slowed-down vehicle and last queued vehicle with empirical evidence from the data,
- Chapter V: describes the methodology of the queue length and traffic volume estimation. Algorithms based on deep learning techniques,
- Chapter VI: reveals the results and analyzes the performance of the queue length and traffic volume estimation algorithms based on the simulation and real-world experiments,
- Chapter VII: draws the conclusions from the experiments and highlights the findings to make the recommendations from the dissertation

CHAPTER II: LITERATURE REVIEW

The estimation of queue length at signalized intersections from trajectory data was introduced as a cutting-edge solution by using different algorithms. Early works in the area started to develop a real-time queue length estimation using trajectory data from CV with the demand of a sufficient percentage of trajectory data (Tan et al., 2021). Since then, the area of queue length estimation has evolved to consider lower market penetration rate (MPR) with relatively higher accuracy. Among early works Skabardonis and Geroliminis (2008), and Vigos et al. (2008), and Liu et al. (2009) developed real-time models of queue length estimation. Since then, there has been a growing attention to the estimating of queue length from connected vehicle data for real-time purposes during the last decade. Almost all works follow either a deterministic or a stochastic approach to estimate the queue length.

2.1. Queue Length and Traffic Volume Estimation

Deterministic methods are mostly built on traffic flow theories by using direct mathematical relationship to estimate the queue length. Ban et al. (2011), Hao and Ban (2015), Liu et al. (2009), Wang et al. (2019), and Wang et al. (2017) determined the shockwave profile to estimate queue length through stochastic approaches that use travel times from connected vehicle trajectory data.

Among the notable works, Cheng et al. (2012), Ramezani and Geroliminis (2015), Li et al. (2017), Yin et al. (2018), and Zheng et al. (2019) utilized shockwave theory in terms of dissipation and forming queues to identify the critical trajectory points of joining and leaving the queue. However, those deterministic methods are capable of providing decent queue length estimations only when there is a sufficient trajectory sample. For example, there is a need of at least two queued probe vehicles to have a decent result based on the mentioned studies.

The stochastic methods depend on probabilistic models to estimate the parameters and the queue length of the cycle. Most of the stochastic models assumed a Poisson distribution of vehicle arrivals and a conditional probability distribution utilized a conditional probability distribution. Comert and Cetin (2011) and Comert (2013) introduced an analytical model to estimate a cycle-by-cycle queue length by estimating the arrival rate through probe vehicle proportion. Hao et al. (2013) and Hao and Ban (2015) estimated a cycle-by-cycle queue length using a Bayesian network method that utilizes the relationship between the forming, queuing, and dissipating positions of the probe vehicles. Tiaprasert et al. (2015) proposed a mathematical model based on discrete wave transform without the use of signal time information or traffic flow characteristics. Li et al. (2017) introduced a queue length estimation model using flow rate and travel time with the consideration of the queue spillover. The model was based on a macroscopic model using a first-in-first-out concept to find the maximum queue length. Rostami Shahrbabaki et al. (2018) proposed a fusion method using the data from a fixed detector an earlier location of the traffic signal approach and the data from connected vehicles. The study modeled a nonlinear function that uses the information from

connected vehicles to identify the number of vehicles in the queue. Zhao et al. (2019) established a queue length distribution model using Bayes theory through analyzing the statistical distribution of the position of queued vehicles. By using the distribution of the traffic flow and the market penetration rate, the mentioned studies could provide reliable estimation results. However, those methods face the challenge of verifying the arrival distribution by empirical data collection and the difficulty of obtaining the market penetration rate of probe vehicles. These two points are considered as the main limitations of both the stochastic and the deterministic methods.

2.2. Traffic Flow Theory

Traffic flow models in terms of shockwave theory and car-following models have been widely considered in the estimation of the traffic characteristic. The need of traffic flow models is explained by the essential role of understanding the nature of traffic flow and the behavior of drivers. The effect of traffic flow theory has been applied directly or indirectly in the estimation or modeling of traffic characteristics.

Shockwave theory was introduced by Lighthill and Whitham (1955) and adopted in traffic theory by Richards (1956). Since then, researchers in transportation engineering started to utilize shockwave theory in different applications of transportation network (Ban et al., 2011; Liu et al., 2009; Michalopoulos et al., 1981; Skabardonis & Geroliminis, 2008; Wu & Liu, 2011; Wu et al., 2011). Among the earliest work about utilizing shockwave theory were Cheng et al. (2012), Cheng et al. (2011), and Ramezani and Geroliminis (2015). A recent work by proposed a queue profile estimation model based on the spatiotemporal propagation of shockwaves (Wang et al., 2020).

Car-following model is necessary to understand the longitudinal behavior of vehicles in the traffic flow. One of the first recognized works in car-following models was introduced by Newell (1961). A significant amount of research followed to explain the car-following behavior to achieve more realistic modeling of the traffic flow (Addison & Low, 1998; Brackstone & McDonald, 1999; Gipps, 1981; Lenz et al., 1999; Newell, 1965; Sharma et al., 2007; Vigos et al., 2008; Zhang & Kim, 2005). The car-following models are influenced by factors different based on the site specifications and driving behavior. An important factor is the discharge headway as it directly affects the parameters of the car-following model (Akçelik & Besley, 2002; Al-Ghamdi, 1999; Hung et al., 2003; Lin & Thomas, 2005; Radhakrishnan & Ramadurai, 2015; Shao & Liu, 2012; Tong & Hung, 2002)

Understanding the behavior of traffic flow has extended to understand the behavior of drivers approaching the signalized intersection and its relation to the macroscopic diagram including queue length (Al-Ghamdi, 1999; Dion et al., 2004; Sheffi & Mahmassani, 1981; Viloria et al., 2000; Yeo & Skabardonis, 2009). Other works attempted to study the relation between signalized intersections and the fundamental traffic diagrams (Kerner et al., 2006; Mühlich et al., 2015; Othayoth & Rao, 2020; Yuan et al., 2017). A good number of studies focused on the queue discharge at signalized intersections and its relation to the traffic capacity (Fourati & Friedrich, 2019, 2021; Li et al., 2017; Liu et al., 2009; Wu & Liu, 2011; Yin et al., 2018; Yuan et al., 2017).

2.3. Deep Learning

The estimation models of traffic flow characteristics started to utilize machine learning and deep learning techniques about two decades ago. The main advantage of data mining models is their capacity in capturing non-linear temporal correlations. A significant amount of research applied machine learning and deep learning in the application of traffic characteristics (Koesdwiady et al., 2016; Lv et al., 2015; Polson & Sokolov, 2017; Wu et al., 2018; Zhang et al., 2019). Support Vector Regression (SVR) is among the first data mining models utilized in the estimation of the traffic flow characteristics such as traffic flow prediction (AiLing et al., 2002; Yang et al., 2014; Zhang & Xie, 2007), travel time prediction (Chun-Hsin et al., 2004), and traffic speed prediction (Vanajakshi & Rilett, 2004; Wang & Shi, 2013).

The ability of deep learning techniques in modeling complex non-linear relationships invited researchers to utilize and different deep learning techniques in traffic flow estimations. Conventional neural network (CNN) is able to capture the local dependencies of traffic data and it is known to be less sensitive to noise in traffic (Li et al., 2020). In another traffic flow application, Song et al. (2017) proposed a speed prediction model based on CNN and Multi-Layer Perceptron (MLP) models. The comparison revealed that CNN demonstrated higher prediction accuracy than MLP. Ma et al. (2017) introduced a speed prediction model utilizing CNN model for a large-scale transportation network. The model revealed a good accuracy in predicting traffic speed for the long term. Another work by Ke et al. (2020) explored the use of CNN in the

prediction of traffic speed based on the correlation between spatiotemporal dimension and traffic volume.

More recently, deep learning techniques have been widely applied in the estimation of traffic characteristics with promising results (Mahmoud et al., 2021, 2022). Among the greatest advantages of deep learning is the flexibility that makes them able to model nonlinearity and distinguish the spatiotemporal features within the traffic flow. There are various versions of neural network based on the structure and the properties such as input cell, hidden cell, recurrent cell, and kernel. Some studies compared different types of neural networks in applications related to the traffic flow on freeways and found that Bayesian Combined Neural Network (BCNN) demonstrated better performance than the single neural network models (NN) and Radial Basis Function Neural Networks (RBFNN) in terms of accuracy (Zheng et al., 2006; Zhu et al., 2014). Another deep learning technique that has been frequently utilized is Long Short-Term Memory (LSTM) in estimating short-term traffic parameters such as cycle-by-cycle traffic volume and queue length (Cui et al., 2020; Mahmoud et al., 2021). Different types of neural network such as Convolutional Neural Network (CNN) have been developed to estimate traffic volume at signalized intersections (Zhang et al., 2019; Zhao et al., 2020; Zheng et al., 2019).

2.4. Summary of Chapter II

For queue length estimation, recent works such as Yao and Tang (2019), Mei et al. (2019), Wang et al. (2020), and Tan et al. (2021) proposed models with relatively improved accuracy. However, the current models face some challenges from two main

aspects including the need of additional information about the traffic flow characteristics and the requirement of more than one sampled vehicle per cycle to achieve a decent accuracy. The additional information is not always available, and it may require data collection in some cases. In fact, the need of market penetration rate opened another stream of research to estimate the market penetration rate (Wong et al., 2019; Zhao et al., 2019). This demand of additional information increases the internal and external dependencies of the queue estimation models. Also, the other aspect of requiring more than one sampled vehicle limits the applicability of the queue estimation models. Therefore, there is a plenty of room for improvement to estimate queue length without external dependency and without the need of more than one sampled vehicle. Zhao et al. (2021) proposed a queue estimation algorithm based on hidden Markov model that utilizes the stopping positions only. Their proposed model considered using 20% of market penetration rate without testing other reasonable rates assuming a constant traffic pattern.

From the literature review of all related works of queue length and traffic volume estimation from sampled trajectory data in connected vehicle environment based on traffic theory, the findings can be summarized as the following:

- There is a lack of independency as the current models require some intersection parameters that might need other types of data collection from the site such as shockwave speed and free-flow speed. This gap limits the use of current estimation models to the intersections where in-site data collection has been previously conducted.

- All the previous works classified vehicles into queued vehicles and non-queued vehicles only. In such classification, the queue length estimation models mainly utilize the queued vehicles only, while the non-queued vehicles are used as a boundary for the model.
- There is a lack of utilizing the information from slowed-down vehicles to estimate the queue length. The uniqueness of this work is utilizing the information of slowed-down vehicle to identify the last queued vehicle.

CHAPTER III: THE DYNAMICS OF TRAFFIC FLOW AT THE SHOCKWAVE DISSIPATION

Most research classifies the traffic flow into stopping (queueing) vehicles and passing vehicles to estimate the traffic characteristics (i.e., traffic volume and queue length). At isolated intersections, a vehicle approaches the intersection with three main possible scenarios:

- Free-flow state (the signal is green, and the queue has already dissipated),
- Jam state (the signal is red, and all vehicles are queued), or
- Capacity state (the signal is green, and the queue is dissipating).

Figure 3.1 displays the trajectories of vehicles approaching the traffic signal in Case A, Case B, and Case C. The vehicles are supposed to approach the intersection within the speed limit, which is known as the free-flow state. When the vehicles arrive to the intersection, they will either continue in Case A (pass the intersection within the speed limit), get into Case B (stop at the traffic signal), or get into Case C (slow down and join the dissipating queue). Case C provides the most valuable information about the traffic characteristics that is worth utilizing. Here, Case C is called a capacity state which includes the saturation state and its transition state as identified by Fourati and Friedrich (2021).

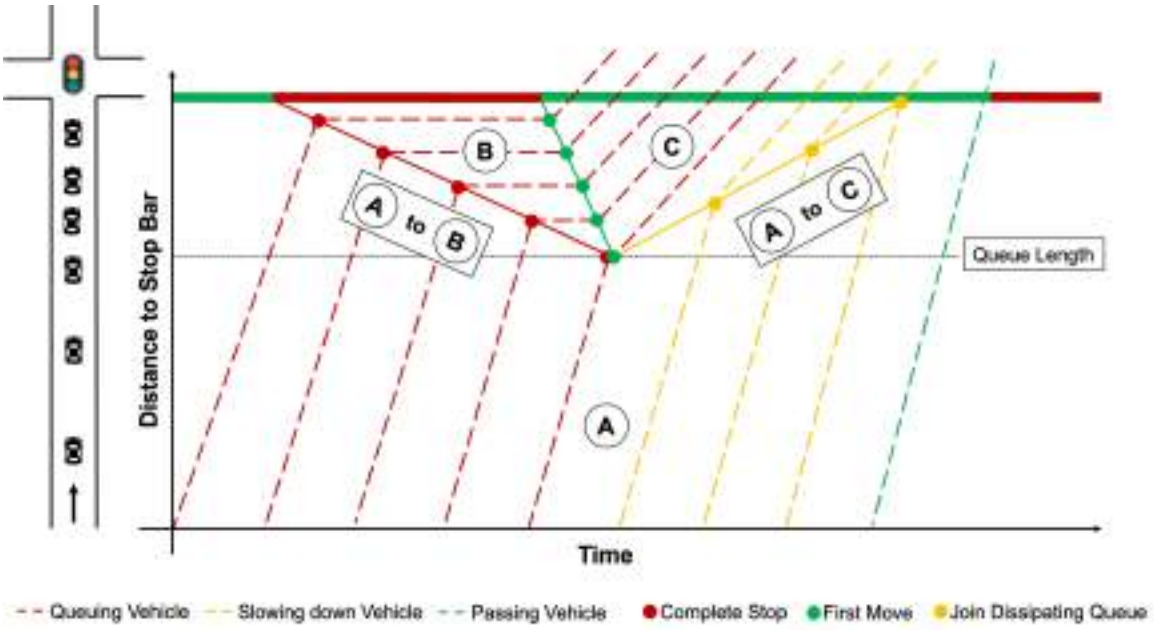

Figure 3.1 The Traffic State During Shockwave Propagation and Dissipation

3.1. The Characteristics of Different Traffic States

The change of vehicles from Case A to Case B provides information about the speed of shockwave propagation (queue formation). However, in a sampled trajectory data with limited market penetration rate, a single queued vehicle does not provide adequate information about the queue formation. On the other hand, a single vehicle that changes from Case A to Case C can provide information about the speed of the shockwave dissipation (queue dissipation), and it can also assist in finding the queue

length and the traffic volume, which is the merit of this work.

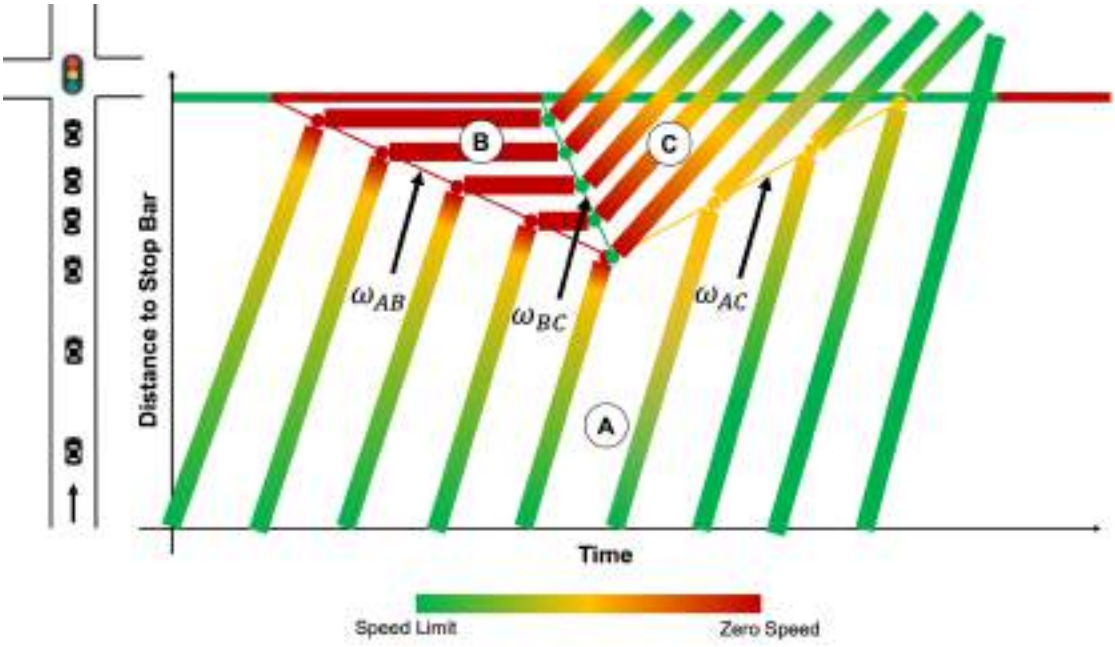

Figure 3.2 The Speed Distribution During Shockwave Propagation and Dissipation

3.1.1. The Queue Dissipation Process

By looking at Figure 3.2, the queue dissipation process begins when the traffic signal turns to green while the speed is zero, and the process of dissipating continues to increase the speed to reach a free-flow speed. In this capacity state (Case C), the sequential departure of vehicles makes the flow saturated, creating a particular follow pattern. In Case B, however, the queue formation follows random patterns due to the random arrival of vehicles. When a vehicle in Case A (free-flow speed) approaches the signalized intersection while the queue is dissipating, the vehicle has to slow down to join the moving queue in the capacity state (Case C). The time, distance, and speed of the slowed-down vehicle can help estimate the stopping position of the last queued vehicle. Finding the stopping position of the last queued vehicle is the most critical piece of

information in identifying the queue length and then the traffic volume. As Figure 3.2 shows, the slope in red formed by the queued vehicles creates the shockwave formation speed (ω_{AB}) based on the arrival rate. The slope in green formed by the first move of vehicles creates the shockwave dissipation speed (ω_{BC}), which is almost constant in most cases. The slope in yellow formed by the slowed-down vehicles creates the forward-moving shockwave speed (ω_{AC}) based on the arrival rate. The significance of the capacity state (Case C) is seen in its ability to connect between the slowed-down vehicles and the last queued vehicle. The information about the capacity state can be obtained from the prior data, while the slowed-down vehicle is obtained from the real-time data of the cycle.

3.1.2. The Queue Dissipation in Relation to the Traffic Flow

The purpose of discussing the different traffic states of the shockwave diagram is to relate the shockwave dissipation. Therefore, it is important to connect the shockwave formation and dissipation with the traffic flow. To visualize this relationship, the following figure is plotted.

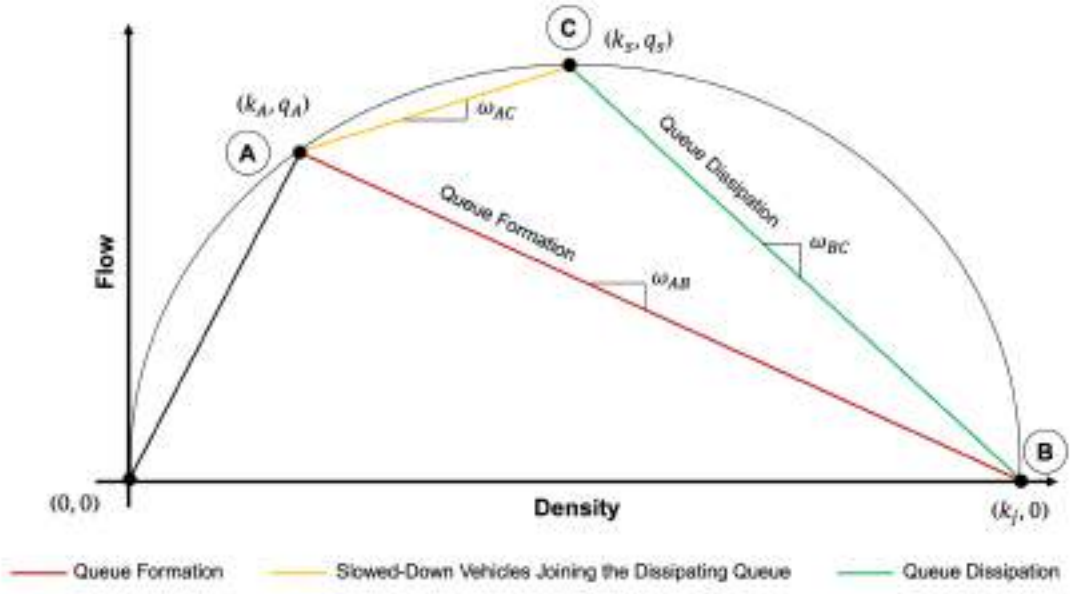

Figure 3.3 Vehicle Classifications and Traffic States on the Fundamental Diagram (Flow Vs Density)

As shown in Figure 3.3, ω_{AC} is the slope between Case A and Case C in terms of flow and density, which both are missing in sampled trajectory data. Since ω_{BC} is relatively constant and the capacity of the intersection is constant as well, the last queued vehicle is following the same departure pattern, which means its speed can indicate its stopping position (the queue length). Moreover, the speed of the slowing down vehicle is related to the speed of the last queued vehicle at Case C based on car-following model. Utilizing all these pieces of information from speed distribution at the capacity state and the slowing down vehicle can lead to an estimate of the stopping position of the last queued vehicle, which represents the queue length. Technically, the furthest (maximum) position of a queued vehicle (p_{QV}) from the stop bar equals the queue length (L_Q) as the following:

$$L_Q = max\ (p_{QV}) \tag{3.1}$$

The relationship between queue length and traffic volume is influenced by the waiting time based on Little's Law (Little, 1961). According to Little's Law, the general relationship is described as the following:

$$L_Q = q \times t_w \tag{3.2}$$

3.2. Slowed-down Vehicles and the Last Queued Vehicle

To understand the interactions between the slowed-down vehicle and the last queued vehicle, the interaction between the two vehicles needs to be established in a microscopic level and macroscopic level. The microscopic interaction is illustrated by the car-following model and the macroscopic interaction is influenced by the traffic state, particularly the queue dissipation.

3.2.1. The Microscopic Interaction in Terms of Car-Following Model

The relationship between the slowed-down vehicle and the last queued vehicle can be described by a car-following model. Most car-following models share certain principles about headway and speed. The slowed-down vehicle (the following vehicle) reacts according to the queued vehicle (the leading vehicle) based on the traffic flow

dynamics. By taking into consideration Newell's car-following model (Newell, 1965), the speed of the slowed-down vehicle when it joins the dissipating queue follows:

$$v_{SD} = min\ (v_d, \frac{S}{T}) \tag{3.3}$$

3.2.2. The Macroscopic Interaction in Terms of the Speed at the Capacity State

Based on Equation (3.3), the speed of the slowed-down vehicle will be correlated with the speed of the last queued vehicle as illustrated in Figure 3.4. The speed of the vehicles in the capacity state is called speed distribution with spatiotemporal consideration. The speed distribution considers the time and distance in the capacity state by obtaining the speed of the queued vehicles as they move from jam state (their stopping positions) to the capacity state (shockwave dissipation). Figure 3.4 shows the interaction between slowed-down vehicles and the queued vehicles with the spatiotemporal speed distribution in the capacity state (Case C).

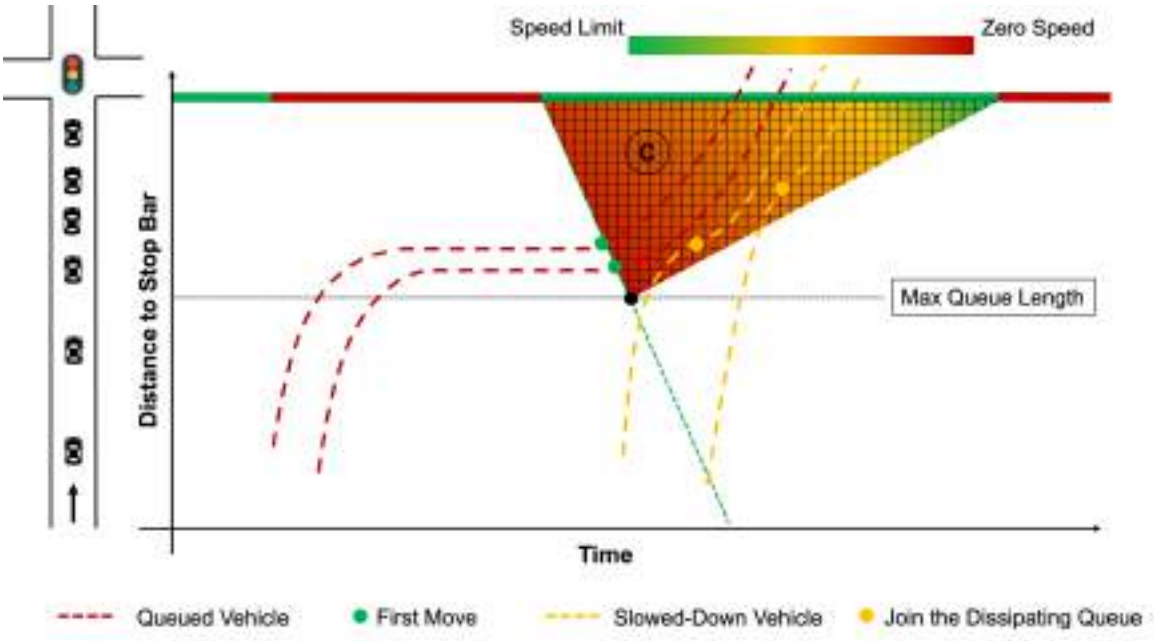

Figure 3.4 The Interactions Between Slowed-down Vehicle and Queued Vehicles in the Capacity State

The first slowed-down vehicle in Figure 3.4 (the one to the left) joined the queue at a spatiotemporal cell closer to the queued vehicle. The speed at this cell is approximately equal to the speed of the queued vehicle. Therefore, uniform speed distribution at the capacity state represents the minimum speed of the last queued vehicle:

$$v_{QV} \geq v_{CS} \tag{3.4}$$

Figure 3.4 also shows a second slowed-down vehicle (to the right) that was extremely distant from the last queued vehicle that approaches the stop bar. This ultimate example justifies the use of the stop bar as the maximum speed of the queued vehicle:

$$v_{QV} \leq v_{SB} \tag{3.5}$$

The jam state at the signalized intersection forces approaching vehicles to slow down even when the signal is green due to the required time for the shockwave to dissipate. That means when slowed-down vehicles approach the moving queue, the free-flow speed will be higher than the speed of the queued vehicles. The increase of the speed of the moving queue during the queue dissipation process means the slowed-down vehicles will increase their speed as well. Therefore, the lowest speed of the slowed-down vehicle will be considered as the moment of joining the moving queue.

3.3. Summary of Chapter III

From the theoretical basis discussed in this chapter, the findings of this chapter can be summarized as the following:

- The queue dissipation and capacity state have a uniform pattern in terms of time, space, and speed,
- The speed of queued vehicles increases with the increase of the green time until the last queued vehicle,
- The slowed-down vehicle interacts with the last queued vehicle based on the car-following model

CHAPTER IV: THE OBSERVATIONAL CHARACTERISTICS OF VEHICLE CLASSIFICATIONS

The role of the prior data is to find the characteristics of the capacity state at the signalized intersection. The speed distribution of the queued vehicles can identify the spatiotemporal propagation and dissipation of the shockwave. This helps to recognize the boundaries of the capacity state and to understand the relation between the queued vehicles and the slowed-down vehicles.

4.1. The Macroscopic Description of the Shockwave

Figures 4.1, 4.2, 4.3, and 4.4 plot the trajectory data of one day from 7 am to 7 pm based on the time, distance, and speed of all vehicles and sampled vehicles. The red line in Figure 4.1 shows the dissipation shockwave speed, and the red shades displays the speed pattern at the capacity state (Case C) based on the entire trajectories of the queued vehicles (100%). The same details about the intersection are still visible in Figure 4.2 from queued vehicles with only a sampled trajectory data (10% only).

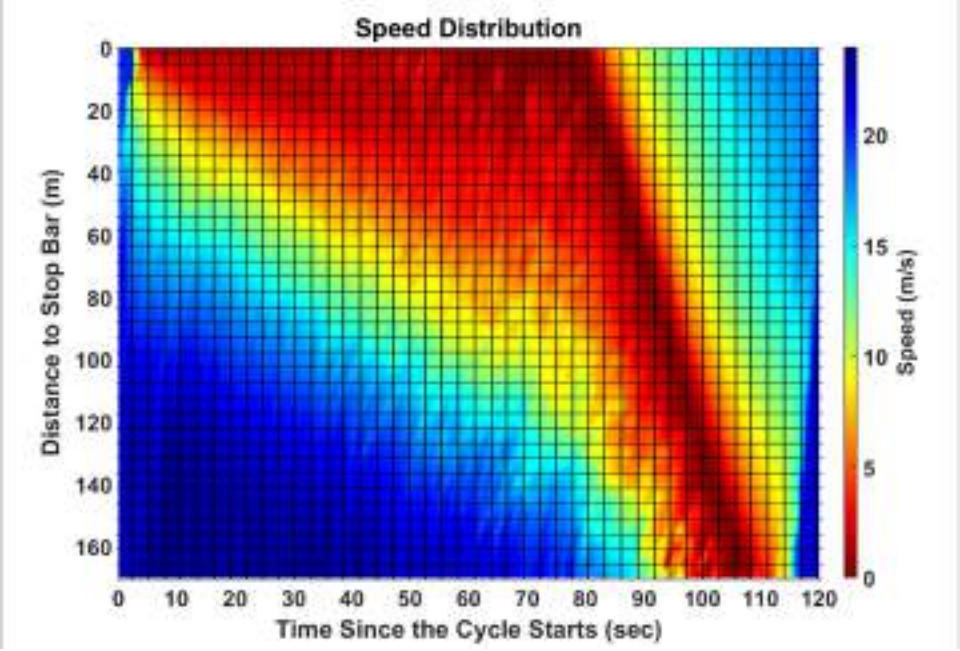

Figure 4.1 The Macroscopic Shockwave Based on the Spatiotemporal Speed Distribution of Queued Vehicles (100%)

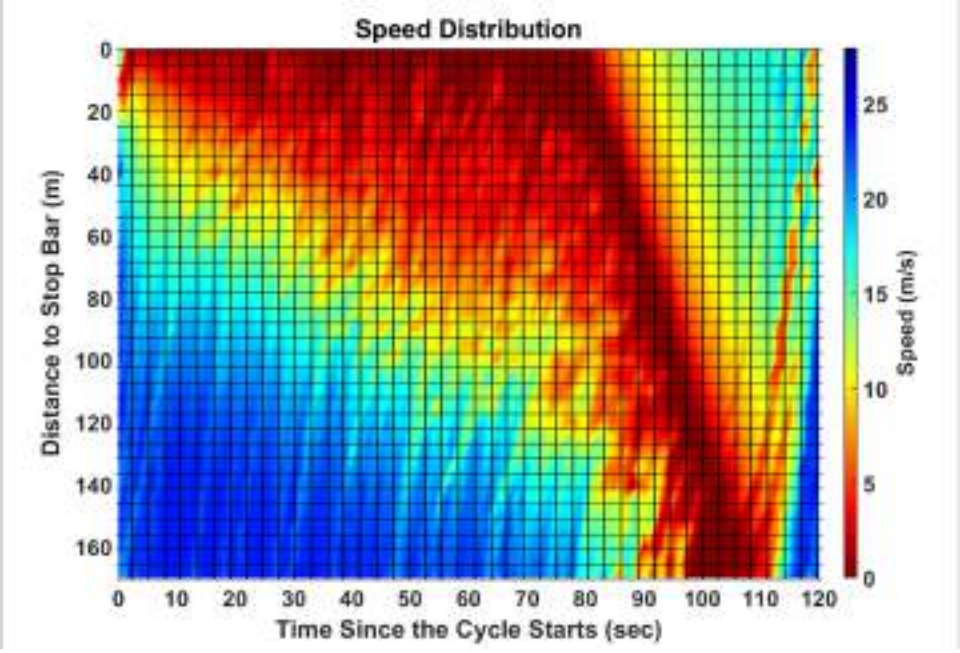

Figure 4.2 The Macroscopic Shockwave Based on the Spatiotemporal Speed Distribution of Queued Vehicles (10%)

Figures 4.3 and 4.4 plot the speed distribution of slowed-down vehicles. The slowed-down vehicle in Figure 4.3 shaped the dissipation shockwave speed (the red slope) due to the relation between the slowed-down vehicles and the queued vehicles. The same details were visible by using a sampled trajectory data (10% only) of the slowed-down vehicles as shown in Figure 4.4. This example from the data establishes empirical evidence of the relation between slowed-down vehicles and the queued vehicles as well as the ability of time, distance, and speed to identify the shockwave propagation and dissipation.

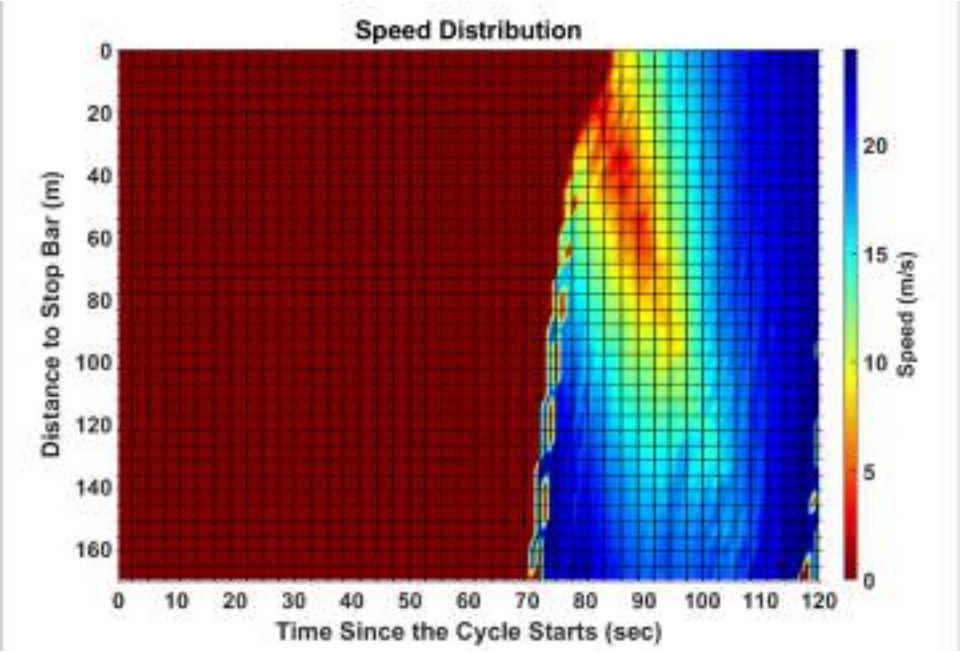

Figure 4.3 The Macroscopic Shockwave Based on the Spatiotemporal Speed Distribution of Slowed-down Vehicles (100%)

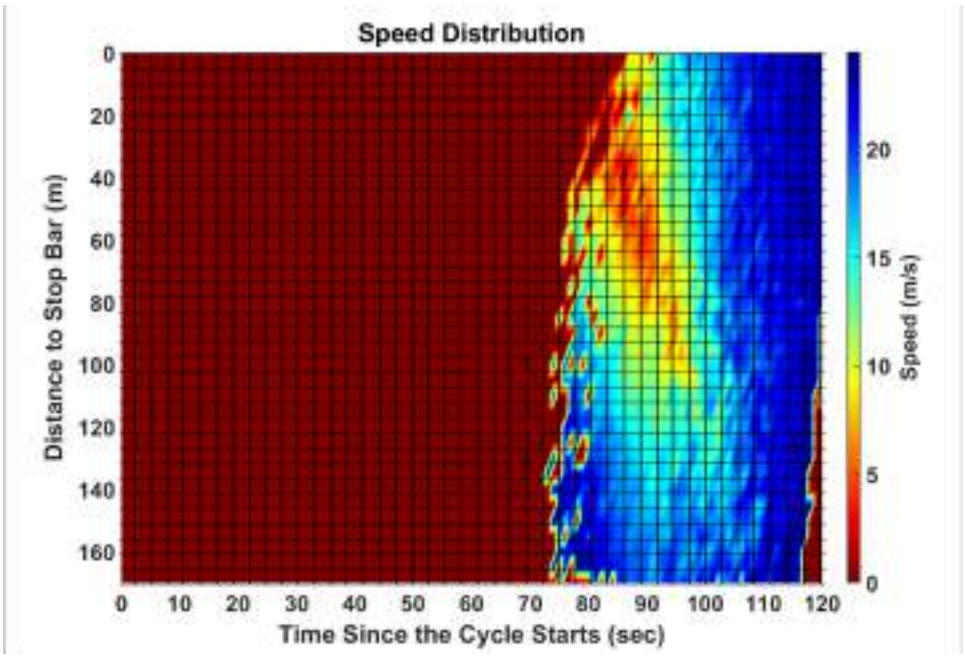

Figure 4.4 The Macroscopic Shockwave Based on the Spatiotemporal Speed Distribution of Slowed-down Vehicles (10%)

4.2. The Interactions Between the Slowed-down Vehicle and the Last Queued Vehicle

Figures 4.5 to 4.10 illustrate empirical evidence of the relationship between the shockwave characteristics, queued vehicles, and slowed-down vehicles. They show the time and position of the first stop of the queued vehicles, the first move of the queued vehicles, and the least speed of the slowed-down vehicles. The backgrounds of the figures are the speed distribution from Figures 4.1 and 4.2 to emphasize the relationship between the shockwave characteristics and the vehicle classifications.

Figures 4.5 to 4.7 are plotted with 100% of the trajectory data, while Figures 4.8 to 4.10 are plotted with only 10% of the trajectory data. The red points in Figure 4.5 are

the first stops of the queued vehicles at the signalized intersection. The red points shaped the jam state (Case B) as Figure 4.5 shows. The green points in Figure 4.6 are the first move of the queued vehicles at the signalized intersection. The green points shaped the dissipation shockwave speed, which is the transition between the jam state (Case B) and the capacity state (Case C) as illustrated in Figure 4.6. It is worth mentioning that the dissipation shockwave speed has a very uniform pattern due to the nature of queue dissipation when vehicles are moving in a repeated sequence. The yellow points in Figure 4.7 are the least speed of the slowed-down vehicles when they are joining the moving queue. The yellow points are scattered in the capacity state (Case C) closer to the shockwave dissipation slope. This finding enhances the relationship between the slowed-down vehicles and the queued vehicles based on the shockwave analysis.

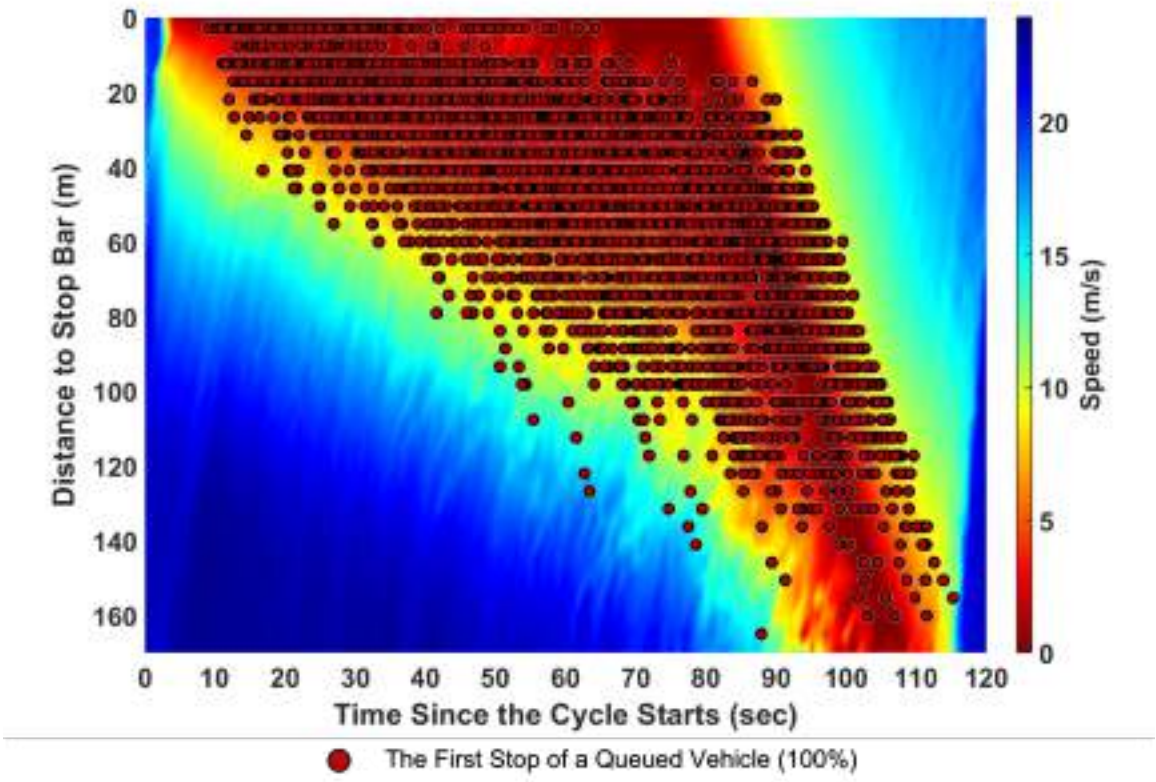

Figure 4.5 The Macroscopic Shockwave based on the Speed Distribution with the First Stop of the Queued Vehicles (100%)

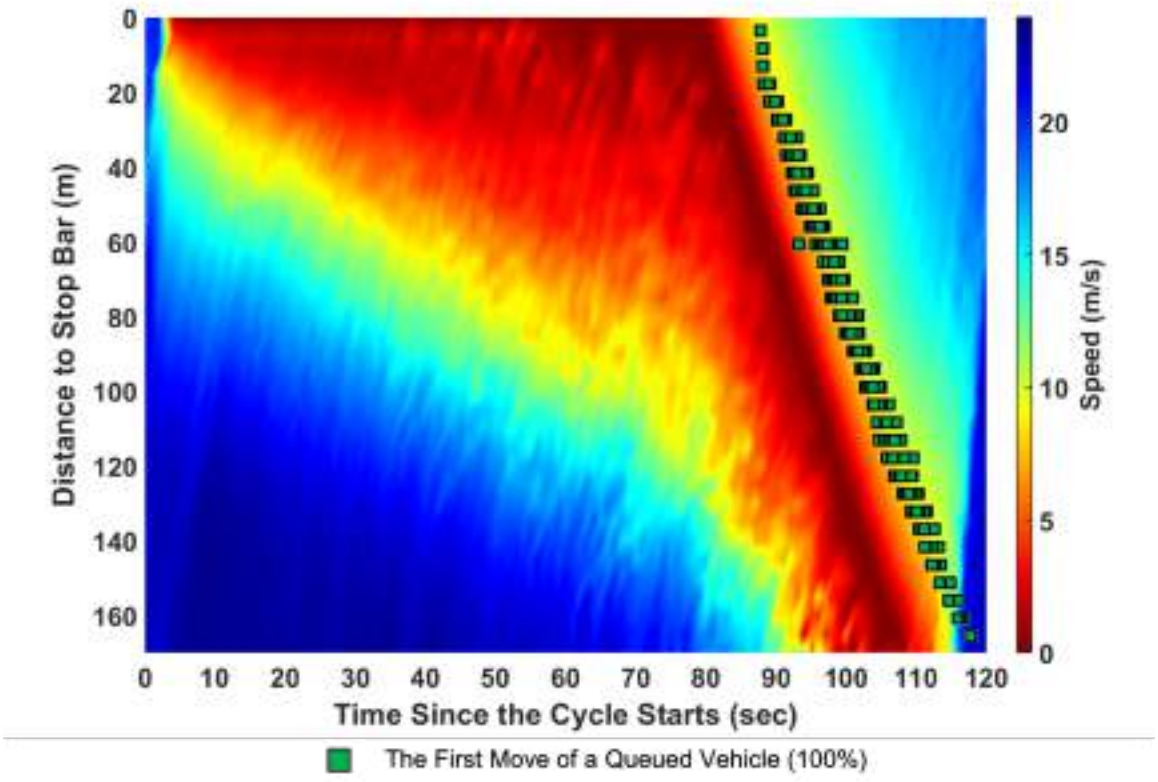

Figure 4.6 The Macroscopic Shockwave based on the Speed Distribution with the First Move of the Queued Vehicles (100%)

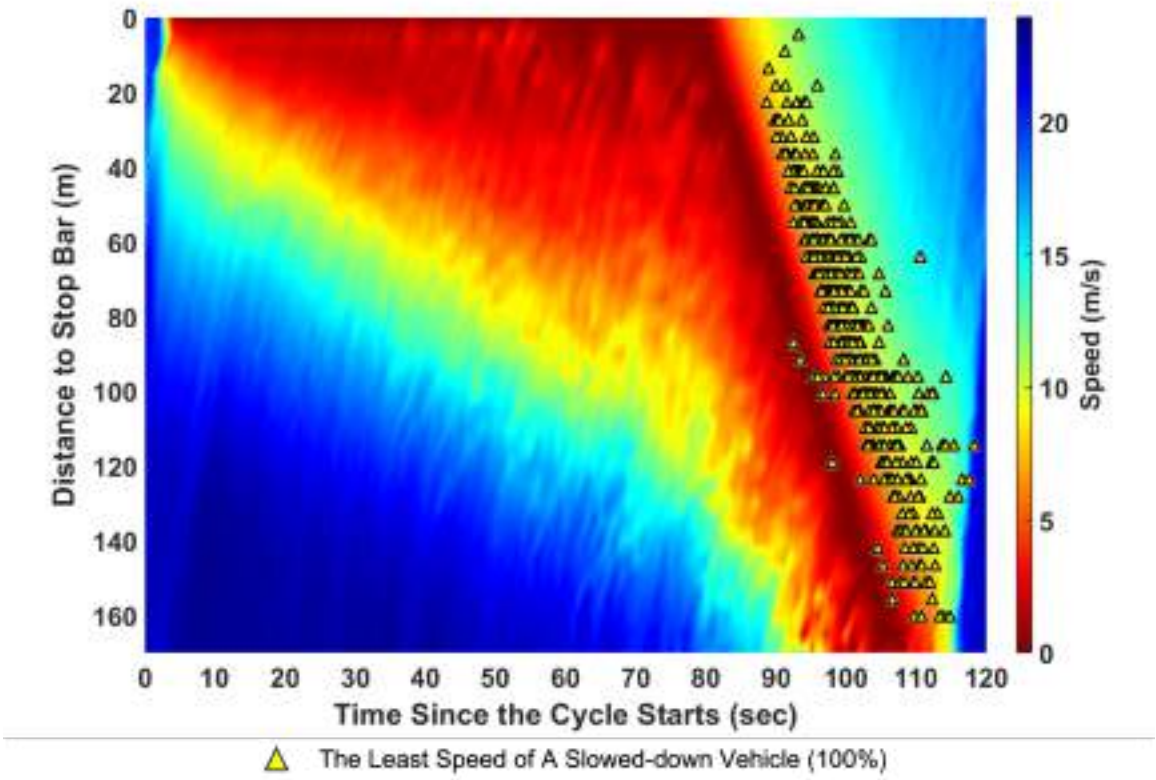

Figure 4.7 The Macroscopic Shockwave based on the Speed Distribution with the Least Speed of the Slowed-down Vehicles (100%)

By looking at Figures 4.8 to 4.10, the same finding from Figures 4.5 to 4.7 can be observed. The only difference is the intensity of red, green, and yellow points due to the lower number of vehicles as a result of selecting a random sample of 10%. This enhances the assumptions the sampled vehicles are able to capture the shockwave characteristics.

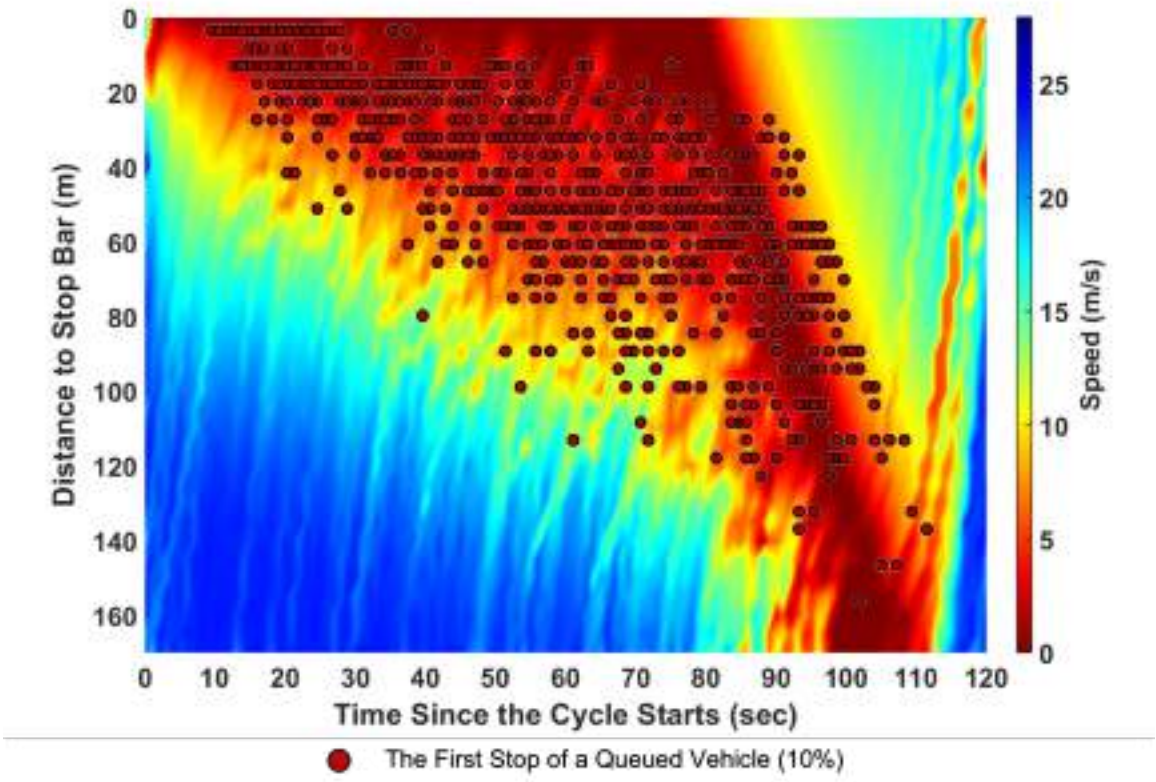

Figure 4.8 The Macroscopic Shockwave based on the Speed Distribution with the First Stop of the Queued Vehicles (10%)

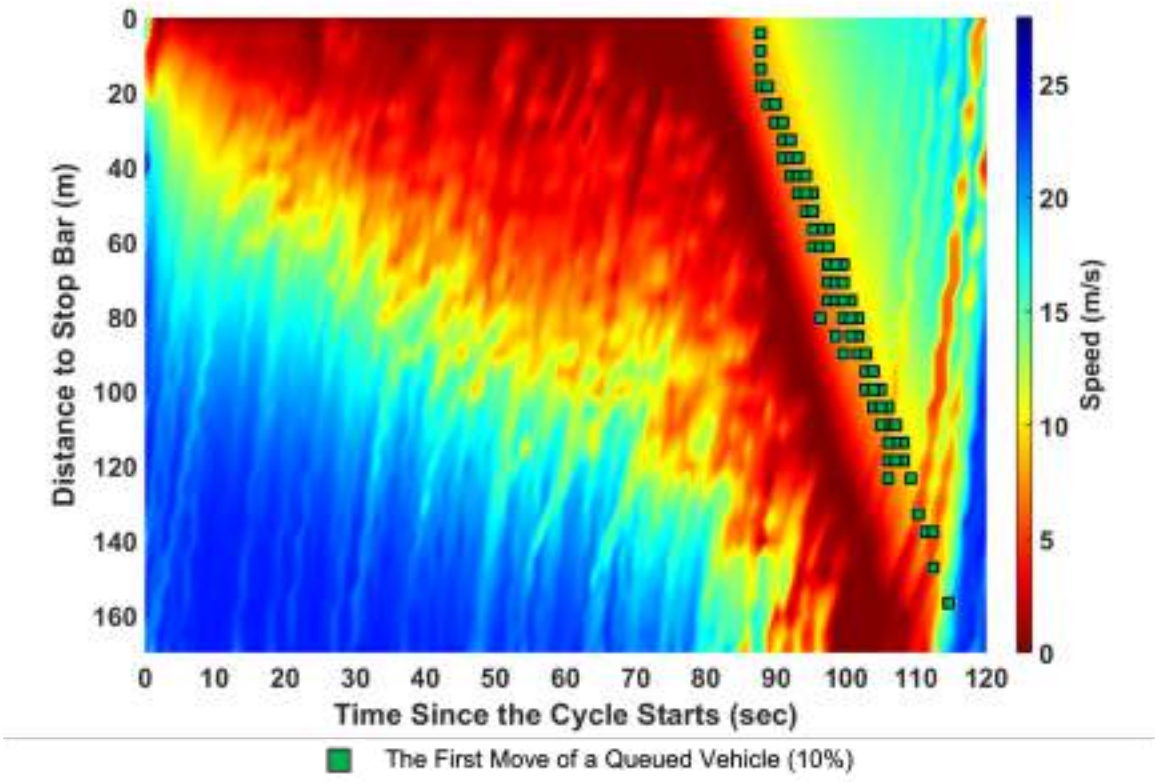

Figure 4.9 The Macroscopic Shockwave based on the Speed Distribution with the First Move of the Queued Vehicles (10%)

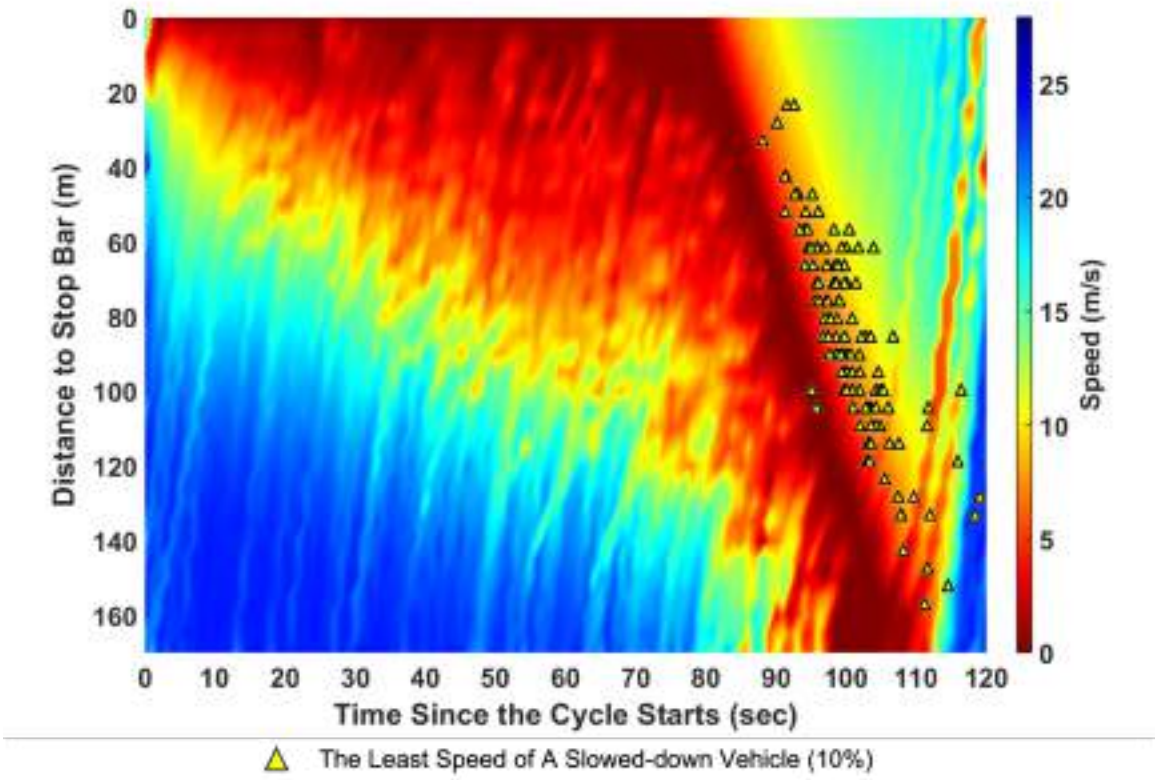

Figure 4.10 The Macroscopic Shockwave based on the Speed Distribution with the Least Speed of the Slowed-down Vehicles (10%)

To enhance the findings from Figures 4.6, 4.7, 4.9, and 4.10 about the relationship between the queued vehicles and the slowed-down vehicles based on the shockwave dissipation, the regressions of vehicle time and position are plotted in Figures 4.11 and 4,12. By looking at Figure 4.11, the linear regression of the departure of the queued vehicles represents the shockwave dissipation speed (slope) with a very high R-squared value of 0.99. The linear regression from the last queued vehicles shaped a similar slope with a relatively high R-squared value of 0.76. Figure 4.11 was plotted using the entire data (100%). The same findings are illustrated by Figure 4.12 based on the sampled trajectory data (10%).

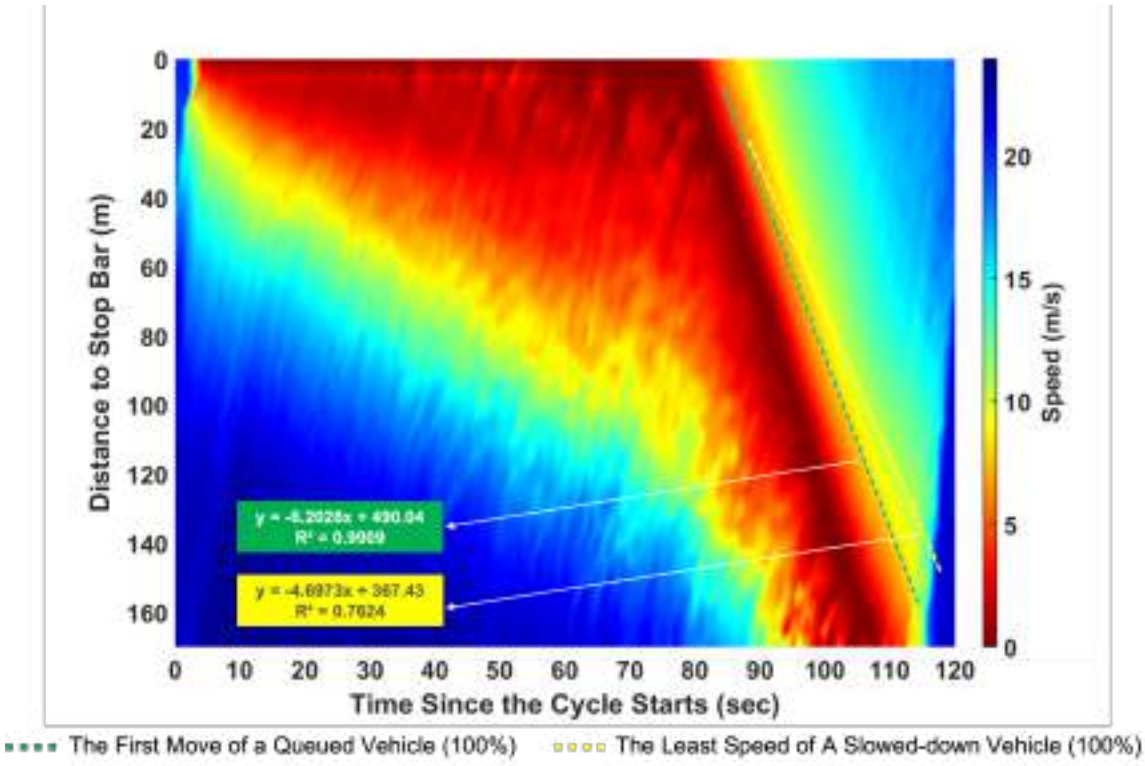

Figure 4.11 The Regression of the Departure of the Queued Vehicles and the Slowed-down Vehicles (100%)

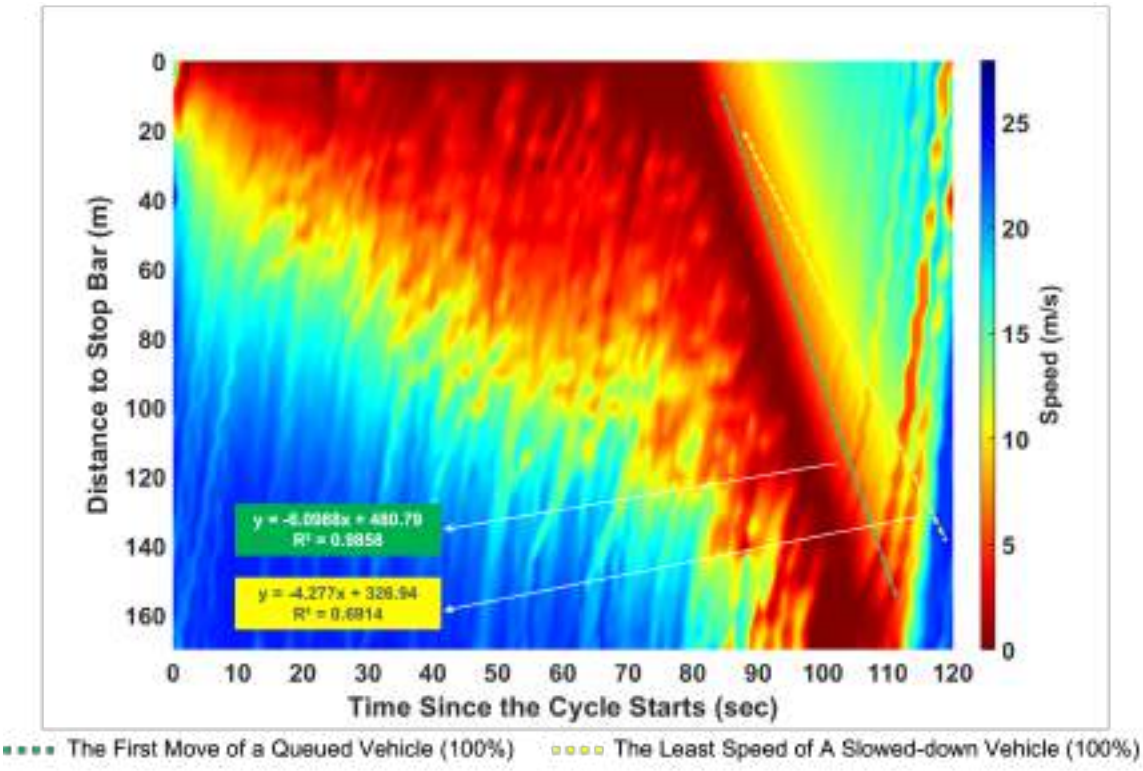

Figure 4.12 The Regression of the Departure of the Queued Vehicles and the Slowed-down Vehicles (10%)

Identifying the moment when a slowed-down vehicle joins the moving queue (the capacity state) is related to the vehicle's speed and acceleration behavior. Since the general behavior of queued vehicles at the capacity state is governed by the acceleration activity to increase the speed after stopping, a slowed-down vehicle decelerates from free-flow speed until joining the moving queue when it starts to accelerate as other queued vehicles in the capacity state. Figure 4.13 illustrates the trajectory data of a typical cycle with queued vehicles, slowed-down vehicles, and a passing vehicle (free-flow speed).

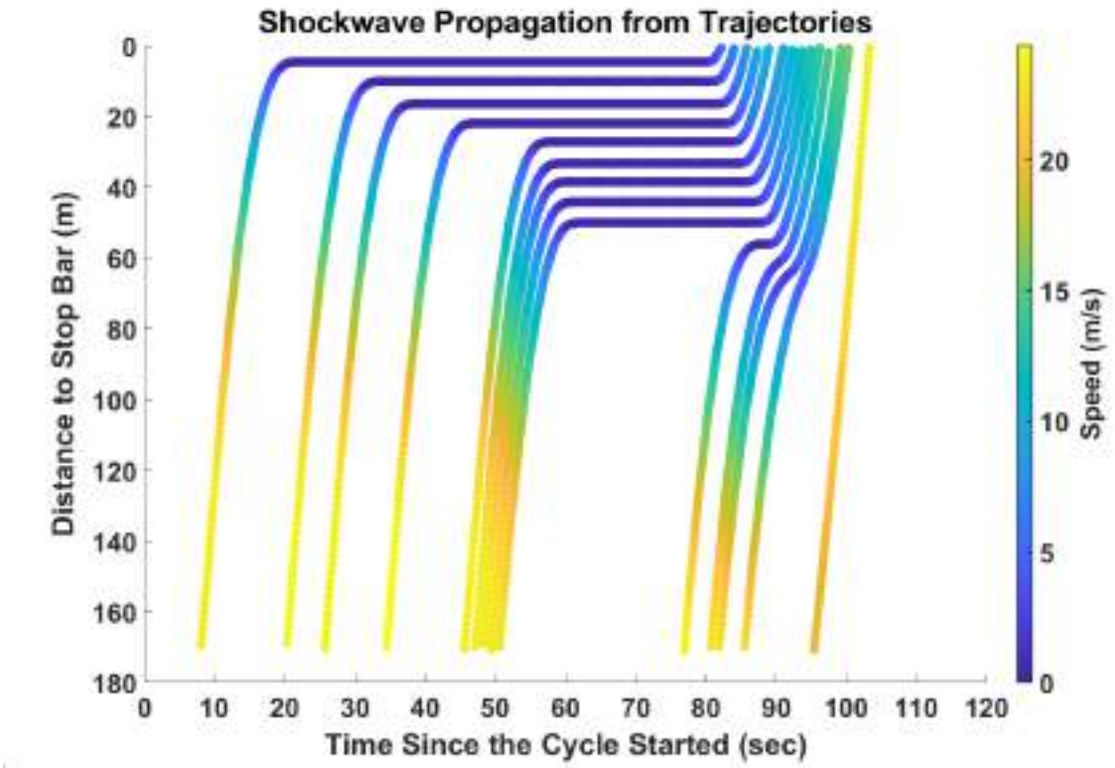

Figure 4.13 The Shockwave Based with Speed on the Time-Space Diagram of One Cycle

The lowest speed of the slowed-down vehicles exists nearby the moving queue before they started to accelerate and increase the speed. Figures 4.14 and 4.15 display the lowest speed of the slowed-down vehicles (SD) in relation to the last queued vehicle in terms of time and distance, respectively. In this example, the lowest speed of all the three slowed-down vehicles happened when the joined the moving queue (in the capacity state) before they started to increase the speed. It is also clear that there is a spatiotemporal proximity between the slowed-down vehicles and last queued vehicle as shown in Figure 4.14 in terms of time proximity and Figure 4.15 in terms of space proximity.

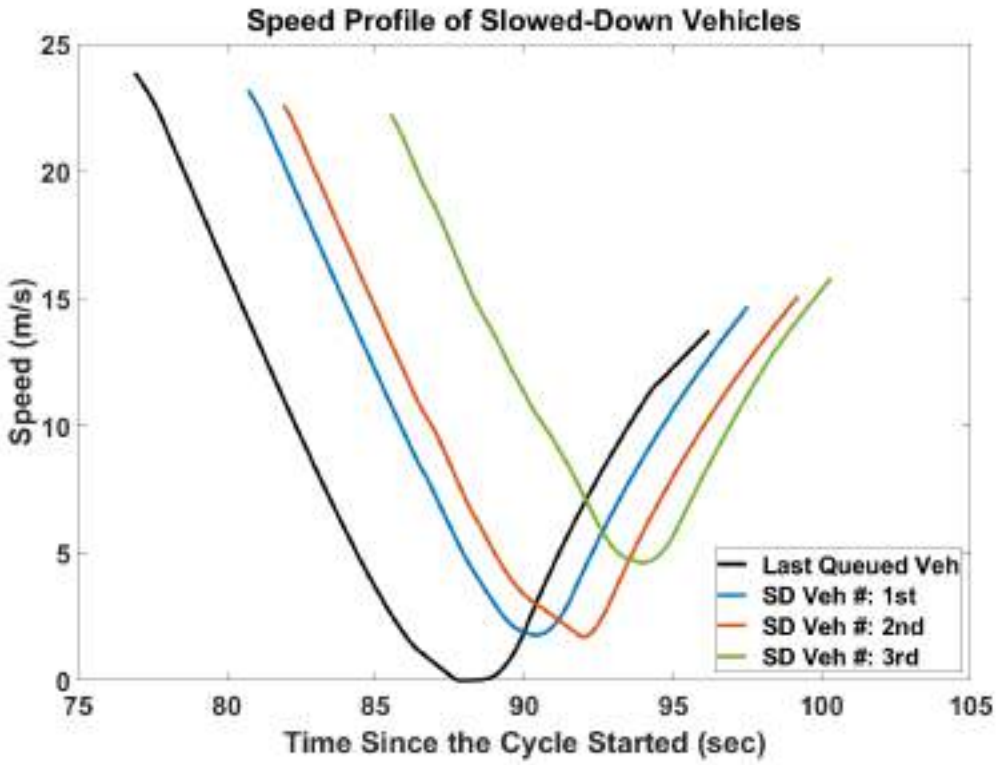

Figure 4.14 The Speed of the Slowed-down Vehicles with Time Joining the Moving Queue

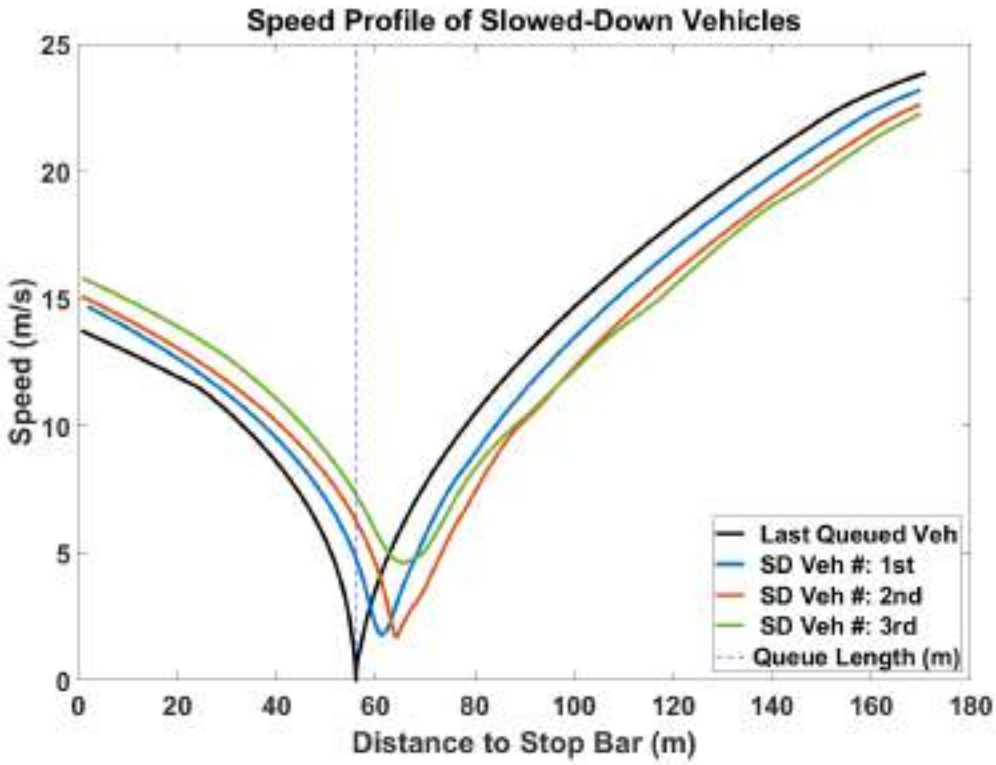

Figure 4.15 The Speed of the Slowed-down Vehicles with Distance Joining the Moving Queue

4.3. Queued Vehicle Characteristics during Shockwave Dissipation

There is no expected relationship between the arrival time of the queued vehicles and their speed at the stop bar. The disassociation is related to the inconsistent arriving pattern of vehicles to the signalized intersection. As Figure 4.16 shows, the time of joining the queue by the vehicles and their speed at the stop bar illustrates scattered points along the X and Y axis. On the other hand, there is an expected relationship between the departure time of the queued vehicles and their speed at the stop bar. The

correlation is based on the expected queue dissipation pattern when the traffic signal is green. By looking at Figure 4.17, the departure time of the queued vehicles and their speed at the stop bar indicates a logarithmic pattern along the X and Y axis. The same logarithmic pattern is expected from the relation between the position of the queued vehicles and their speed at the stop bar. Figure 4.18 plots the position of the queued vehicles and their speed at the stop bar, which indicates almost an identical pattern that was found in Figure 4.17. This is justified by the high correlation between the queue position and the departure time of the queued vehicles.

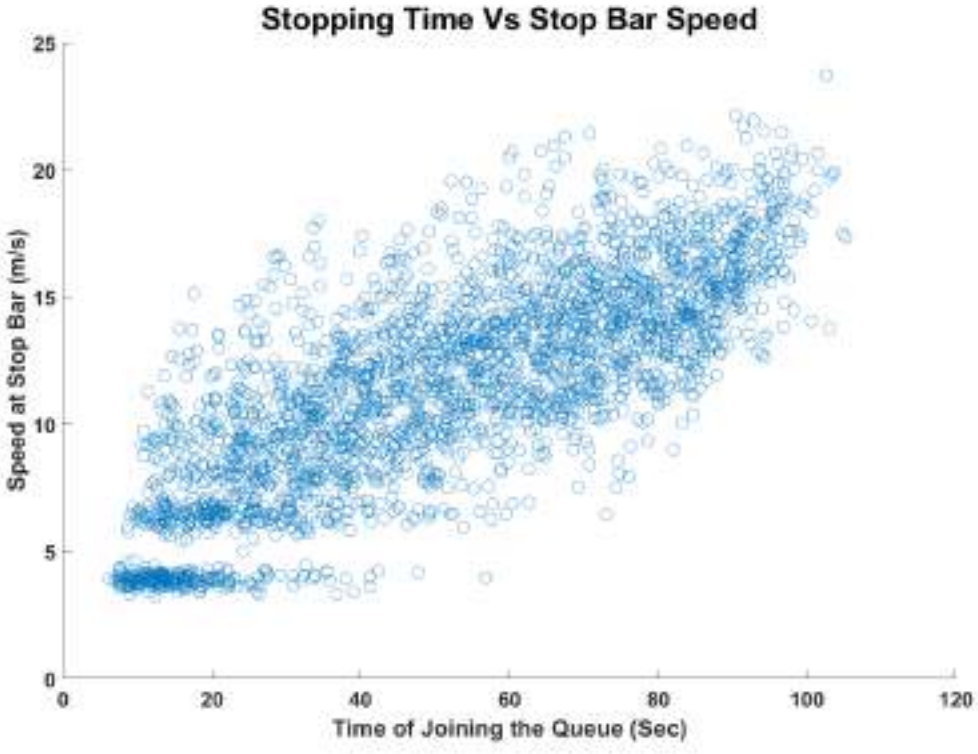

Figure 4.16 The Time of the First Stop of the Queued Vehicles and the Speed at the Stop Bar

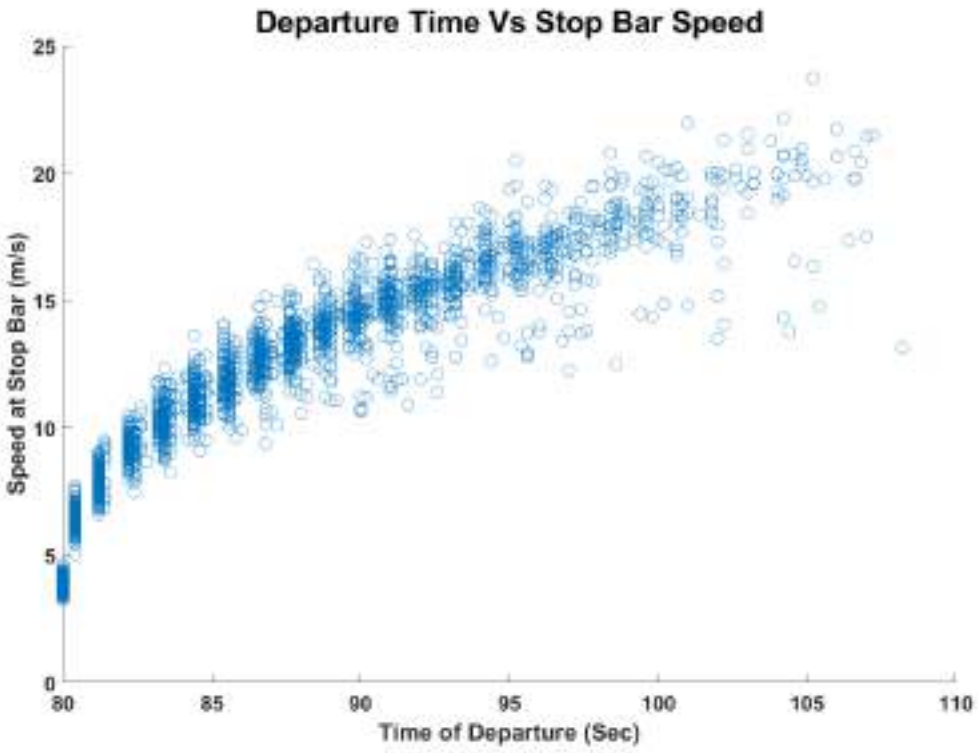

Figure 4.17 The Time of the First Move of the Queued Vehicles and the Speed at the Stop Bar

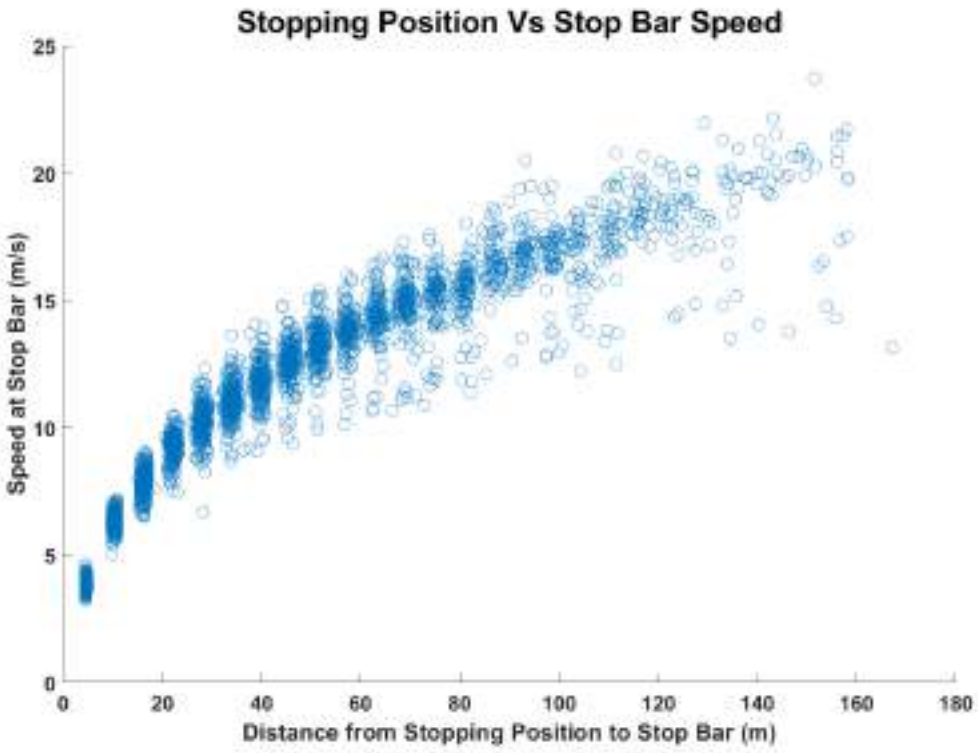

Figure 4.18 The Stopping Position of the Queued Vehicles and the Speed at the Stop Bar

Based on Figure 4.17 and 4.18, the stopping position, the departure time, and the speed at the stop bar have a clear relationship. Therefore, Figure 4.19 is plotted to explore the relationship between the stopping position, the departure time, and the speed at the stop bar in one graph. By looking at Figure 4.19, the three variables are highly correlated due to the nature of queue dissipation process, as mentioned earlier.

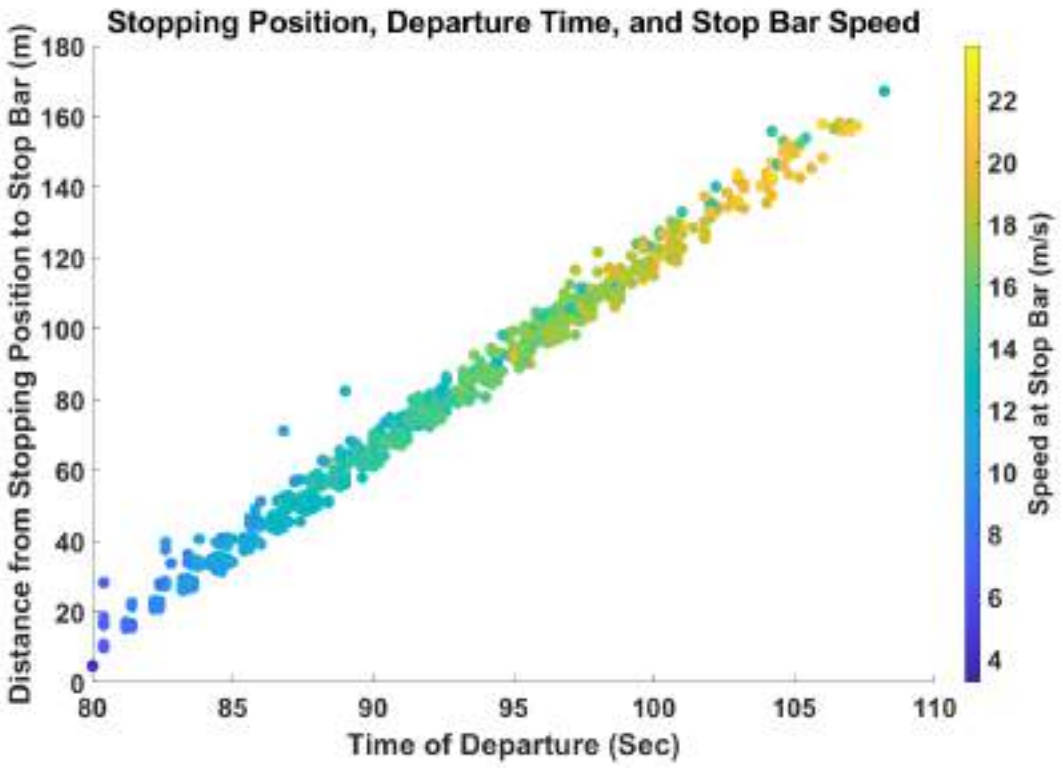

Figure 4.19 The Relationship between Stopping Position, Departure Time, and the Speed at the Stop Bar

4.4. Slowed-down Vehicle Interactions with Queue Length and Traffic Volume

The least speed of the slowed-down vehicles is considered in this work as the moment of joining the moving queue and the key of estimating the traffic volume. Figures 4.20 to 4.23 explore the relationship of the slowed-down vehicle characteristics int terms of time, distance, and speed with other factors such as queued vehicle speed, queue length, and traffic volume. Figure 4.20 shows the least speed of the slowed-down vehicles on the time-space diagram. The lowest speed (dark blue) aligns with queued

vehicle departure found in Figure 4.19. When shorter queues exist, the least speed of the slowed-down vehicles increase as a result of the faster queue dissipation process. Figure 4.21 shows the speed difference between the slowed-down vehicle and the queued vehicle. The negative speed difference indicates a higher speed of the slowed-down vehicles than the queued vehicle. There are multiple cases of negative speed difference that happened way before the slope of the shockwave dissipation (upper left of the figure), which are treated as outliers.

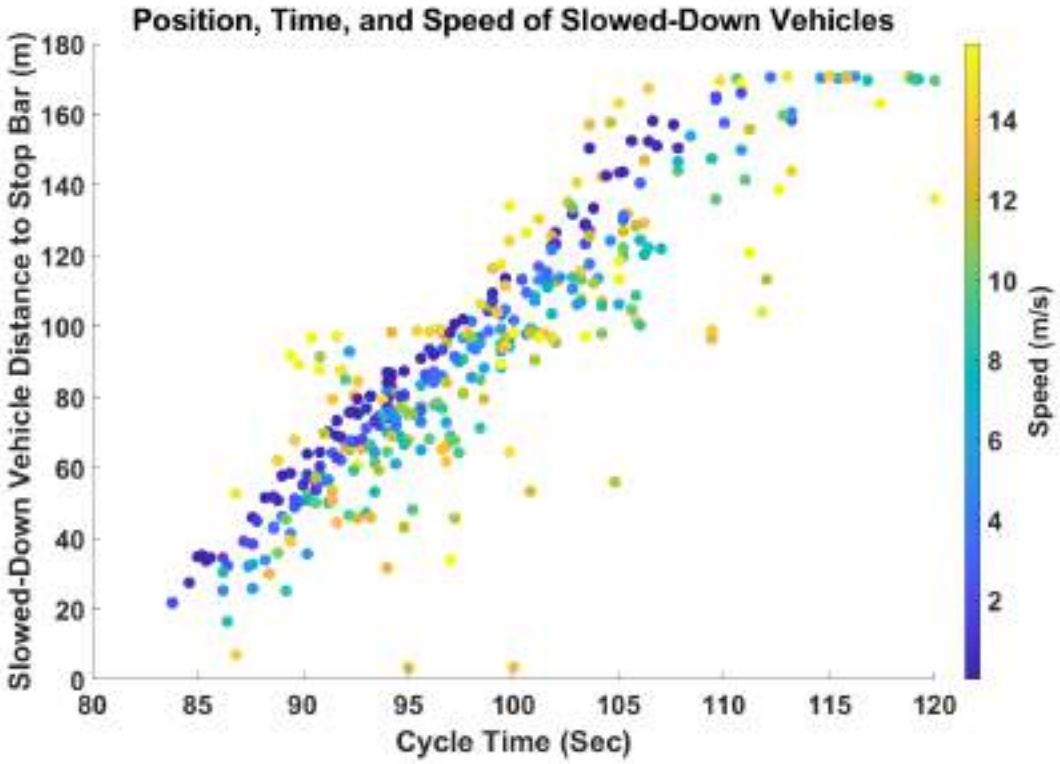

Figure 4.20 The Interactions between the Time, Position, and Least Speed of the Slowed-down Vehicles

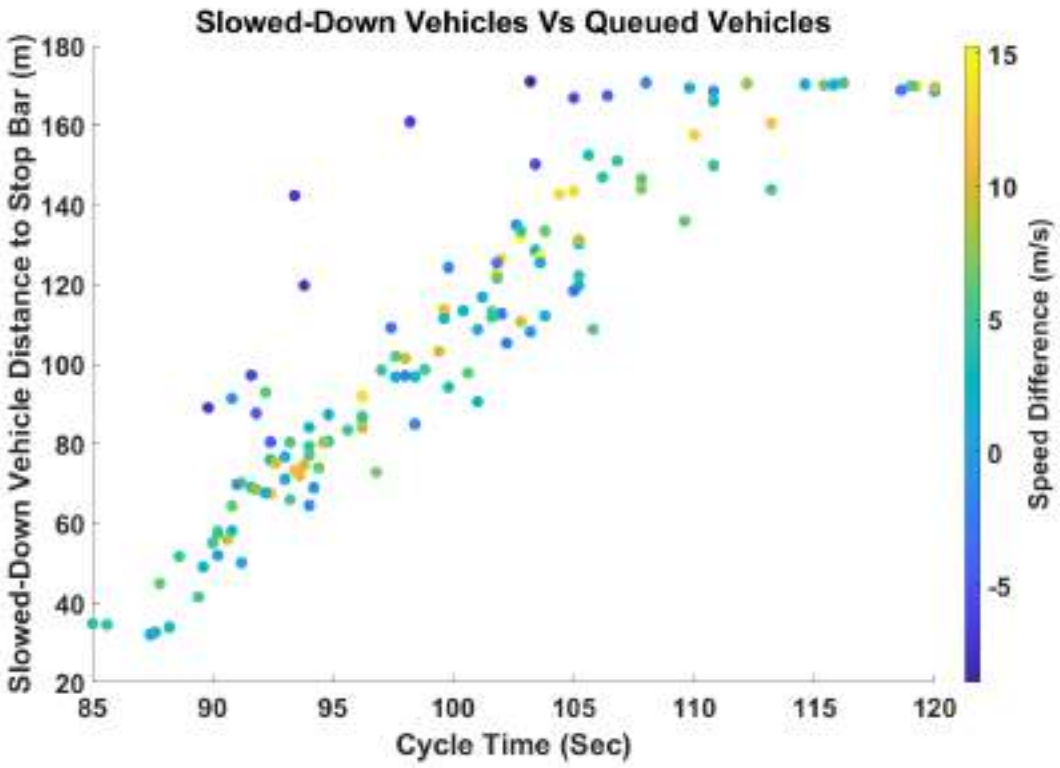

Figure 4.21 The Interactions between the Time, Position, and Speed Difference of the Slowed-down Vehicles and the Last Queued Vehicles

To investigate the relationship between the slowed-down vehicle characteristics and the queue length and traffic volume, Figures 4.22 and 4.23 are plotted, respectively. Figure 4.22 indicates clear effects of the least speed, time, and distance of the slowed-down vehicles on the queue length. The same effect is visible on the traffic volume as shown in Figure 4.23. This is another empirical evidence of the of the relationship between the slowed-down vehicle and the last queued vehicle in identifying the traffic flow characteristics.

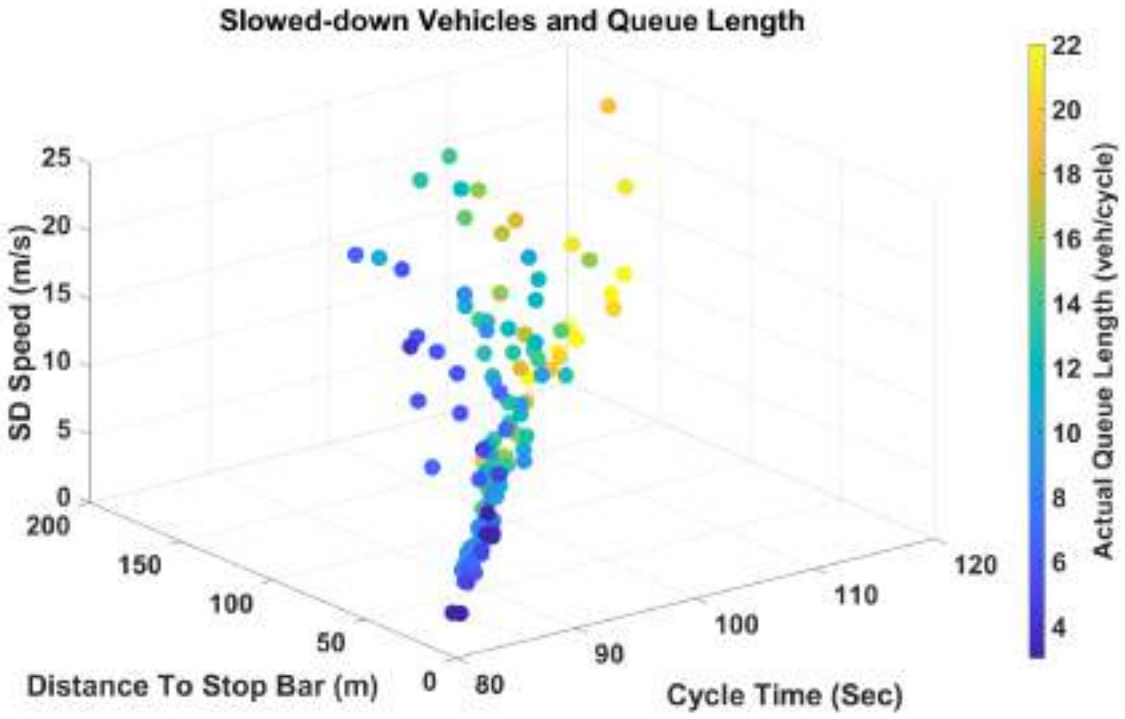

Figure 4.22 The Interactions between the Time, Position, Least Speed of the Slowed-down Vehicles, and the Queue Length

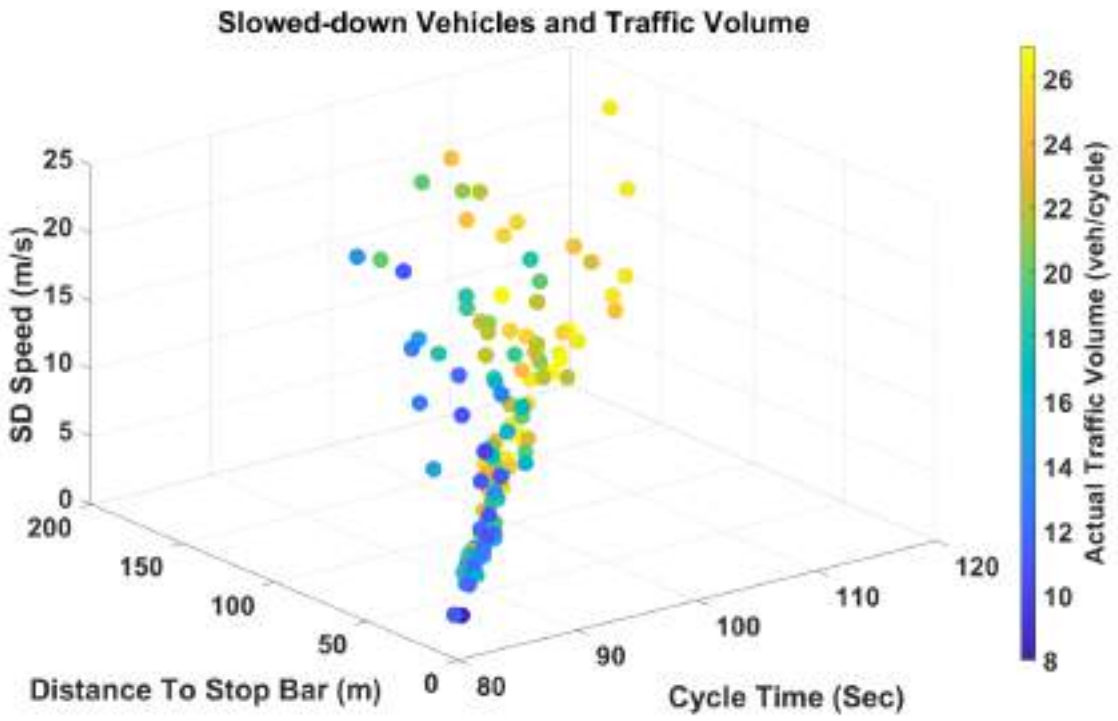

Figure 4.23 The Interactions between the Time, Position, Least Speed of the Slowed-down Vehicles, and the Queue Length

4.5. The Relationship between Queue Length and Traffic Volume

The influence of the slowed-down vehicles on the queue length is justified earlier as there is a relationship with the last queued vehicle. The effect of the slowed-down vehicles on the traffic volume is justified by the high correlation between the queue length and the traffic volume. If a signalized intersection has the same arrival distribution and the same red time, the increase of traffic volume will increase the queue length.

Figure 4.24 plots the queue length and the traffic volume for more than 60 cycles. The figure illustrates a high level of correlation between the two key flow characteristics, which justifies the utilization of the slowed-down vehicles and queue length in estimating the traffic volume as will be described in the following sections.

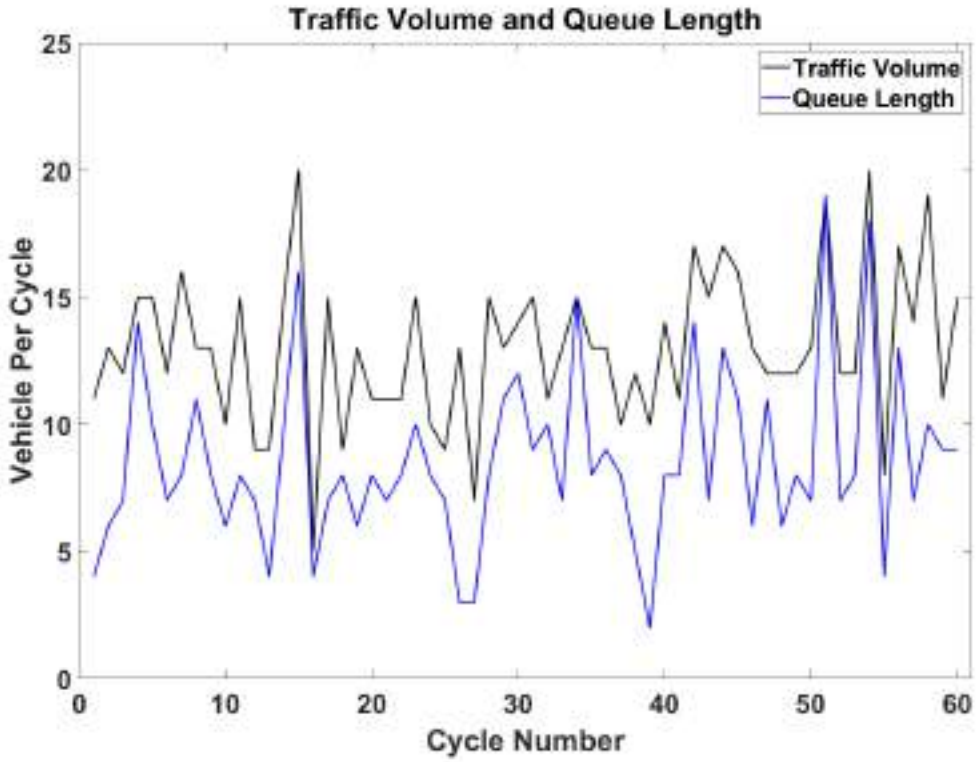

Figure 4.24 The Empirical Relationship between Queue length and Traffic Volume

4.6. Summary of Chapter IV

From the empirical indications discussed in this chapter, the findings of this chapter can be summarized as the following:

- The macroscopic shockwave can be illustrated by the speed distribution based on a sampled trajectory data,

- There is a relationship between the slowed-down vehicles and the last queued vehicles around the dissipation shockwave based on the macroscopic shockwave,
- There is a spatiotemporal proximity between the slowed-down vehicles and the last queued vehicles from the empirical cycle results,
- The departure time and the distance to the stop bar are associated with the speed at the stop bar,
- The speed of the queued vehicles at the stop bar increase with the increase of the green time,
- The least speed of the slowed-down vehicles is correlated with the green time and distance,
- The least speed of the slowed-down vehicles is associated with the queue length and the traffic volume,
- At the same signalized intersection, there is a correlation between the queue length and the traffic volume.

CHAPTER V: THE ESTIMATION MODELS BASED ON DEEP LEARNING

Utilizing the prior data (at least one day) provides valuable information about the traffic characteristics during different patterns at the signalized intersection. This dataset is a sample of the traffic flow at the site of interest, and the percentage of the sampled vehicles is based on the market penetration rate. The major training models that lead to the queue length estimation are:

- Speed at the stop bar,
- Speed at the capacity state, and
- Queue position.

The traffic volume is calculated based on the flow rate during the red time. With the increase of each time interval, the speed at the stop bar in the capacity state area increases due to the queue departure process. With the fact that the time headway at the stop bar decreases with the increase of green time, the traffic flow and the speed of vehicles increase with time as well. Flow has an inverse relationship with the headway and a direct relationship with speed and density as the following:

$$q_i = \frac{n_i}{t_i} = \frac{n_i}{\sum_1^{n_i} h_i} = \frac{1}{h_\sigma} = v_\sigma \times k_\sigma \quad (5.1)$$

Therefore, the increase of speed at the stop bar with time can be utilized as the maximum limit of the speed of queued vehicles and, eventually, can be integrated in the queue estimation algorithm as will be described in the following sections.

Assuming a uniform acceleration behavior, the speed of the queued vehicle at the stop bar indicates its stopping position. Based on the relationship between speed, distance, and time, the stopping position of the queued vehicle can be obtained as the following:

$$p_{QV} = v_{SB} \times t_m \tag{5.2}$$

Also, the time since the first move and the speed at the capacity state indicates the stopping position of the queued vehicle:

$$p_{QV} = v_{QV} \times t_m \tag{5.3}$$

The time since the first move of the queued vehicle is related to the vehicle sequence at the queue and the time since the green time started:

$$t_m = t_G - t_i \tag{5.4}$$

The queue position is the sum of the moving distance from the stopping position and the distance to the stop bar:

$$p_{QV} = d_m + d_{SB} \quad (5.5)$$

In fact, the speed of the queued vehicle since its first move can indicate its stopping position:

$$v_{QV} = \frac{d_m}{t_m} \quad (5.6)$$

5.1.1. Speed at the Stop Bar

The stop bar represents the limit of the capacity state (Case C) as appears in Figure 4. The speed of the queued vehicles at the stop bar can be estimated based on the green time by relying on the training dataset and deep learning techniques as the following:

$$v_{SB} = f(t_G) \quad (5.7)$$

5.1.2. Speed Distribution at the Capacity State

If the acceleration of vehicles and the sequence of moving are constant, the speed at each combination of time and distance is constant too. This means the speed distribution at the capacity state is a function of time and distance, which can be represented in term of cells as appears in Figure 3.4 The increase of speed is associated with the increase of time and distance. Modeling this relationship is influenced by the

acceleration profile of the individual queued vehicles and their time sequence of moving. Therefore, deep learning is utilized to estimate the speed distribution at the capacity state based on all queued vehicles in the training dataset using the green time and distance to the stop bar as the following:

$$v_{CS} = f(t_G, d_{QV}) \tag{5.8}$$

5.1.3. Identifying Queue Position

Due to the complexity of including different factors such as acceleration and perception-reaction time, modeling the time of the first move based on the queue position can be difficult to achieve. Therefore, deep learning techniques can be utilized to identify the queue position (p_{QV}) based on the green time and speed from the training data as the following:

$$p_{QV} = f(t_G, v_{QV}) \tag{5.9}$$

5.2. The Estimation of Queue Length from Cycle Data

When all models are trained from the prior data, from now on, the slowed-down vehicles in the cyclic data can be implemented in the models to estimate the queue position of the last queued vehicle (queue length).

5.2.1. Speed of the Last Queued Vehicle

The time of the moment the slowed-down vehicle joins the moving queue will be implemented in the training model of the stop bar speed (Equation 5.7):

$$v_{SB} = f(t_{SD}) \tag{5.10}$$

The time and distance of the moment the slowed-down vehicle joins the moving queue will be implemented in the training model of the speed distribution at the capacity state:

$$v_{CS} = f(t_{SD}, d_{SD}) \tag{5.11}$$

The speed of the last queued vehicle needs to be estimated based on stop bar speed and speed at the capacity state (speed distribution). Estimating the speed of the last queued vehicle is described as the following:

$$v_{EQV} = f(v_{SB}, v_{CS}) \tag{5.12}$$

Based on the mentioned speed limits stated in Equations (3.4) and (3.5), the speed of last queued vehicle is a value between the speed distribution and the speed at the stop bar as the following:

$$v_{CS} < v_{EQV} < v_{SB} \tag{5.13}$$

The distance between the slowed-down vehicle and the last queued vehicle is unattainable due to the variation in space headway and the possibility of having other slowed-down vehicles between the consider slowed-down vehicle and the last queued vehicle. Therefore, the estimated speed of the queued vehicle is modeled as the following:

$$v_{EQV} = \frac{v_{CS}+v_{SB}}{2} \tag{5.14}$$

5.2.2. Final Queue Length Model

The time from the slowed-down vehicle and the estimated speed of the last queued vehicle will be implemented in the training model of the queued vehicle position as the following:

$$L_{EQ} = f(t_{SD}, d_{SD}, v_{EQV}) \tag{5.15}$$

5.2.3. Final Traffic Volume Model

As Figure 4.22 showed, there is a high correlation between the queue length and the traffic volume. The relationship between queue length and traffic volume is influenced by the waiting time based on Little's Law. According to Little's Law, the general relationship is described in Equation (3.2). To find the traffic volume, the estimated queue length will be utilized to obtain the traffic flow for the period from the

red time to the time when the slowed-down vehicle joined the dissipating queue. Since the slowed-down vehicle is considered in the traffic flow, one more vehicle is added to the queue length. The traffic flow is calculated as the following:

$$q_E = \frac{L_{EQ}+1}{t_{SD}} \tag{5.16}$$

To compute the traffic volume per cycle, the traffic follow is multiplied by the cycle time as the following:

$$V_E = q_E \times C \tag{5.17}$$

5.3. The Process and Components of the Estimation Algorithms

Figure 5.1 is the flowchart of estimating traffic volume, and it explains the process in terms of data inputs, models, and outputs. The algorithm requires a prior trajectory dataset with the traffic signal information of the intersection (without the need of traffic volume nor queue length information). From the prior dataset, the queued vehicle trajectories will be utilized to obtain three models including speed distribution model, stop bar speed model, and queuing position model by using deep learning technique (ANN). After that, the traffic volume of any future cycle can be estimated through the trajectories of slowed-down vehicles.

Figure 5.1 The Flowchart of the Estimation Algorithm of Queued Vehicles and Traffic Volume

5.4. The Inputs and Output of the Algorithm

As the flowchart in Figure 5.1 shows, the training and testing datasets from the prior data are utilized to find three essential models related to the speed distribution at the capacity state, queuing position of vehicles from speed at the capacity state, and the speed at the stop bar. The speed distribution model relies on the green time and the distance to

the stop bar as inputs. The queuing position model is based on tracking the green time and the speed of each queued vehicle at the capacity state with the stopping position being constant for each vehicle. Table 5.1 summarizes the inputs and outputs of the training models of the speed distribution and the queuing position. For the stop bar speed model, the green time is the only influencing variable that has been used as an input in the model due to the direct relationship between the green time and the speed at the stop bar, which has been demonstrated earlier in the area (Lee & Chen, 1986).

Table 5.1 Training Models from Queued Vehicles

Speed Distribution Model		**Queuing Position Model**	
Input	**Output**	**Input**	**Output**
Green Time (t_G)	Speed (v_{CS})	Green Time (t_G)	Queuing Position (p_{QV})
Distance to Stop Bar (d_{QV})		Speed (v_{QV})	

The slowed-down vehicle trajectories from the real-time cycle data will be implemented in the three models. From the cycle data, the least speed of the slowed-down vehicle and its corresponding green time and distance to stop bar will be used to estimate the speed of the queued vehicle (v_{EQV}) as per Equation (5.14). The estimated value of v_{EQV} is then implemented in the queuing position model to estimate the queue length. The validation model based on the slowed-down vehicles is summarized in Table 5.2.

Table 5.2 Validation Models Using Slowed-down Vehicles

Validation (Speed Distribution)		**Validation (Estimated Queue Length)**	
Input	**Output**	**Input**	**Output**
Green Time (t_{SD})	Speed (v_{CS})	Green Time (t_{SD})	Queue Length (L_{EQ})
Distance to Stop Bar (d_{SD})		Distance to Stop Bar (d_{SD})	
		Estimated Speed (v_{EQV})	

The estimated queue length is the key in the finding the flow rate that eventually leads to the traffic volume of the cycle as described in Equation (5.17).

5.5. Deep Learning Technique for the Estimation Models

Estimating a continuous output variable such as speed and stopping position can be done through different types of deep leaning models. However, MLP, a type of ANN, is suitable for estimation purposes rather than interpretation purposes. MLP is known as a provider of an efficient representation of the characteristics of the data with high accuracy and reasonable development time. The MLP was applied using the machine learning software WEKA. The appendix includes information about the software and the used MLP package.

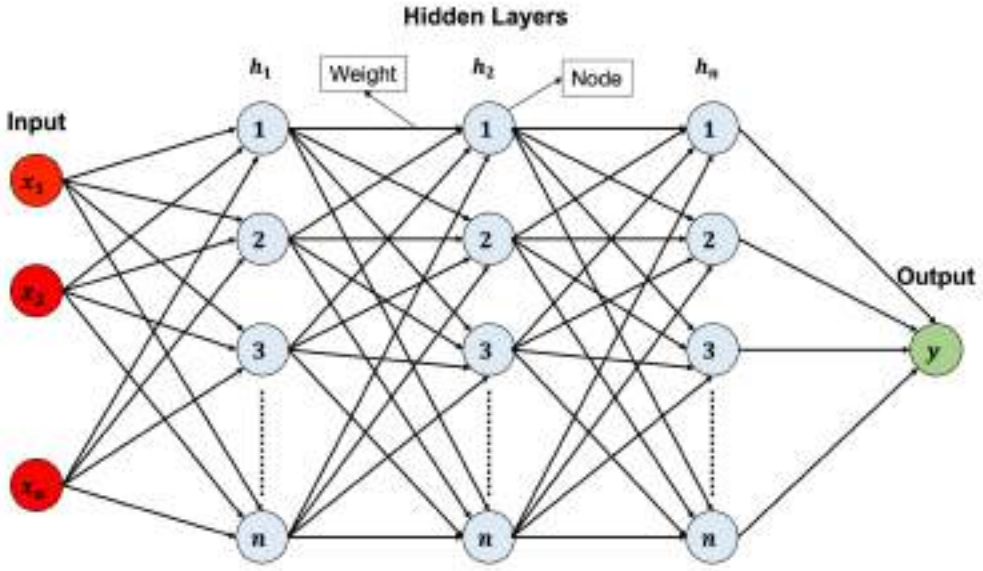

Figure 5.2 The General Structure of ANN with Inputs, Outputs, and Hidden Layers

Figure 5.2 illustrates the general structure of ANN where (x) represents the selected inputs and (y) represents the output based on the estimation model. The structure of MLP relies on (x) as the main inputs of the model and (y) as the main output (prediction). Between the inputs and the output, there are hidden layers (h) and neurons that can be modified based on the nature of the data. The neurons are linked by connectors with weights (w), which are also modifiable. The final output (y) in the estimation models using MLP is described as the following:

$$y = \sigma(z) = \frac{1}{1+e^{-z}} \tag{5.18}$$

The logistic function is represented by the sigmoid activation function (σ). The variable (z) is based on a non-linear activation function, which aims to create non-linearity into the output of the neurons, and can be described as the following:

$$z = \sum(x \cdot w) + b \tag{5.19}$$

The value (b) a bias that creates an offset to move the entire activation function to the left or right towards output values. The summation of the vectors (x) and (w) is the dot product of the vectors as the following:

$$\sum(x \cdot w) = (x_1 \cdot w_1) + (x_2 \cdot w_2) + \cdots + (x_n \cdot w_n) \tag{5.20}$$

The inputs (x) and outputs (y) are different in each of the three models: speed distribution, speed at the stop bar, and queuing position. The details of inputs and outputs are as described in the previous section.

In most of ANN applications, one and two hidden layers are widely used as there is no theoretical reason for deciding more than two hidden layers. For the number of neurons, researchers have been using multiple rule-of-thumb methods as a start point to determine the optimal number of neurons in the hidden layers by considering the number of inputs and outputs (Ibnu Choldun R et al., 2020; Stathakis, 2009). In this work, the adopted rule-of thumb method is number of hidden neurons to be less than twice the size of the input layer. Therefore, one to three hidden layers have been tested with combinations of different number of neurons. The best combination of hidden layers and hidden neuros for each model was selected based on the accuracy of the testing results.

Figure 5.3 shows the selected structure of the MLP for the last step of finding the queue length.

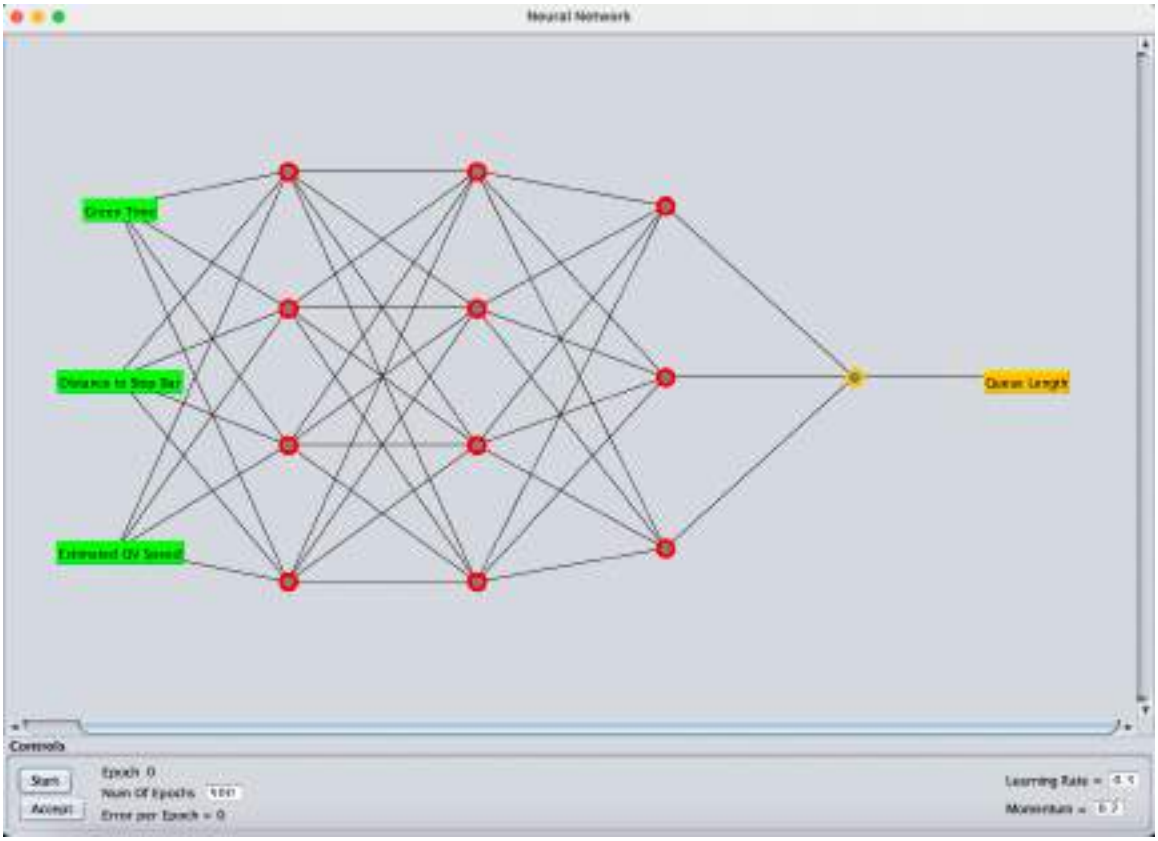

Figure 5.3 The Structure of the adopted MLP Structure with Inputs, Outputs, and Hidden Layers

5.6. Summary of Chapter V

From the methodology discussed in this chapter, the findings of this chapter can be summarized as the following:

- By utilizing deep learning technique, multilayer perceptron (MLP), three models are formed:
    - The speed at the stop bar model based on the green time,

    - The speed distribution model based on the green time and distance to the stop bar,
    - The queue length estimation model based on the green time and the estimated speed of the last queued vehicle.
- The speed of the last queued vehicles is formulated as the average speed between the stop bar and the capacity state
- The traffic volume estimation is based on the traffic flow at the arrival of the slowed-down vehicle by dividing the queue length and one more slowed-vehicle by the time of the least speed vehicle.

CHAPTER VI: THE VALIDATION OF THE ESTIMATION MODELS

The second and third objectives of this dissertation are to propose a queue length model and to develop a traffic volume estimation model. The two developed models in Chapter V needs to be evaluated. The results in this chapter are dedicated to analyzing the performance of the proposed models.

6.1. Experiment Design

To analyze and evaluate the performance of the algorithm, four experiments have been conducted on simulation and real-world data. The first experiment is a simulation-based with the aim of testing the accuracy of the queue length algorithm and the effect of different factors. The second experiment examined the queue length estimation algorithm on real-world data (NGSIM). The third experiment evaluates the traffic volume estimation algorithm on simulation data algorithm and tests the effect of different factors on the estimation accuracy. The fourth experiment examined the traffic volume estimation algorithm on NGSIM data. The experiments in this work assume that the signalized intersection is isolated with a pre-timed signal control and the lane-changing activities are neglected.

6.1.1. Simulation Experiment

The signalized intersection in the simulation has three lanes with middle lane (through) is being studied as it appears in Figure 6.1. The scenarios were implemented in the simulation software package (VISSIM).

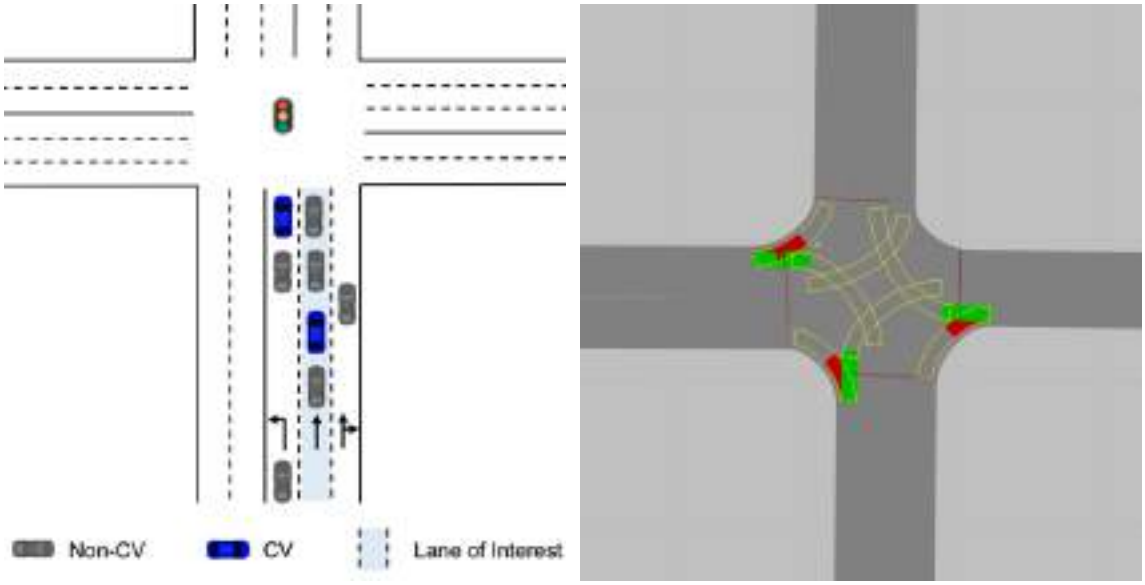

(a) (b)

Figure 6.1 The Conceptual Design of the Site in the Experiments

The traffic signal has 120-sec cycle length, and the through lane has 40-sec green phase. To evaluate the model with different traffic volumes, the traffic flow fluctuates between high, moderate, and low traffic flow. Table 6.1 shows the minimum and maximum traffic flow and queue lengths of the validation dataset at the simulated signalized intersection.

Table 6.1 The Traffic Characteristics of the Site in the Simulation Experiment

	Traffic Flow (Veh/hr/ln)	Traffic Volume (Veh/Cycle/ln)	Queue Length (Veh/Cycle/ln)	Traffic Signal (Sec)	
Min	270	9	4	**Green Time**	40
Max	960	32	19	**Cycle Length**	120

The simulation results created a prior data of a full day from 7:00 AM to 7:00 PM. The samples of 5%, 10%, 15%, 20% have been randomly selected from the trajectories to study different market penetration rate. In most cases in the analysis, market penetration rate of 10% was selected. The data contains cycle time during red and green, distance to stop bar, and speed. The real-time data (cycle data) is another day from 1:00 PM to 1:30 PM and from 4:00 PM to 5:00 PM.

6.1.2. Real-world Experiment

The real-world experiment has been implemented on the through lane in the second signalized intersection of NGSIM data (Atlanta, Georgia) as shown in Figure 6.2. A disadvantage about NGSIM is that the dataset was collected for only 15 minutes in peak period and 15 minutes in off-peak period. In this work, the off-peak data has been utilized as prior dataset to train and test the models, and the peak data has been utilized to validate the algorithm. The major limitation of NGSIM dataset is the short period, especially for data mining and deep learning models. However, several studies have

utilized NGSIM in data mining and deep learning applications (Jazayeri et al., 2021; Jiang et al., 2019; Mercat et al., 2019; Shi et al., 2021).

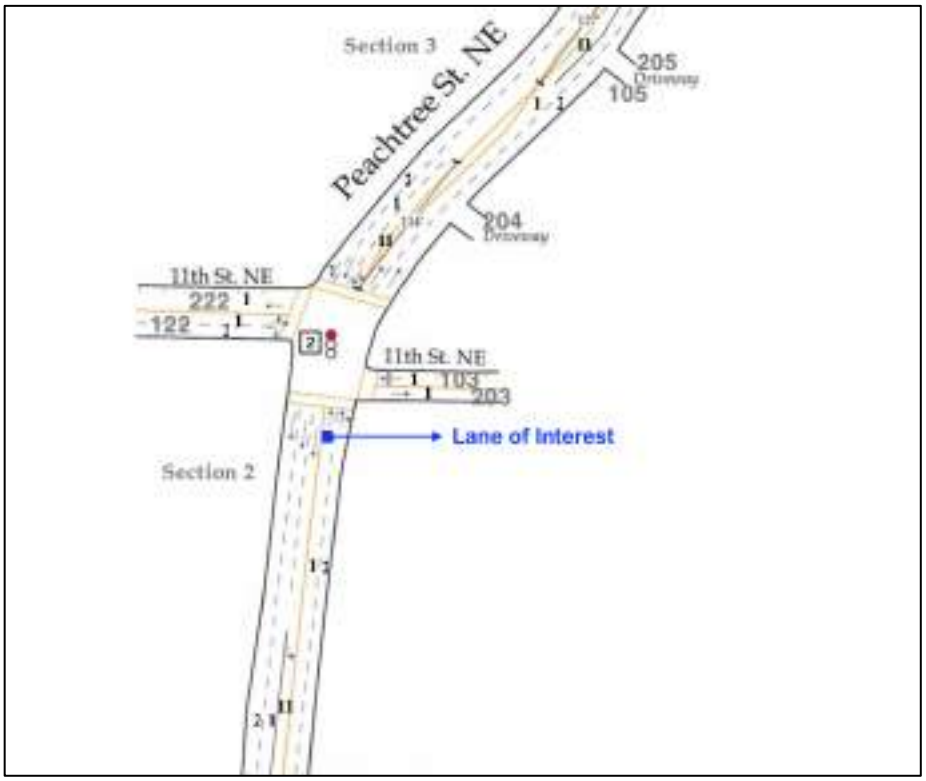

Figure 6.2 The Site Description of the Real-world Experiment (Cambridge Systematics, 2007)

The cycle time during red and green, distance to stop bar, and speed of queued vehicles in the prior dataset (off-peak) has been processed to find the estimation models. The peak data was, firstly, processed to find the traffic volume and queue length of each cycle. Then, the slowed-down trajectories of the real-time dataset (peak) have been implemented in the estimation models. Table 6.2 summarizes the traffic details of the validation dataset in the real-world experiment.

Table 6.2 The Traffic Characteristics of the Real-world Experiment

	Traffic Volume (Veh/Cycle/ln)	**Queue Length (Veh/Cycle/ln)**	**Traffic Signal (Sec)**	
Min	4	2	**Green Time**	32
Max	14	7	**Cycle Length**	100

6.2. Measure of Effectiveness

The evaluation of performance requires a comparison between the ground truth and the predicted value. The Mean Absolute Percentage Error (MAPE) calculates the percentage of error by comparing the actual value with the estimated value to observe the variation in traffic volume. In this paper, MAPE will be used as the performance evaluation measurement, and it can be calculated as the following:

$$MAPE = \frac{1}{n}\sum_{t=1}^{n}\left|\frac{A_t - E_t}{A_t}\right| \quad (6.1)$$

Where: n is number of times the summation iteration, A_t is actual value, and E_t is estimated value.

6.3. The Performance of Queue Length Estimation Model

The performance of the queue length estimation model is evaluated based on the measure of effectiveness (MAPE) to assess the accuracy of the algorithm for simulation data and real-world data.

6.3.1. Queue Length Estimation Analysis of the Simulation Experiment

The results of the simulation of 33 cycles during peak and off-peak (1:00 PM to 1:30 PM and 4:00 PM to 5:00 PM) is shown in the following table. The accuracy of the model during the 33 cycles was 86.53% as MAPE was 13.44%. The results are based on (10%) penetration rate. The results in the table indicate some cases of overestimation and underestimation. To have a deeper look at the results, Figure 6.3 is also plotted with traffic volume, actual queue length, and estimated queue length.

Table 6.3 The Results of the Queue Length Estimation Model for Simulation Data

Cycle	Traffic Volume (Veh/ln/Cycle)	Queue Length (Veh/ln/Cycle)	Estimation (Veh/ln/Cycle)	APE(%)
1	24	11	9.9	9.18%
2	12	5	4.1	17.82%
3	26	16	15.1	6.08%
4	27	18	16.1	10.46%
5	22	10	8.5	14.85%
6	25	15	13.2	12.19%

7	23	11	10.0	8.89%
8	19	7	6.6	6.25%
9	16	5	5.2	4.52%
10	20	10	10.1	0.12%
11	12	5	4.3	14.79%
12	18	7	6.4	8.61%
13	17	8	7.2	9.88%
14	26	14	12.7	9.58%
15	25	12	11.0	8.13%
16	23	12	10.9	9.37%
17	24	11	9.8	11.26%
18	7	3	2.4	18.11%
19	20	9	7.9	11.40%
20	15	6	7.4	22.56%
21	18	8	9.1	13.14%
22	13	3	3.6	20.79%
23	16	6	7.8	29.84%
24	22	10	11.8	17.80%
25	13	4	4.9	22.75%
26	18	9	12.8	42.50%
27	26	13	13.9	7.01%
28	11	5	5.5	9.69%
29	21	11	12.0	9.20%
30	11	5	5.1	1.38%
31	12	4	5.2	29.55%
32	12	5	5.9	17.97%
33	18	6	6.5	7.96%
Min APE				**0.12%**
Max APE				**42.50%**
STD				**8.74%**

MAPE	13.44%

From Figure 6.3, the estimation algorithm demonstrated an excellent performance as it followed the fluctuation of the traffic length along different cycles. As the figure shows, there are more overestimations than underestimations by the algorithm. The overestimation seems to be associated with the longer queues. This might be because the higher probability of having more slowed-down vehicles in front of the utilized slowed-down vehicle when the queue is longer. This raises a question about the effect of different variables in the performance of the algorithm. Also, it urges the investigation of which slowed-down vehicle to use when there are two slowed-down vehicles in one cycle. To answer those questions, the section of The Effective Factors in the Queue Length Estimation Model is included to investigate the relationship between the performance of the model and green time, distance to stop bar, speed of the slowed-down vehicle, and the sequence of the used vehicle among the slowed-down vehicle in the cycle.

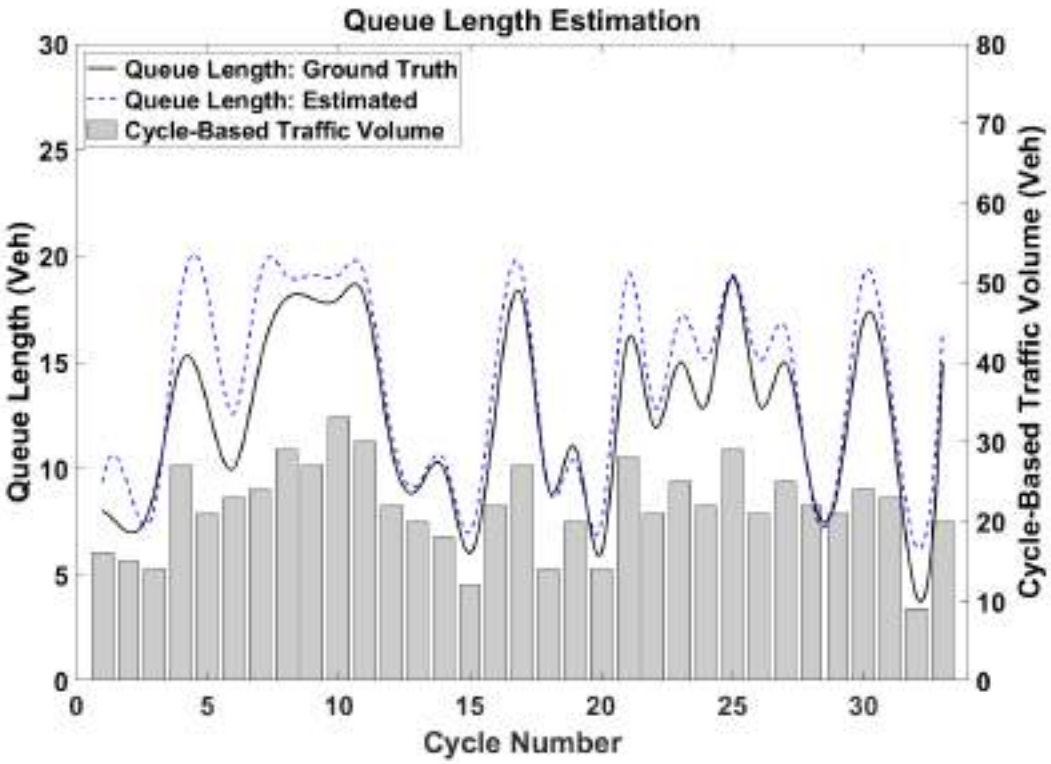

Figure 6.3 Th Performance of the Queue Length Estimation Model in the Simulation Experiment

6.3.2. Queue Length Analysis of the Real-world Experiment

Due to the limited amount of data in the validation data (only 15 minutes), one slowed-down vehicle was randomly selected for each cycle. NGSIM data has nine cycles during the 15-minute dataset where seven of them had slowed-down vehicles. The results of the algorithm demonstrated an MAPE of 21.97%, which means an accuracy of 78.03%. The following table summarizes the performance of the algorithm.

Table 6.4 The Results of the Queue Length Estimation Model for Real-world Data

Cycle	Traffic Volume (Veh/ln/Cycle)	Queue Length (Veh/ln/Cycle)	Estimation (Veh/ln/Cycle)	APE (%)
1	7	2	2.1	33.68%
2	9	2	2.5	11.27%
3	3	3	2.6	8.66%
4	5	3	3.1	4.42%
5	5	4	1.4	60.10%
6	9	4	3.8	5.42%
7	14	7	4.3	30.24%
Min APE				**4.42%**
Max APE				**60.10%**
STD				**20.54%**
MAPE				**21.97%**

To visualize the performance of the algorithm across the cycles, Figure 6.4 shows the estimated and actual queue lengths along with the traffic volume. There is one significant underestimation in cycle 5 with 60.1% MAPE. After investigating the data, it was found that the stopping position of the last queued vehicle had been changing before it started the acceleration process. In other words, the last queued vehicle kept an extremely long distance with the leading vehicle before it reduced the gap when the traffic signal turned green. This significant underestimation influenced the final MAPE of the algorithm, and if it was replaced with the second higher APE (33.68%), the MAPE would be 17.86%. The short period of training data (only 15 minutes) can be an effective factor in increasing the MAPE as it limits learning all the traffic patterns. Larger training dataset is expected to lower the MAPE and increase the accuracy of the algorithm.

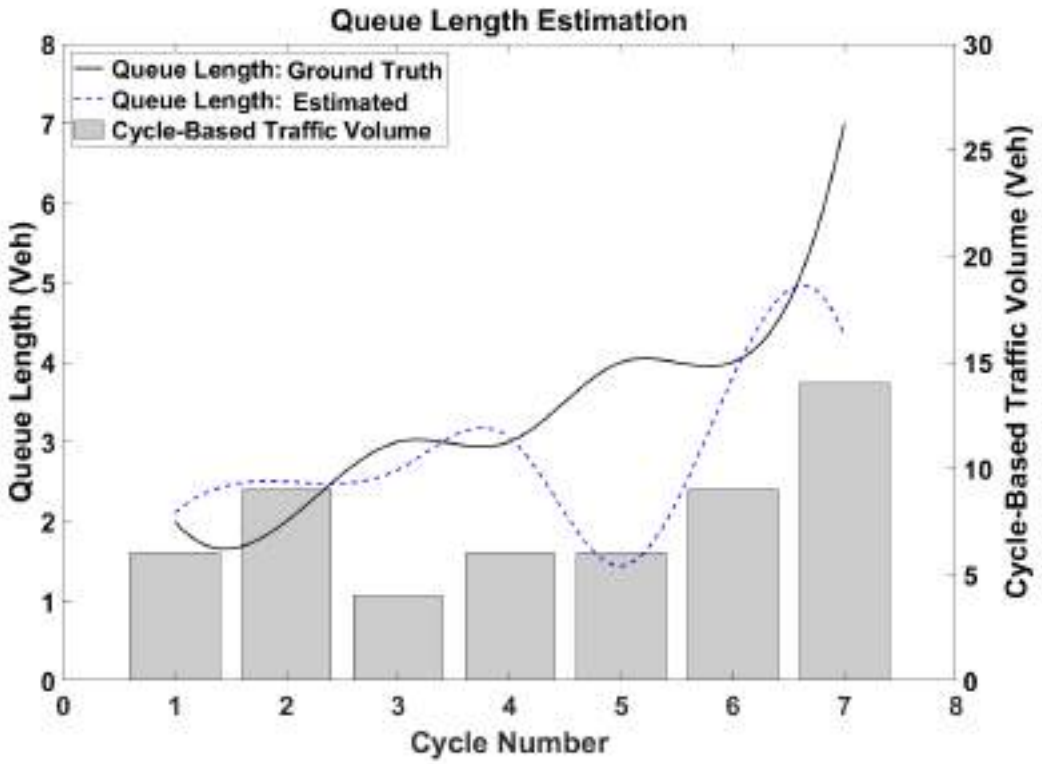

Figure 6.4 Th Performance of the Queue Length Estimation Model in the Real-world Experiment

6.3.3. The Effective Factors in the Queue Length Estimation Model

To instigate the effective factors in the queue length estimation model, the MAPE was plotted against different inputs. In this investigation, the simulation data has been utilized as it provides higher sample data.

By looking at Figures 6.5 to 6.8, there seems to be a correlation between the queue length and MAPE of the algorithm. In other words, the accuracy of the model increases with the increase of the queue length. This might be because the longer queue provides higher probability of the slowed-down vehicle to be closer to the last queued

vehicle. This is enhanced by Figures 6.5 and 6.6 where higher green time and longer distance from the bar are associated with lower MAPE (higher accuracy).

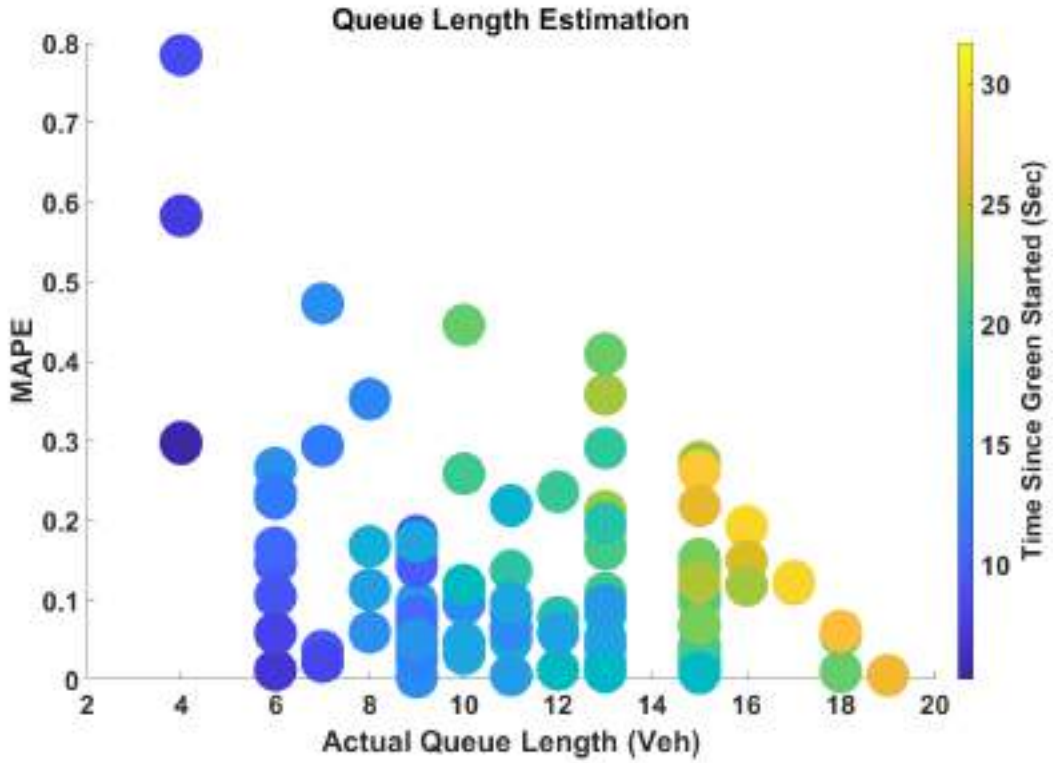

Figure 6.5 Th Effect of Cycle Time on the Performance of the Queue Length Estimation Model

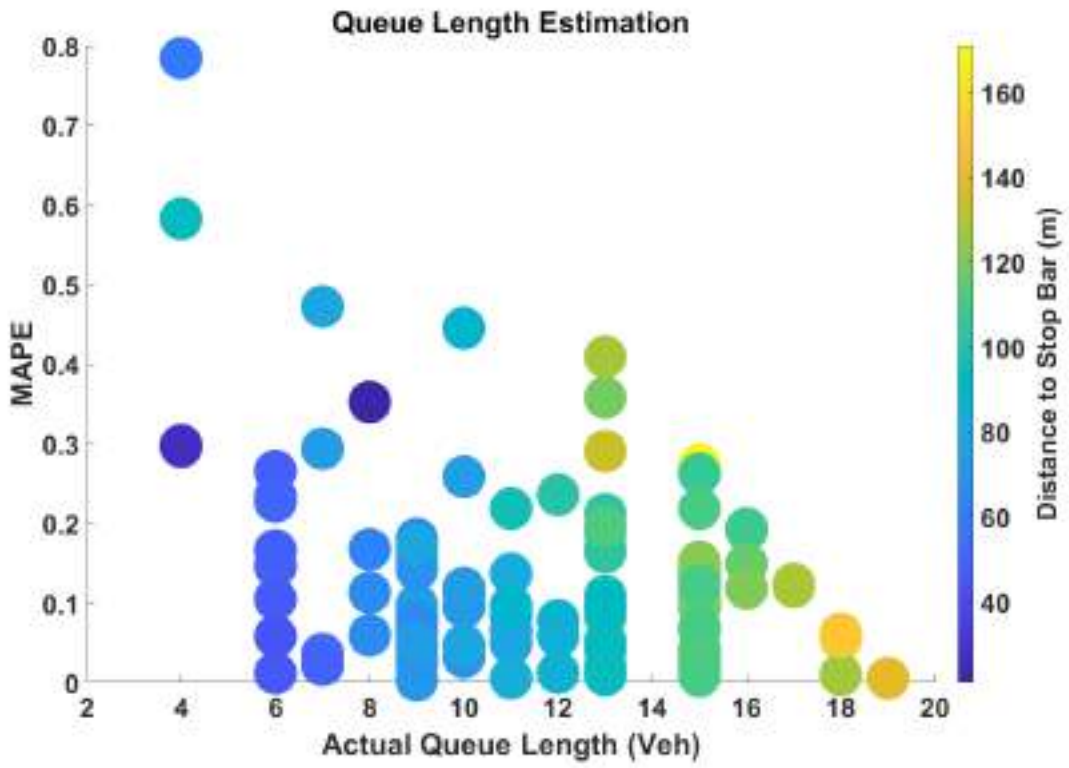

Figure 6.6 Th Effect of Distance on the Performance of the Queue Length Estimation Model

To have a closer look at the relationship between MAPE and the most effective factors, Figures 6.7 and 6.8 are plotted with the speed of the slowed-down vehicle and its sequence after the last queued vehicle, respectively. From both figures, the lower MAPE is scattered in the lower speed and lower sequence of slowed-down vehicles. The relation between the speed and sequence of slowed-down vehicle is justified by the nature of queue dissipation process as the speed at capacity state keeps increasing during the green time, which means the earlier slowed-down vehicle in sequence will have a lower speed. Therefore, when there is more than one slowed-down vehicle in one cycle, the earlier in the sequence will be selected for queue length estimation. This is a significant

consideration when different penetration rates are compared. With higher penetration rates, there are higher probability of having more slowed-down vehicles.

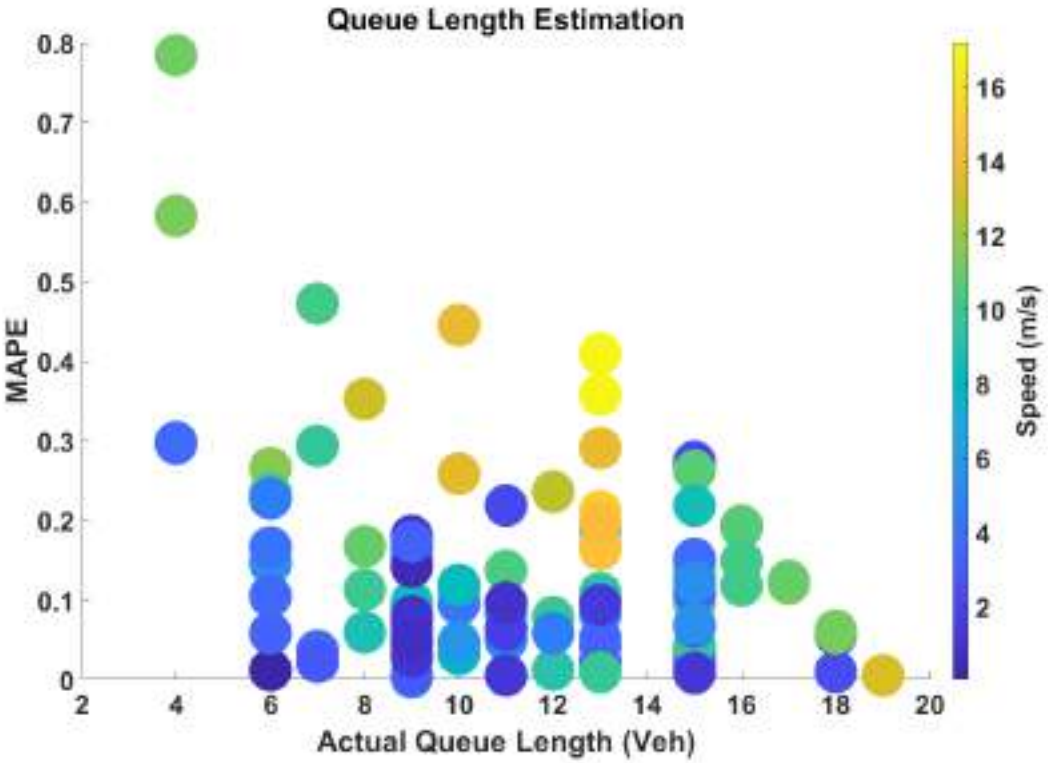

Figure 6.7 Th Effect of the Speed on the Performance of the Queue Length Estimation Model

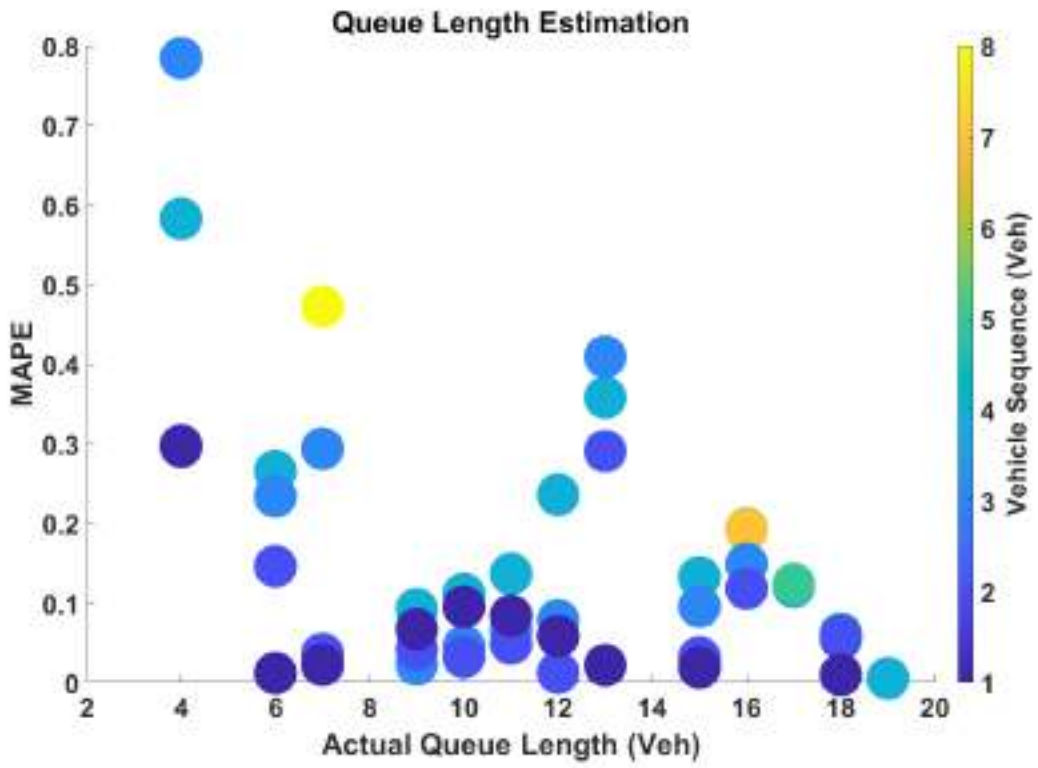

Figure 6.8 Th Effect of the Vehicle Sequence on the Performance of the Queue Length Estimation Model

To have a better visualization of the relationship between the characteristics of the slowed-down vehicles and the estimation accuracy, Figure 6.9 is plotted. The sequence of the slowed-down vehicle has a direct relationship with the MAPE. In other words, the model demonstrated a higher accuracy when the slowed-down vehicle has a closer distance to the queued vehicle. The lower MAPE (higher accuracy) is associated with the lower slowed-down sequence, lower speed, and longer queue length.

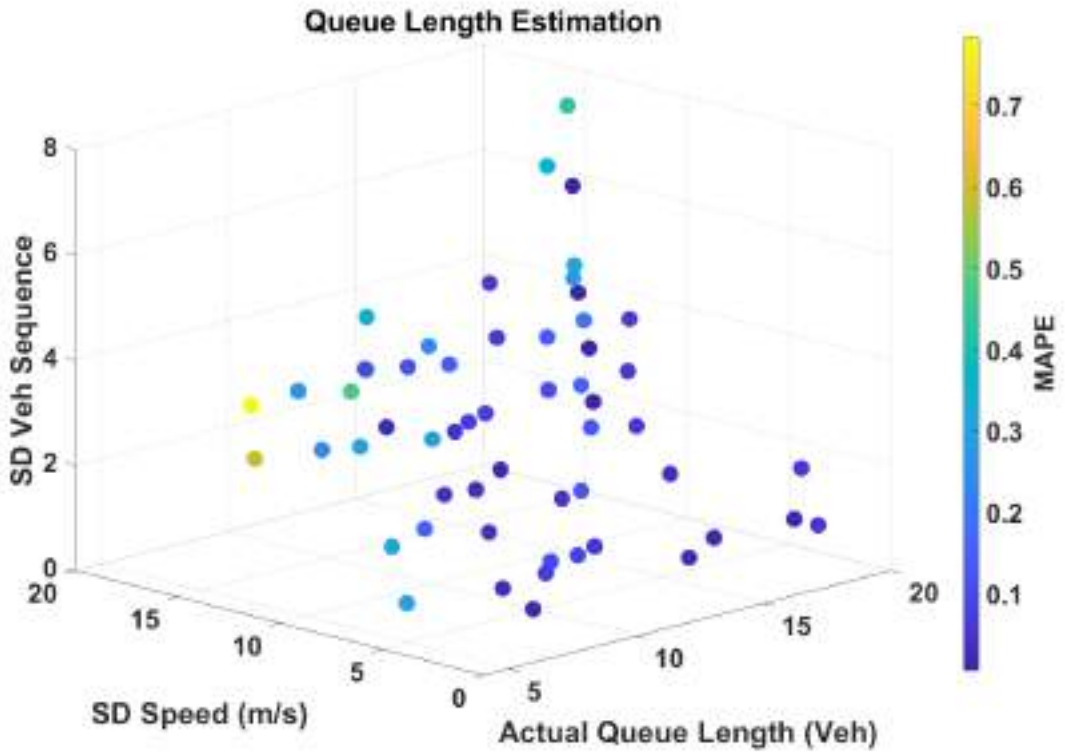

Figure 6.9 Th Effect of Speed and Sequence of the Slowed-down Vehicle on the Performance of the Queue Length Estimation Model

The data about the relationship between slowed-down vehicle characteristics and the accuracy of the queue length estimation as appeared in Figures 6.5 to 6.9 are summarized in the following table.

Table 6.5 The Data of the Slowed-down Vehicle Characteristics and the Accuracy of the Queue Length Estimation

SD Speed (m/s)	Time (s)	Distance (m)	Traffic Volume (veh)	Queue Length (veh)	MAPE (%)

10.97	96.5	62.75	16	7	16.74%
9.79	92	74.46	15	6	29.39%
0.92	91	74.38	14	8	7.94%
8.64	106.3	111.58	27	14	21.84%
16.96	102.2	127.47	21	12	40.95%
13.51	100.7	73.77	23	9	72.00%
15.49	105.5	150.85	24	14	27.36%
11.96	111.7	138.07	29	17	6.15%
16.82	109.9	169.49	27	17	6.15%
11.78	105.8	156.05	33	17	6.14%
10.33	109	128.39	30	16	6.10%
9.48	98.4	78.51	22	10	6.59%
11.00	96.2	62.97	20	8	2.29%
8.90	97	72.12	18	9	4.54%
4.09	90.7	48.29	12	5	16.61%
7.41	98.1	107.03	22	12	16.37%
5.22	106.4	145.69	27	17	6.12%
6.49	94.5	69.81	14	8	0.29%
1.60	93.2	80.02	20	10	6.23%
10.43	92.4	49.3	14	5	23.40%
10.58	109.2	109.23	28	15	19.12%
9.90	99.1	87.67	21	11	7.80%
9.48	103.5	117.07	25	14	14.19%
6.25	99.8	107.94	22	12	16.53%
14.09	108.8	129.34	29	17	0.51%
14.60	101	103.93	21	12	62.00%
3.09	100.9	119.67	25	14	10.88%
1.08	92.5	70.1	22	8	2.88%
3.70	94.7	74.17	21	8	6.09%
11.79	108.1	124.39	24	16	12.23%

4.23	97.6	99.72	23	12	8.21%
11.40	87.4	94.11	9	3	58.26%
10.56	103	113.73	20	14	9.56%
10.03	94.9	66.39	16	7	11.30%
9.79	92	74.46	15	6	29.39%
0.73	89.1	62.29	14	8	18.02%
5.42	102.6	111.55	27	14	6.90%
16.96	102.2	127.47	21	12	40.95%
13.51	100.7	73.77	23	9	25.87%
10.14	101.3	119.68	24	14	10.67%
11.96	111.7	138.07	29	17	6.15%
1.93	103.8	138.6	27	17	5.96%
11.65	102.7	161.36	33	17	5.85%
9.99	105.6	134.1	30	16	5.87%
9.48	98.4	78.51	22	10	6.59%
11.00	96.2	62.97	20	8	2.29%
7.88	95.8	70.44	18	9	3.21%
3.63	89.2	46.71	12	5	10.49%
7.41	98.1	107.03	22	12	16.37%
5.22	106.4	145.69	27	17	6.12%
6.49	94.5	69.81	14	8	0.29%
1.60	93.2	80.02	20	10	6.23%
5.39	90	48.45	14	5	14.61%
10.21	105.7	116.88	28	15	14.91%
9.16	97.9	85.42	21	11	1.25%
2.90	106.2	170.97	25	14	27.37%
6.25	99.8	107.94	22	12	16.53%
14.09	108.8	129.34	29	17	0.51%
14.60	101	103.93	21	12	16.40%
1.97	99.3	115.32	25	14	6.69%

1.08	92.5	70.1	22	8	2.88%
3.70	94.7	74.17	21	8	6.09%
11.32	111	122.72	24	16	12.38%
4.23	97.6	99.72	23	12	8.21%
4.50	86.7	28.57	9	3	29.82%
10.56	103	113.73	20	14	9.56%

There is an effect of the market penetration rate on the performance of the model. Table 6.6 shows the results of testing 5%, 10%, 15%, and 20%. A direct relationship between percentage of the sampled vehicles (market penetration rate) and the accuracy of the model. The maximum accuracy is almost 100% and the minimum accuracy is approximately 38%. The results indicate a bigger gap in MAPE (larger accuracy improvement) between 5% MPR and 10% MPR. The improvement of MAPE tends to become smaller between 10% MPR, 15% MPR, and 20% MPR. This might be because the increase of market penetration rate will be less likely to change the slowed-down vehicle to be earlier in the sequence.

Table 6.6 The Results of the Queue Length Estimation with Different MPR

	MPR (5%)	**MPR (10%)**	**MPR (15%)**	**MPR (20%)**
MAPE	19.16%	13.44%	9.17%	7.36%
Min APE	0.12%	0.12%	0.01%	0.01%
Max APE	62.26%	62.26%	62.26%	32.1%
STD APE	13.37%	8.74%	7.63%	5.94%

Figure 6.10 demonstrates a better performance of the algorithm with the increase of the market penetration rate (MPR). Obviously, the lowest MPR of 5% shows the highest MAPE and the highest MPR of 20% provides the lowest MAPE. The highest

MAPE was 19.16% (accuracy of 80.84%) and the lowest was 7.36% (accuracy of 92.64%).

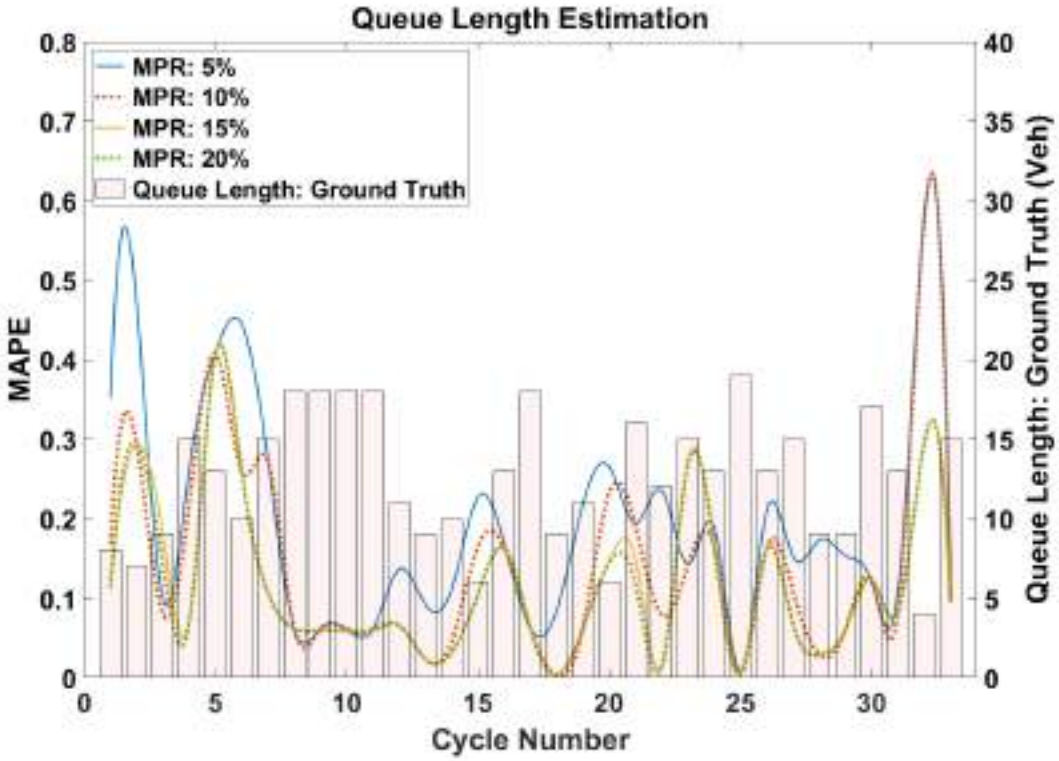

Figure 6.10 The Performance of the Queue Length Estimation Model with Different MPR

6.4. The Performance of Traffic Volume Estimation Model

The performance of the queue length estimation model is evaluated based on the measure of effectiveness (MAPE) to assess the accuracy of the algorithm for simulation data and real-world data.

6.4.1. Traffic Volume Estimation Analysis of the Simulation Experiment

By applying the algorithm on the validation dataset, the MAPE was 11.85%, which means an accuracy of 88.15%. The maximum MAPE was 27.68% and the minimum MAPE was 0.31% (accuracy of 72.32% and 99.69%). The following table summarizes the results of the model for each cycle based on the simulation data.

Table 6.7 The Results of the Traffic Volume Estimation Model for Simulation Data

Cycle	Traffic Volume (Veh/ln/Cycle)	Queue Length (Veh/ln/Cycle)	Traffic Volume Estimation (Veh/ln/Cycle)	APE (%)
1	17	11	15	13.92%
2	16	8	12	25.66%
3	25	22	26	2.41%
4	22	15	19	15.60%
5	17	14	18	6.52%
6	22	13	17	24.39%
7	23	18	21	7.35%
8	24	18	22	6.50%
9	21	13	17	17.70%
10	11	5	8	26.12%
11	14	10	14	0.33%
12	13	8	11	11.81%
13	12	8	12	2.60%
14	16	9	13	18.83%
15	22	18	22	1.49%
16	18	13	17	6.48%

17	23	13	17	27.68%
18	10	5	8	18.92%
19	8	6	9	13.39%
20	11	8	12	4.67%
21	25	20	24	3.63%
22	16	12	16	0.31%
23	17	10	14	18.78%
24	14	11	15	6.26%
25	23	15	19	16.85%
26	25	15	19	25.87%
27	21	15	19	11.58%
28	25	19	22	13.36%
29	20	17	21	3.45%
30	9	6	9	3.02%
Min APE				**0.31%**
Max APE				**27.68%**
STD APE				**8.67%**
MAPE				**11.85%**

To have a deeper look at the performance of the model, the estimation of the 30 cycles is plotted in Figure 6.11. From the figure, an excellent performance by the model can be observed as estimated traffic volume followed the fluctuation of the actual traffic volume along different cycles. There seems to be more underestimations than overestimations by the algorithm. This might be because the traffic flow from the queued vehicles is less than the traffic flow in the entire cycle. Also, there is a probability of having more slowed-down vehicles in front of the utilized slowed-down vehicle.

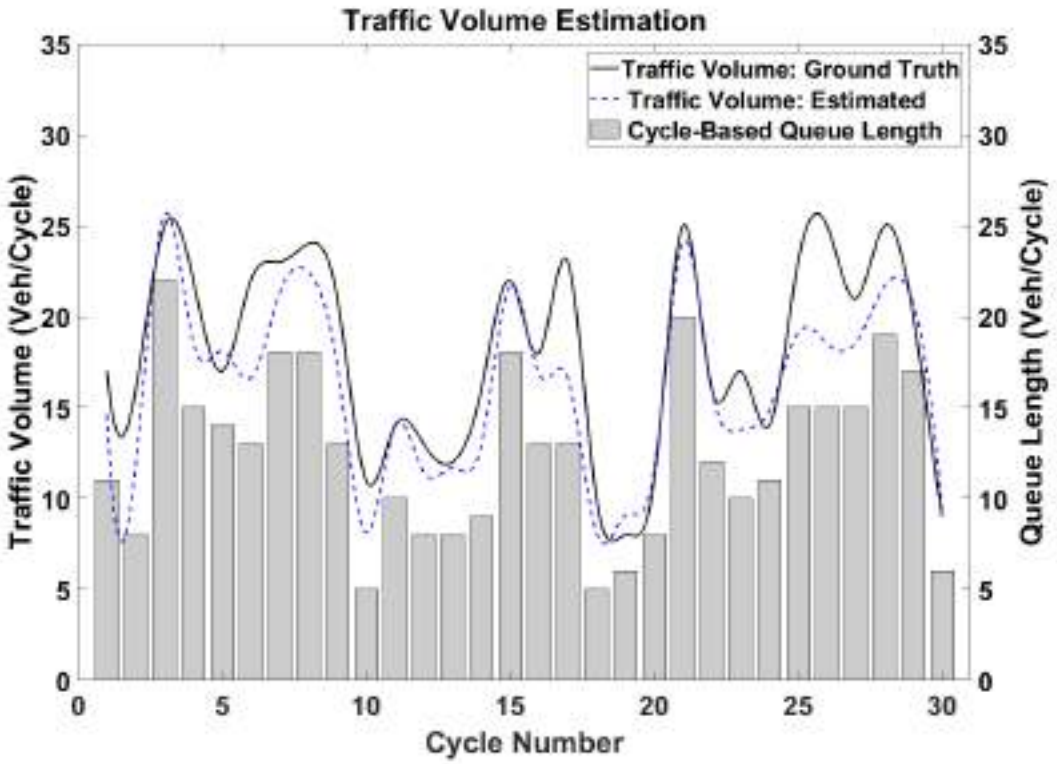

Figure 6.11 Th Performance of the Traffic Volume Estimation Model in the Simulation Experiment

6.4.2. Traffic Volume Estimation Analysis of the Real-world Experiment

Because NGSIM data has a relatively small dataset of 15 minutes, only one slowed-down vehicle was randomly selected from each cycle. The validation data has nine cycles during the 15-minute dataset where six of them had complete trajectories with at least one slowed-down vehicle. The performance of the algorithm on real-world data demonstrated an MAPE of 23.57% (accuracy of 76.43%). Table 6.8 includes a summary of the performance of the algorithm for the six cycles.

Table 6.8 The Results of the Traffic Volume Estimation Model for Simulation Data

Cycle	Traffic Volume (Veh/ln/Cycle)	Queue Length (Veh/ln/Cycle)	Traffic Volume Estimation (Veh/ln/Cycle)	APE (%)
1	6	2	4	25.67%
2	9	2	7	22.22%
3	4	3	5	36.34%
4	5	3	5	2.44%
5	5	4	6	27.52%
6	8	4	6	27.24%
Min APE				**2.44%**
Max APE				**36.34%**
STD				**11.36%**
MAPE				**23.57%**

Figure 6.12 shows the estimated and actual queue lengths along with the traffic volume. There is more underestimation than overestimation as found in the performance of the model on simulation data. The lower accuracy of the real-world data compared to the simulation might be related to the two main reasons. First, the prior dataset (for training and testing) of NGSIM is relatively low that it does not represent different the traffic patterns, which might influence the accuracy of the models. The second reason is the low traffic volume and the low queue length per cycle in the signalized intersection explored in NGSIM dataset.

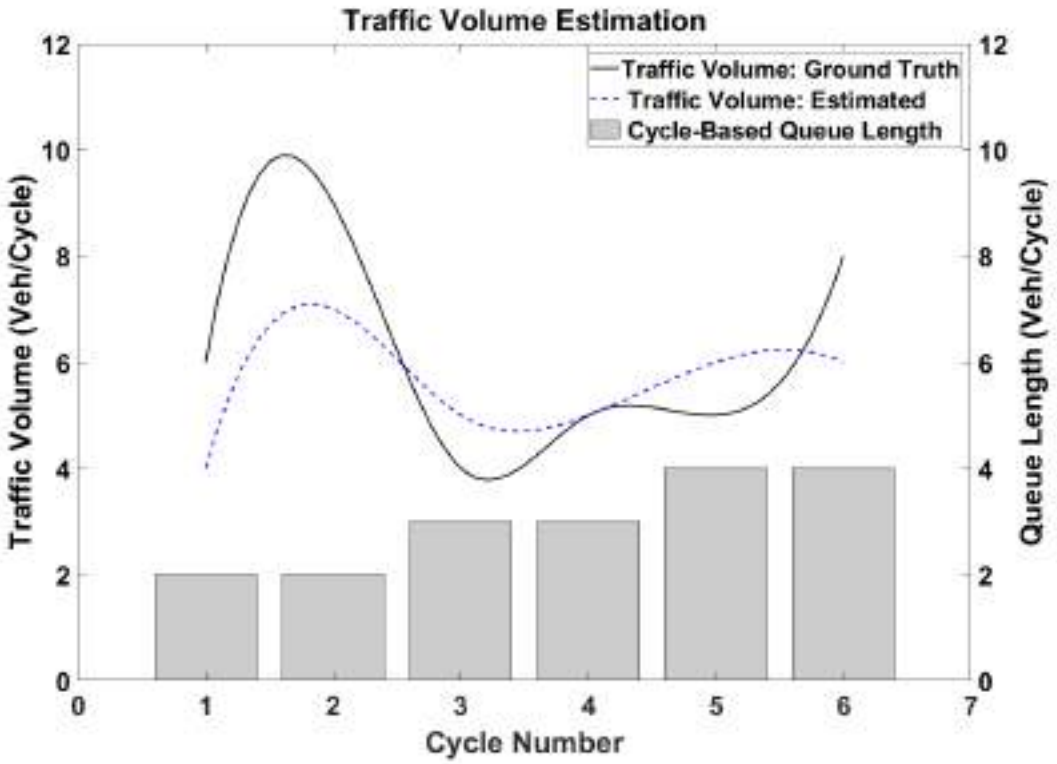

Figure 6.12 Th Performance of the Traffic Volume Estimation Model in the Real-world Experiment

6.4.3. The Effective Factors in the Traffic Volume Estimation Model

To instigate the effective factors in the traffic volume estimation model, the MAPE was plotted against different inputs. In this investigation, the simulation data has been utilized as it provides higher sample data.

From Figure 6.13, more accuracy (lower MAPE) was achieved when the time since green phase started was longer. This simply because the calculated flow rate closer to the end of the cycle covers almost longer time of the cycle, which means it represents almost the entire cycle. A similar finding in Figure 6.14 about the relationship between the distance to the stop bar and the MAPE. The longer the distance from the stop bar

yields a lower MAPE. This might be because the further the slowed-down vehicle from the stop bar means the longer the queue, which means longer time of the cycle.

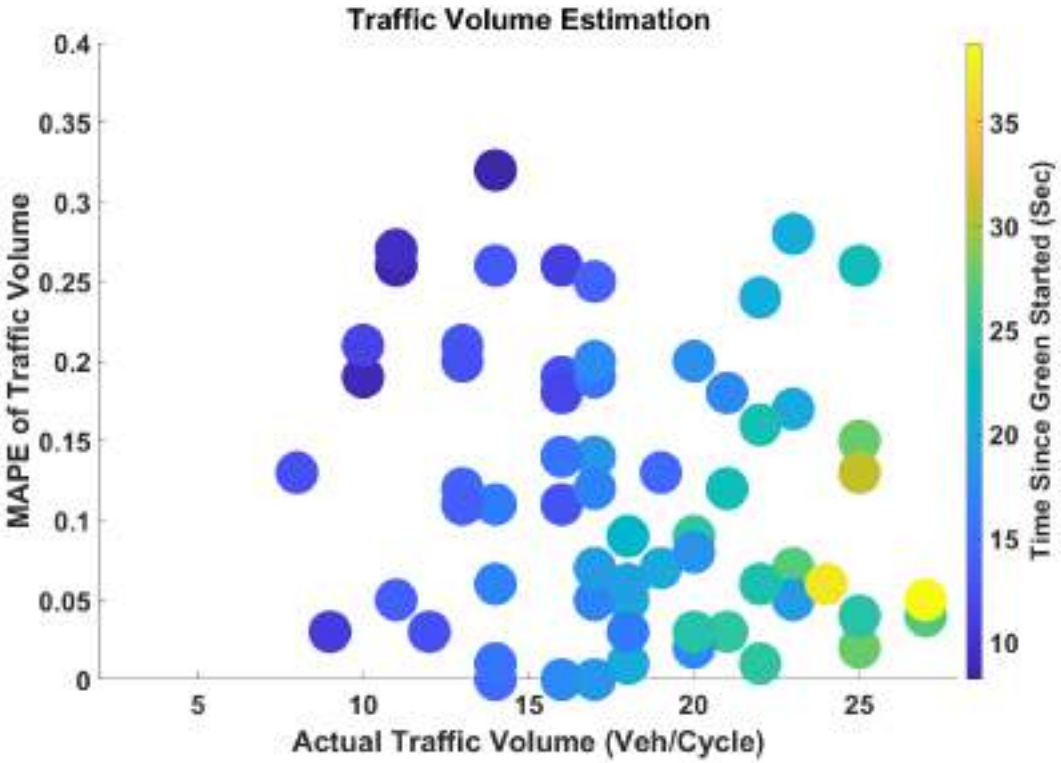

Figure 6.13 Th Effect of the Time on the Performance of the Traffic Volume Estimation Model

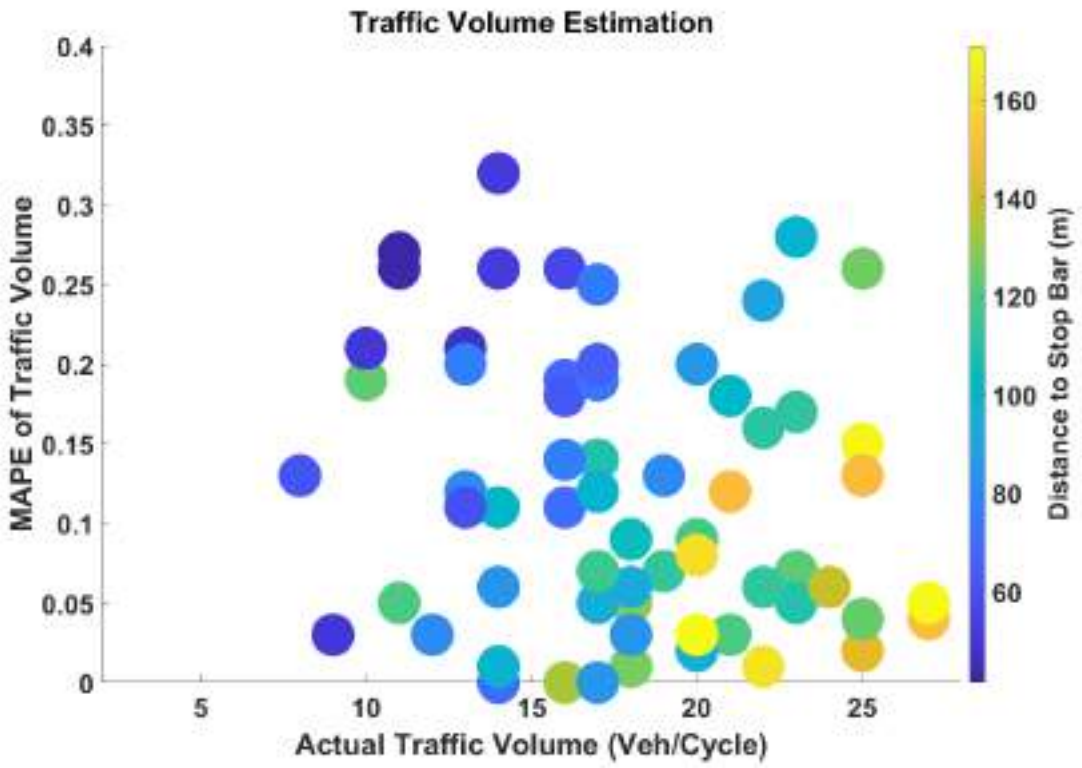

Figure 6.14 Th Effect of the Distance on the Performance of the Traffic Volume Estimation Model

The findings in Figures 6.13 and 6.14 are supported by the finding from Figure 6.15 where there was also a correlation between the number of queued vehicles and MAPE. The higher number of queued vehicles allows the flow rate part based on queue length in the algorithm to cover a larger portion. This is emphasized by Figure 6.16 when the queued vehicles are represented in terms of a ratio of the entire traffic flow.

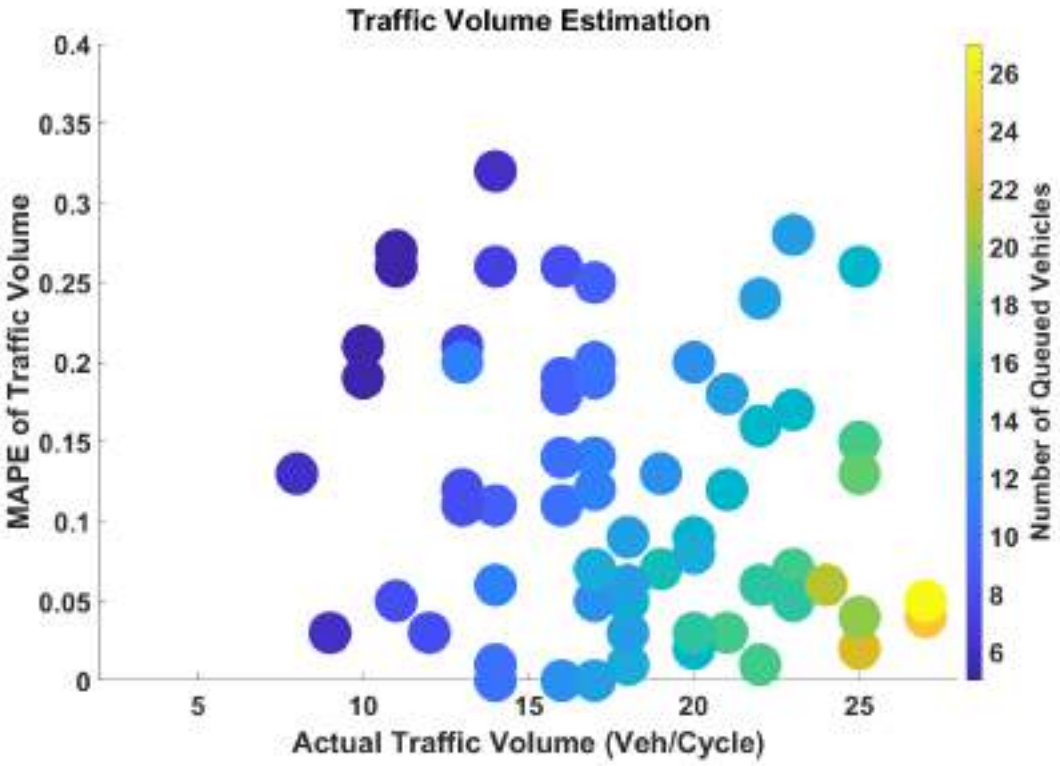

Figure 6.15 Th Effect of the Queue Length on the Performance of the Traffic Volume Estimation Model

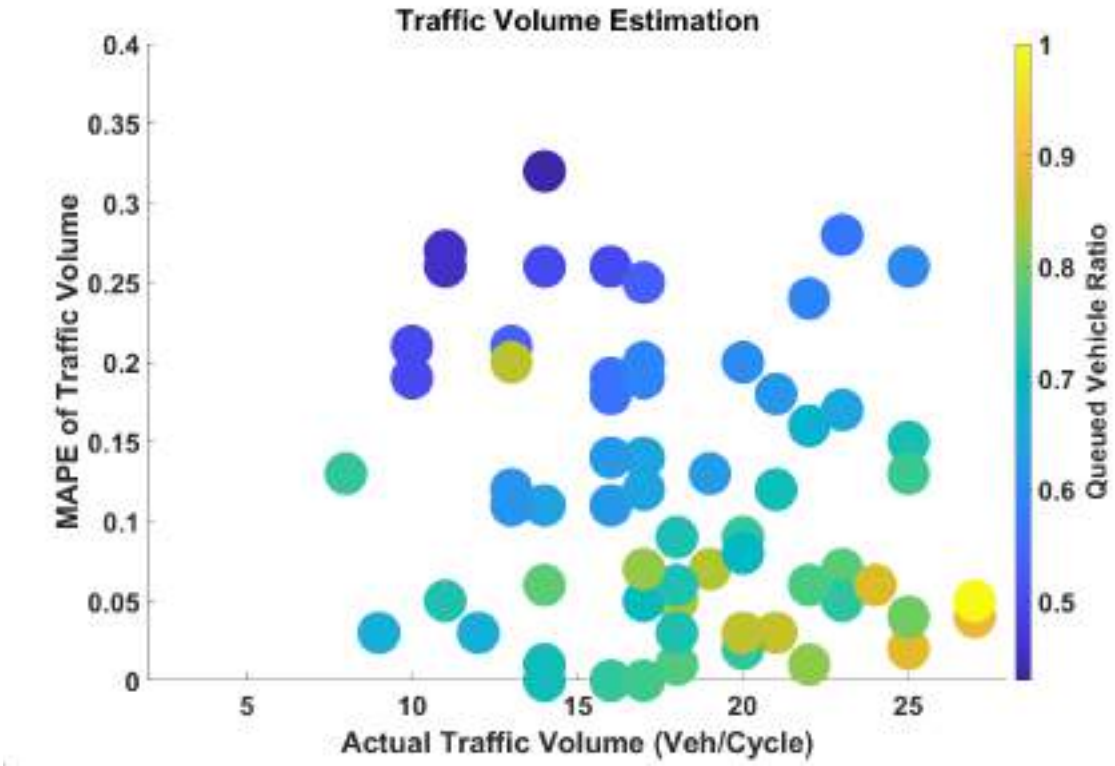

Figure 6.16 Th Effect of the Queued Vehicle Ratio on the Performance of the Traffic Volume Estimation Model

The data about the relationship between slowed-down vehicle characteristics and the accuracy of the traffic volume estimation as appeared in Figures 6.13 to 6.16 are summarized in the following table.

Table 6.9 The Data of the Slowed-down Vehicle Characteristics and the Accuracy of the Traffic Volume Estimation

SD Speed (m/s)	Time (s)	Distance (m)	Traffic Volume (veh)	Queue Length (veh)	MAPE (%)
14.2027778	101.2	130.38	15	18	5.40%

17.6722222	98.4	108.98	11	17	13.92%
0.3	90.8	64.4	8	16	25.66%
9.48333333	107.8	144.02	22	25	2.41%
16.2555556	103.4	169.3	15	22	15.60%
5.38611111	99.4	93.1	14	17	6.52%
11.0361111	101	90.53	13	22	24.39%
6.84166667	107	121.98	18	23	7.35%
2.97777778	101.6	113.24	18	24	6.50%
0.14722222	97.2	100.72	13	21	17.70%
3.66111111	88.6	42.73	5	11	26.12%
7.41388889	94.6	68.79	10	14	0.33%
4.74444444	102.2	113.88	18	22	1.41%
7.86944444	93.2	51.57	7	14	26.43%
13.2833333	94.2	81.21	8	13	11.81%
8.82222222	93	47.28	7	13	20.60%
0.02777778	92.4	75.93	11	13	19.88%
9.6	105.2	119.72	18	21	3.20%
4.81111111	89.4	41.45	5	11	26.78%
13.6472222	92.4	80.45	8	12	2.60%
2.86388889	92.8	70.54	10	16	11.10%
11.8861111	96.8	95.34	12	17	5.20%
1.08055556	92.4	67.44	9	16	18.83%
0.43333333	106.8	151.07	24	27	4.04%
9.79166667	100.4	113.4	16	19	6.94%
8.94722222	118.8	170.41	27	27	4.75%
10.1555556	105.2	122.23	18	22	1.49%
15.3583333	100.6	126.51	14	18	0.60%
15.425	99.8	134.09	13	18	6.48%
10.8888889	101	98.65	13	23	27.68%
6.30555556	97.6	96.8	15	20	1.64%

20.9305556	107.8	169.35	18	25	15.40%
15.625	105	118.42	15	20	8.57%
4.04166667	91	56.13	8	16	25.82%
16.275	98.2	160.9	14	20	8.35%
18.1444444	88.8	123.16	5	10	18.92%
2.31944444	94	74.12	9	17	24.91%
14.1833333	95.4	98.76	10	14	1.17%
15.4527778	92.6	60.88	6	8	13.39%
18.7333333	93.8	119.81	8	11	4.67%
5.11111111	104.6	124.27	20	25	3.63%
1.475	94.6	80.33	12	19	13.21%
16.1638889	97.2	133.62	12	16	0.31%
0.3	99	109.38	17	23	5.14%
11.3138889	99.4	94.01	13	18	6.10%
13.3388889	99	116.42	14	17	6.95%
5.34166667	98	85.6	12	20	20.41%
1.61388889	91.6	62.81	9	16	18.12%
12.9888889	91.4	50.56	5	10	21.23%
19.8055556	117.2	138.07	21	24	6.14%
18.6	102.2	105.31	13	18	8.68%
4.21944444	95.6	73.02	10	17	18.78%
2.61111111	95.6	76.23	10	16	13.70%
13.9527778	96.6	98.72	11	17	12.31%
9.32777778	97.4	64.25	10	17	20.28%
12.4805556	96.8	84.07	11	14	6.26%
14.6888889	105	163.24	18	22	1.30%
17.8527778	96.2	101.72	9	14	10.90%
2.27777778	100.4	113.11	15	23	16.85%
6.50555556	104	113.6	17	22	5.59%
3.51388889	96.2	84.04	13	18	2.98%

11.8944444	103.6	125.5	15	25	25.87%
20.7944444	103.4	150.2	15	21	11.58%
19.7944444	110.8	149.66	19	25	13.36%
9.74722222	98.4	84.97	13	17	0.43%
19.0833333	104.4	170.95	17	20	3.45%
9.94444444	90.6	50.07	6	9	3.02%
0.125	88.2	51.53	6	14	31.97%
11.3805556	93.6	59.3	8	13	11.24%
11.6138889	103.8	112.2	15	22	15.92%

The effect of market penetration rate on the performance of the algorithm is significantly high when MPR of 5% is compared with MPR of 20%. When 5% of vehicle trajectories are considered, MAPE was 16.01% (accuracy of approximately 84%), while MPR of 20% yields an MAPE of 7.81% (accuracy of 92.19%). The following table summarizes the effect of multiple market penetration rates on the performance of the system.

Table 6.10 The Results of the Travel Volume Estimation with Different MPR

	MPR (5%)	**MPR (10%)**	**MPR (15%)**	**MPR (20%)**
MAPE	16.01%	11.85%	9.72%	7.81%
Min APE	0.40%	0.31%	0.20%	0.24%
Max APE	38.14%	27.68%	24.91%	21.31%
STD APE	11.81%	8.67%	7.41%	5.76%

From Figure 6.17 the increase of the market penetration rate demonstrated an improved performance of the algorithm. By looking at the figure, there is bigger gap between the MPR of 5% and 10% in terms of MAPE, which indicates a larger

improvement of the accuracy of the model. The improvement seems less when the MPR of 10% increase to 15% and then to 20%. This might be because the flow rate value with the increase of market penetration rate was not highly influenced to change the traffic volume estimation.

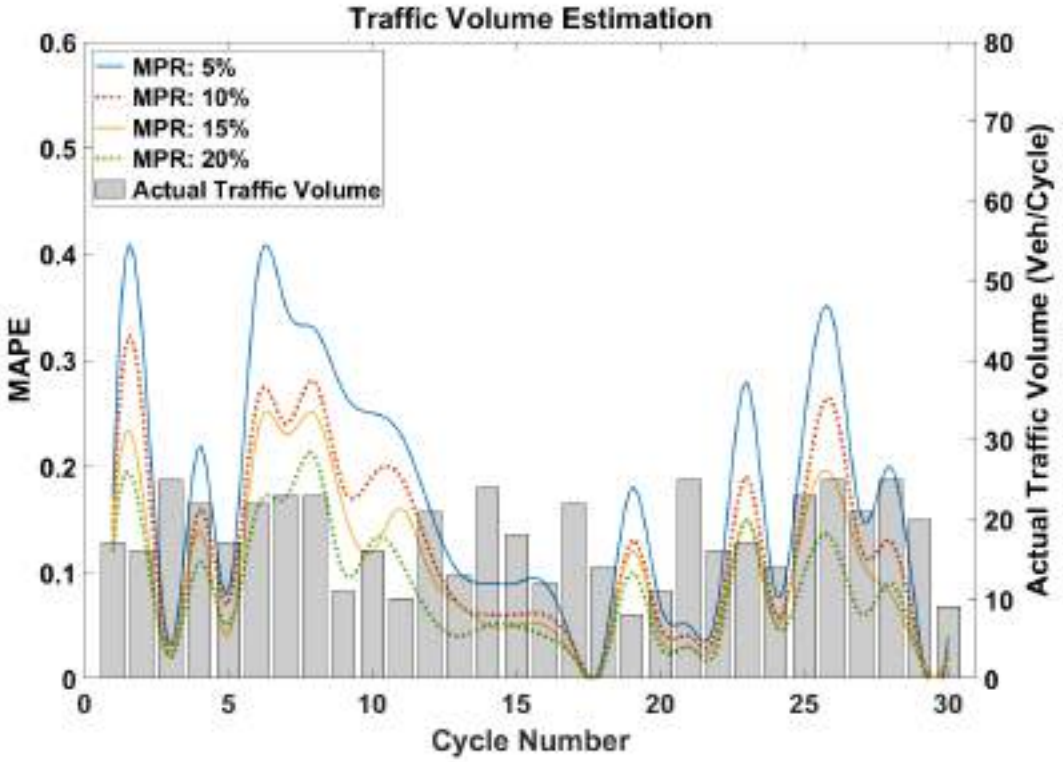

Figure 6.17 Th Performance of the Traffic Volume Estimation Model with Different MPR

6.5. Summary of Chapter VI

From the results from the simulation and real-world experiments, the findings of this chapter can be summarized as the following:

- The queue length results of the simulation experiment demonstrated an adequate MAPE of 13.44% (accuracy of 86.56%),
- The results of the queue length algorithm applied on real-world data demonstrated an MAPE of 21.97% (78.03% accuracy),
- The performance of the traffic volume algorithm on simulation data demonstrated an excellent MAPE of 11.8% (88.2% accuracy),
- The performance of the algorithm based on real-world data from demonstrated an MAPE of 23.57% (76.43% accuracy),
- Lower MAPE of the queue length estimation was achieved when the time since green phase started and the distance to the stop bar were longer,
- There was a correlation between the queue length and the accuracy of the queue estimation model,
- The effect of market penetration rate on the performance of the algorithm is significantly high when MPR of 5%, and
- The improvement of MAPE tends to become smaller between 10% MPR, 15% MPR, and 20% MPR.

CHAPTER VII: CONCLUSIONS AND RECOMMENDATIONS

This dissertation proposed a sophisticated model based on slowed-down vehicle trajectories to estimate real-time queue length and traffic volume from connected vehicles. The model tackles the low market penetration rate by relying on the spatiotemporal speed distribution of the queued vehicle to learn from the data about the propagation and dissipation of the shockwave through a deep learning technique. The significance of this work is highlighted by avoiding external dependencies of other parameters and the ability to estimate traffic volume with one sampled vehicle per cycle. The model is based on only a prior dataset of trajectories with signal time information and trajectories from real-time cycle data.

The four objectives of this paper are (1) establishing a relationship between the slowed-down vehicle and last queued vehicle based on shockwave theory and the capacity state; (2) utilizing only a prior dataset and a deep learning technique to identify the last queued vehicle information based on the slowed-down vehicle; (3) proposing a queue length estimation algorithm based on lower market penetration rates; and (4) developing a traffic volume estimation algorithm considering the queue length estimation model.

7.1. Conclusions

By achieving the first two objectives of this dissertation, the conclusions are formed by the observations from Chapter III and Chapter IV. The significant findings can be highlighted as the following:

- The queue dissipation and capacity state have a uniform pattern in terms of time, space, and speed,
- The speed of queued vehicles increases with the increase of the green time until the last queued vehicle,
- The slowed-down vehicle interacts with the last queued vehicle based on the car-following model
- The macroscopic shockwave can be illustrated by the speed distribution based on a sampled trajectory data,
- There is a relationship between the slowed-down vehicles and the last queued vehicles around the dissipation shockwave based on the macroscopic shockwave,
- There is a spatiotemporal proximity between the slowed-down vehicles and the last queued vehicles from the empirical cycle results,
- The departure time and the distance to the stop bar are associated with the speed at the stop bar,
- The speed of the queued vehicles at the stop bar increase with the increase of the green time,

- The least speed of the slowed-down vehicles is correlated with the green time and distance,
- The least speed of the slowed-down vehicles is associated with the queue length and the traffic volume,
- At the same signalized intersection, there is a correlation between the queue length and the traffic volume.

Achieving the third and fourth objectives is determined by the performance of the models in estimating the actual values of the queue length and traffic volume. To analyze and evaluate the performance of the algorithm, four experiments have been conducted on simulation and real-world data. The first experiment is a simulation-based with the aim of testing the accuracy of the queue length algorithm and the effect of different factors. The second experiment examined the queue length estimation algorithm on real-world data (NGSIM). The third experiment evaluates the traffic volume estimation algorithm on simulation data algorithm and tests the effect of different factors on the estimation accuracy. The fourth experiment examined the traffic volume estimation algorithm on NGSIM data.

- The queue length results of the simulation experiment demonstrated an adequate MAPE of 13.44% (accuracy of 86.56%),
- The results of the queue length algorithm applied on real-world data demonstrated an MAPE of 21.97% (78.03% accuracy),
- The performance of the traffic volume algorithm on simulation data demonstrated an excellent MAPE of 11.8% (88.2% accuracy),

- The performance of the algorithm based on real-world data from demonstrated an MAPE of 23.57% (76.43% accuracy),
- Lower MAPE of the queue length estimation was achieved when the time since green phase started and the distance to the stop bar were longer,
- There was a correlation between the queue length and the accuracy of the queue estimation model,
- The effect of market penetration rate on the performance of the algorithm is significantly high when MPR of 5%,
- The improvement of MAPE tends to become smaller between 10% MPR, 15% MPR, and 20% MPR.

7.2. Recommendation and Future Directions

The proposed estimation models based on slowed-down vehicles revealed an adequate accuracy by using only a prior trajectory dataset with low market penetration rate. From the findings of this dissertation, the recommendations are summarized as the following:

- The proposed model can be applied in real-world scenarios for both real-time applications and off-line applications,
- The consideration of non-queued vehicles, particularly slowed-down vehicles, can provide a positive impact on the estimation models of queue length and traffic volume based on this dissertation and might also provide positive impact on the estimation of other traffic characteristics,

- The utilization of slowed-down vehicles can be integrated with other vehicle classifications, particularly queued vehicles and passing vehicles, in one holistic estimation model,
- Other variables such as acceleration and vehicle length can be included in the dataset to improve the accuracy of the estimation models.

The models in this dissertation are limited to the cycles with slowed-down vehicles only considering an isolated signalized intersection. Another limitation is the short period of the NGSIM dataset, which did not only affect the results, but also restricted the investigation of MPR and other factors. The models consider stable driving conditions without any influence of external factors such as weather or accident. Although unusual conditions may affect the models, this work is limited to normal driving conditions.

Future work might consider incorporating all vehicle classifications (slowed-down vehicles, queued vehicles, and passing vehicles) in one holistic model. Also, future work may consider applying a sensitivity analysis of MPR and other factors on a larger real-world dataset. Also, future work might consider incorporating slowed-down vehicle information with other vehicle classifications, i.e., queued vehicles and passing vehicles, in one holistic model. Another aspect of future work might consider other variables such as acceleration and vehicle length to improve the accuracy of the estimation models.

REFERENCES

Addison, P. S., & Low, D. J. (1998). A novel nonlinear car-following model. *Chaos: An Interdisciplinary Journal of Nonlinear Science, 8*(4), 791-799. https://doi.org/10.1063/1.166364

AiLing, D., XiangMo, Z., & LiCheng, J. (2002, 6-6 Sept. 2002). Traffic flow time series prediction based on statistics learning theory. Proceedings. The IEEE 5th International Conference on Intelligent Transportation Systems,

Akçelik, R., & Besley, M. (2002). Queue Discharge Flow and Speed Models for Signalised Intersections. In M. A. P. Taylor (Ed.), *Transportation and Traffic Theory in the 21st Century* (pp. 99-118). Emerald Group Publishing Limited. https://doi.org/10.1108/9780585474601-006

Al-Ghamdi, A. S. (1999, 1999/01/01). Entering Headway for Through Movements at Urban Signalized Intersections. *Transportation Research Record, 1678*(1), 42-47. https://doi.org/10.3141/1678-06

Ban, X., Hao, P., & Sun, Z. (2011, 2011/12/01/). Real time queue length estimation for signalized intersections using travel times from mobile sensors. *Transportation Research Part C: Emerging Technologies, 19*(6), 1133-1156. https://doi.org/https://doi.org/10.1016/j.trc.2011.01.002

Brackstone, M., & McDonald, M. (1999, 1999/12/01/). Car-following: a historical review. *Transportation Research Part F: Traffic Psychology and Behaviour, 2*(4), 181-196. https://doi.org/https://doi.org/10.1016/S1369-8478(00)00005-X

Cheng, Y., Qin, X., Jin, J., & Ran, B. (2012, 2012/01/01). An Exploratory Shockwave Approach to Estimating Queue Length Using Probe Trajectories. *Journal of Intelligent Transportation Systems, 16*(1), 12-23. https://doi.org/10.1080/15472450.2012.639637

Cheng, Y., Qin, X., Jin, J., Ran, B., & Anderson, J. (2011, 2011/01/01). Cycle-by-Cycle Queue Length Estimation for Signalized Intersections Using Sampled Trajectory Data. *Transportation Research Record, 2257*(1), 87-94. https://doi.org/10.3141/2257-10

Chun-Hsin, W., Jan-Ming, H., & Lee, D. T. (2004). Travel-time prediction with support vector regression. *IEEE Transactions on Intelligent Transportation Systems, 5*(4), 276-281. https://doi.org/10.1109/TITS.2004.837813

Comert, G. (2013, 2013/09/01/). Simple analytical models for estimating the queue lengths from probe vehicles at traffic signals. *Transportation Research Part B: Methodological, 55*, 59-74. https://doi.org/https://doi.org/10.1016/j.trb.2013.05.001

Comert, G., & Cetin, M. (2011). Analytical Evaluation of the Error in Queue Length Estimation at Traffic Signals From Probe Vehicle Data. *IEEE Transactions on Intelligent Transportation Systems, 12*(2), 563-573. https://doi.org/10.1109/TITS.2011.2113375

Cui, Z., Ke, R., Pu, Z., & Wang, Y. (2020, 2020/09/01/). Stacked bidirectional and unidirectional LSTM recurrent neural network for forecasting network-wide traffic state with missing values. *Transportation Research Part C: Emerging Technologies, 118*, 102674. https://doi.org/https://doi.org/10.1016/j.trc.2020.102674

Dion, F., Rakha, H., & Kang, Y.-S. (2004, 2004/02/01/). Comparison of delay estimates at under-saturated and over-saturated pre-timed signalized intersections. *Transportation Research Part B: Methodological, 38*(2), 99-122. https://doi.org/https://doi.org/10.1016/S0191-2615(03)00003-1

Fourati, W., & Friedrich, B. (2019, 2019/10/01). Trajectory-Based Measurement of Signalized Intersection Capacity. *Transportation Research Record, 2673*(10), 370-380. https://doi.org/10.1177/0361198119848412

Fourati, W., & Friedrich, B. (2021, 2021/09/01/). A method for using crowd-sourced trajectories to construct control-independent fundamental diagrams at signalized links. *Transportation Research Part C: Emerging Technologies, 130*, 103270. https://doi.org/https://doi.org/10.1016/j.trc.2021.103270

Gipps, P. G. (1981, 1981/04/01/). A behavioural car-following model for computer simulation. *Transportation Research Part B: Methodological, 15*(2), 105-111. https://doi.org/https://doi.org/10.1016/0191-2615(81)90037-0

Hao, P., & Ban, X. (2015, 2015/12/01/). Long queue estimation for signalized intersections using mobile data. *Transportation Research Part B: Methodological, 82*, 54-73. https://doi.org/https://doi.org/10.1016/j.trb.2015.10.002

Hao, P., Sun, Z., Ban, X., Guo, D., & Ji, Q. (2013, 2013/11/01/). Vehicle index estimation for signalized intersections using sample travel times. *Transportation Research Part C: Emerging Technologies, 36*, 513-529. https://doi.org/https://doi.org/10.1016/j.trc.2013.06.018

Hung, W. T., Tian, F., & Tong, H. Y. (2003). Discharge headway at signalized intersections in Hong Kong. *Journal of Advanced Transportation, 37*(1), 105-117. https://doi.org/https://doi.org/10.1002/atr.5670370105

Ibnu Choldun R, M., Santoso, J., & Surendro, K. (2020, 2020//). Determining the Number of Hidden Layers in Neural Network by Using Principal Component Analysis. Intelligent Systems and Applications, Cham.

Jazayeri, M. S., Jahangiri, A., & Machiani, S. G. (2021). *Predicting Vehicle Trajectories at Intersections using Advanced Machine Learning Techniques (SDSU-01-01)* Version V1) VTTI. https://doi.org/doi:10.15787/VTT1/AKKZ6V

Jiang, H., Chang, L., Li, Q., & Chen, D. (2019, 5-7 Sept. 2019). Trajectory Prediction of Vehicles Based on Deep Learning. 2019 4th International Conference on Intelligent Transportation Engineering (ICITE),

Ke, R., Li, W., Cui, Z., & Wang, Y. (2020, 2020/04/01). Two-Stream Multi-Channel Convolutional Neural Network for Multi-Lane Traffic Speed Prediction Considering Traffic Volume Impact. *Transportation Research Record, 2674*(4), 459-470. https://doi.org/10.1177/0361198120911052

Kerner, B. S., Klenov, S. L., & Hiller, A. (2006, March 01, 2006). Criterion for traffic phases in single vehicle data and empirical test of a microscopic three-phase traffic theory. *Journal of Physics A Mathematical General, 39*, 2001-2020. https://doi.org/10.1088/0305-4470/39/9/002

Koesdwiady, A., Soua, R., & Karray, F. (2016). Improving Traffic Flow Prediction With Weather Information in Connected Cars: A Deep Learning Approach. *IEEE Transactions on Vehicular Technology, 65*(12), 9508-9517. https://doi.org/10.1109/TVT.2016.2585575

Lee, J., & Chen, R. (1986). Entering headway at signalized intersections in a small metropolitan area. *Transportation Research Record, 1091*, 117-126.

Lenz, H., Wagner, C. K., & Sollacher, R. (1999, 1999/01/01). Multi-anticipative car-following model. *The European Physical Journal B - Condensed Matter and Complex Systems, 7*(2), 331-335. https://doi.org/10.1007/s100510050618

Li, F., Tang, K., Yao, J., & Li, K. (2017, 2017/01/01). Real-Time Queue Length Estimation for Signalized Intersections Using Vehicle Trajectory Data. *Transportation Research Record, 2623*(1), 49-59. https://doi.org/10.3141/2623-06

Li, W., Wang, J., Fan, R., Zhang, Y., Guo, Q., Siddique, C., & Ban, X. (2020, 2020/02/01/). Short-term traffic state prediction from latent structures: Accuracy vs. efficiency. *Transportation Research Part C: Emerging Technologies, 111*, 72-90. https://doi.org/https://doi.org/10.1016/j.trc.2019.12.007

Lighthill, M. J., & Whitham, G. B. (1955). On kinematic waves I. Flood movement in long rivers. *Proceedings of the Royal Society of London. Series A. Mathematical and*

Physical Sciences, 229(1178), 281-316. https://doi.org/doi:10.1098/rspa.1955.0088

Lin, F.-B., & Thomas, D. R. (2005, 2005/01/01). Headway Compression during Queue Discharge at Signalized Intersections. *Transportation Research Record, 1920*(1), 81-85. https://doi.org/10.1177/0361198105192000110

Little, J. D. C. (1961). A Proof for the Queuing Formula: L= λ W. *Operations Research, 9*(3), 383-387. http://www.jstor.org/stable/167570

Liu, H. X., Wu, X., Ma, W., & Hu, H. (2009, 2009/08/01/). Real-time queue length estimation for congested signalized intersections. *Transportation Research Part C: Emerging Technologies, 17*(4), 412-427. https://doi.org/https://doi.org/10.1016/j.trc.2009.02.003

Lv, Y., Duan, Y., Kang, W., Li, Z., & Wang, F. (2015). Traffic Flow Prediction With Big Data: A Deep Learning Approach. *IEEE Transactions on Intelligent Transportation Systems, 16*(2), 865-873. https://doi.org/10.1109/TITS.2014.2345663

Ma, X., Dai, Z., He, Z., Ma, J., Wang, Y., & Wang, Y. (2017). Learning Traffic as Images: A Deep Convolutional Neural Network for Large-Scale Transportation Network Speed Prediction. *Sensors, 17*(4), 818. https://www.mdpi.com/1424-8220/17/4/818

Mahmoud, N., Abdel-Aty, M., Cai, Q., & Yuan, J. (2021, 2021/03/01/). Predicting cycle-level traffic movements at signalized intersections using machine learning models. *Transportation Research Part C: Emerging Technologies, 124*, 102930. https://doi.org/https://doi.org/10.1016/j.trc.2020.102930

Mahmoud, N., Abdel-Aty, M., Cai, Q., & Yuan, J. (2022, 2022/02/05/). Estimating cycle-level real-time traffic movements at signalized intersections. *Journal of Intelligent Transportation Systems*. https://doi.org/https://doi.org/10.1080/15472450.2021.1890072

Mei, Y., Gu, W., Chung, E. C. S., Li, F., & Tang, K. (2019, 2019/12/01/). A Bayesian approach for estimating vehicle queue lengths at signalized intersections using probe vehicle data. *Transportation Research Part C: Emerging Technologies, 109*, 233-249. https://doi.org/https://doi.org/10.1016/j.trc.2019.10.006

Mercat, J., Zoghby, N. E., Sandou, G., Beauvois, D., & Gil, G. P. (2019). Kinematic Single Vehicle Trajectory Prediction Baselines and Applications with the NGSIM Dataset. *arXiv preprint arXiv:1908.11472*.

Michalopoulos, P. G., Stephanopoulos, G., & Stephanopoulos, G. (1981, 1981/02/01/). An application of shock wave theory to traffic signal control. *Transportation Research*

Part B: Methodological, 15(1), 35-51. https://doi.org/https://doi.org/10.1016/0191-2615(81)90045-X

Mühlich, N., Gayah, V. V., & Menendez, M. (2015, 2015/01/01). Use of Microsimulation for Examination of Macroscopic Fundamental Diagram Hysteresis Patterns for Hierarchical Urban Street Networks. *Transportation Research Record, 2491*(1), 117-126. https://doi.org/10.3141/2491-13

Newell, G. F. (1961). Nonlinear Effects in the Dynamics of Car Following. *Operations Research, 9*(2), 209-229. https://doi.org/10.1287/opre.9.2.209

Newell, G. F. (1965). Instability in dense highway traffic, a review. *Proceedings of the Second International Symposium on the Theory of Traffic Flow, London 1963.*

Othayoth, D., & Rao, K. V. K. (2020, 2020/01/01/). Investigating the Relation between Level of Service and Volume-to-Capacity ratio at Signalized Intersections under Heterogeneous Traffic Condition. *Transportation Research Procedia, 48*, 2929-2944. https://doi.org/https://doi.org/10.1016/j.trpro.2020.08.190

Polson, N. G., & Sokolov, V. O. (2017, 2017/06/01/). Deep learning for short-term traffic flow prediction. *Transportation Research Part C: Emerging Technologies, 79*, 1-17. https://doi.org/https://doi.org/10.1016/j.trc.2017.02.024

Radhakrishnan, S., & Ramadurai, G. (2015, 2015/01/01/). Discharge Headway Model for Heterogeneous Traffic Conditions. *Transportation Research Procedia, 10*, 145-154. https://doi.org/https://doi.org/10.1016/j.trpro.2015.09.064

Ramezani, M., & Geroliminis, N. (2015, 2015/06/01). Queue Profile Estimation in Congested Urban Networks with Probe Data [https://doi.org/10.1111/mice.12095]. *Computer-Aided Civil and Infrastructure Engineering, 30*(6), 414-432. https://doi.org/https://doi.org/10.1111/mice.12095

Richards, P. I. (1956). Shock Waves on the Highway. *Operations Research, 4*(1), 42-51. https://doi.org/10.1287/opre.4.1.42

Ripley, B. D. (1996). *Pattern Recognition and Neural Networks*. Cambridge University Press. https://doi.org/DOI: 10.1017/CBO9780511812651

Rostami Shahrbabaki, M., Safavi, A. A., Papageorgiou, M., & Papamichail, I. (2018, 2018/07/01/). A data fusion approach for real-time traffic state estimation in urban signalized links. *Transportation Research Part C: Emerging Technologies, 92*, 525-548. https://doi.org/https://doi.org/10.1016/j.trc.2018.05.020

Shao, C.-q., & Liu, X.-m. (2012, 2012/11/20). Estimation of Saturation Flow Rates at Signalized Intersections. *Discrete Dynamics in Nature and Society, 2012*, 720474. https://doi.org/10.1155/2012/720474

Sharma, A., Bullock, D. M., & Bonneson, J. A. (2007, 2007/01/01). Input–Output and Hybrid Techniques for Real-Time Prediction of Delay and Maximum Queue Length at Signalized Intersections. *Transportation Research Record, 2035*(1), 69-80. https://doi.org/10.3141/2035-08

Sheffi, Y., & Mahmassani, H. (1981, 1981/02/01). A Model of Driver Behavior at High Speed Signalized Intersections. *Transportation Science, 15*(1), 50-61. https://doi.org/10.1287/trsc.15.1.50

Shi, X., Zhao, D., Yao, H., Li, X., Hale, D. K., & Ghiasi, A. (2021, 2021/12/01/). Video-based trajectory extraction with deep learning for High-Granularity Highway Simulation (HIGH-SIM). *Communications in Transportation Research, 1*, 100014. https://doi.org/https://doi.org/10.1016/j.commtr.2021.100014

Skabardonis, A., & Geroliminis, N. (2008, 2008/05/06). Real-Time Monitoring and Control on Signalized Arterials. *Journal of Intelligent Transportation Systems, 12*(2), 64-74. https://doi.org/10.1080/15472450802023337

Song, C., Lee, H., Kang, C., Lee, W., Kim, Y. B., & Cha, S. W. (2017, 11-14 June 2017). Traffic speed prediction under weekday using convolutional neural networks concepts. 2017 IEEE Intelligent Vehicles Symposium (IV),

Stathakis, D. (2009, 2009/04/20). How many hidden layers and nodes? *International Journal of Remote Sensing, 30*(8), 2133-2147. https://doi.org/10.1080/01431160802549278

Tan, C., Yao, J., Tang, K., & Sun, J. (2021). Cycle-Based Queue Length Estimation for Signalized Intersections Using Sparse Vehicle Trajectory Data. *IEEE Transactions on Intelligent Transportation Systems, 22*(1), 91-106. https://doi.org/10.1109/TITS.2019.2954937

Tiaprasert, K., Zhang, Y., Wang, X. B., & Zeng, X. (2015). Queue Length Estimation Using Connected Vehicle Technology for Adaptive Signal Control. *IEEE Transactions on Intelligent Transportation Systems, 16*(4), 2129-2140. https://doi.org/10.1109/TITS.2015.2401007

Tong, H. Y., & Hung, W. T. (2002, 2002/01/01/). Neural network modeling of vehicle discharge headway at signalized intersection: model descriptions and results. *Transportation Research Part A: Policy and Practice, 36*(1), 17-40. https://doi.org/https://doi.org/10.1016/S0965-8564(00)00035-5

Vanajakshi, L., & Rilett, L. R. (2004, 14-17 June 2004). A comparison of the performance of artificial neural networks and support vector machines for the prediction of traffic speed. IEEE Intelligent Vehicles Symposium, 2004,

Vigos, G., Papageorgiou, M., & Wang, Y. (2008, 2008/02/01/). Real-time estimation of vehicle-count within signalized links. *Transportation Research Part C: Emerging Technologies, 16*(1), 18-35. https://doi.org/https://doi.org/10.1016/j.trc.2007.06.002

Viloria, F., Courage, K., & Avery, D. (2000). Comparison of Queue-Length Models at Signalized Intersections. *Transportation Research Record, 1710*(1), 222-230. https://doi.org/10.3141/1710-26

Wang, J., & Shi, Q. (2013, 2013/02/01/). Short-term traffic speed forecasting hybrid model based on Chaos–Wavelet Analysis-Support Vector Machine theory. *Transportation Research Part C: Emerging Technologies, 27*, 219-232. https://doi.org/https://doi.org/10.1016/j.trc.2012.08.004

Wang, S., Huang, W., & Lo, H. K. (2019, 2019/07/01/). Traffic parameters estimation for signalized intersections based on combined shockwave analysis and Bayesian Network. *Transportation Research Part C: Emerging Technologies, 104*, 22-37. https://doi.org/https://doi.org/10.1016/j.trc.2019.04.023

Wang, Z., Cai, Q., Wu, B., Zheng, L., & Wang, Y. (2017, 2017/01/01/). Shockwave-based queue estimation approach for undersaturated and oversaturated signalized intersections using multi-source detection data. *Journal of Intelligent Transportation Systems, 21*(3), 167-178. https://doi.org/https://doi.org/10.1080/15472450.2016.1254046

Wang, Z., Zhu, L., Ran, B., & Jiang, H. (2020, 2020/11/01/). Queue profile estimation at a signalized intersection by exploiting the spatiotemporal propagation of shockwaves. *Transportation Research Part B: Methodological, 141*, 59-71. https://doi.org/https://doi.org/10.1016/j.trb.2020.08.009

Wong, W., Shen, S., Zhao, Y., & Liu, H. X. (2019, 2019/08/01/). On the estimation of connected vehicle penetration rate based on single-source connected vehicle data. *Transportation Research Part B: Methodological, 126*, 169-191. https://doi.org/https://doi.org/10.1016/j.trb.2019.06.003

Wu, X., & Liu, H. X. (2011, 2011/12/01/). A shockwave profile model for traffic flow on congested urban arterials. *Transportation Research Part B: Methodological, 45*(10), 1768-1786. https://doi.org/https://doi.org/10.1016/j.trb.2011.07.013

Wu, X., Liu, H. X., & Geroliminis, N. (2011, 2011/01/01/). An empirical analysis on the arterial fundamental diagram. *Transportation Research Part B: Methodological, 45*(1), 255-266. https://doi.org/https://doi.org/10.1016/j.trb.2010.06.003

Wu, Y., Tan, H., Qin, L., Ran, B., & Jiang, Z. (2018, 2018/05/01/). A hybrid deep learning based traffic flow prediction method and its understanding. *Transportation*

Research Part C: Emerging Technologies, 90, 166-180. https://doi.org/https://doi.org/10.1016/j.trc.2018.03.001

Yang, Z., Mei, D., Yang, Q., Zhou, H., & Li, X. (2014, 2014/08/12). Traffic Flow Prediction Model for Large-Scale Road Network Based on Cloud Computing. *Mathematical Problems in Engineering, 2014*, 926251. https://doi.org/10.1155/2014/926251

Yao, J., & Tang, K. (2019, 2019/12/01/). Cycle-based queue length estimation considering spillover conditions based on low-resolution point detector data. *Transportation Research Part C: Emerging Technologies, 109*, 1-18. https://doi.org/https://doi.org/10.1016/j.trc.2019.10.003

Yeo, H., & Skabardonis, A. (2009). Understanding Stop-and-go Traffic in View of Asymmetric Traffic Theory. In W. H. K. Lam, S. C. Wong, & H. K. Lo (Eds.), *Transportation and Traffic Theory 2009: Golden Jubilee: Papers selected for presentation at ISTTT18, a peer reviewed series since 1959* (pp. 99-115). Springer US. https://doi.org/10.1007/978-1-4419-0820-9_6

Yin, J., Sun, J., & Tang, K. (2018, 2018/12/01). A Kalman Filter-Based Queue Length Estimation Method with Low-Penetration Mobile Sensor Data at Signalized Intersections. *Transportation Research Record, 2672*(45), 253-264. https://doi.org/10.1177/0361198118798734

Yuan, K., Knoop, V. L., & Hoogendoorn, S. P. (2017). A Microscopic Investigation Into the Capacity Drop: Impacts of Longitudinal Behavior on the Queue Discharge Rate. *Transportation Science, 51*(3), 852–862. https://doi.org/10.1287/trsc.2017.0745

Zhang, H., Liu, H. X., Chen, P., Yu, G., & Wang, Y. (2020). Cycle-Based End of Queue Estimation at Signalized Intersections Using Low-Penetration-Rate Vehicle Trajectories. *IEEE Transactions on Intelligent Transportation Systems, 21*(8), 3257-3272. https://doi.org/10.1109/TITS.2019.2925111

Zhang, H. M., & Kim, T. (2005, 2005/06/01/). A car-following theory for multiphase vehicular traffic flow. *Transportation Research Part B: Methodological, 39*(5), 385-399. https://doi.org/https://doi.org/10.1016/j.trb.2004.06.005

Zhang, W., Yu, Y., Qi, Y., Shu, F., & Wang, Y. (2019, 2019/11/29). Short-term traffic flow prediction based on spatio-temporal analysis and CNN deep learning. *Transportmetrica A: Transport Science, 15*(2), 1688-1711. https://doi.org/10.1080/23249935.2019.1637966

Zhang, Y., & Xie, Y. (2007, 2007/01/01). Forecasting of Short-Term Freeway Volume with v-Support Vector Machines. *Transportation Research Record, 2024*(1), 92-99. https://doi.org/10.3141/2024-11

Zhao, L., Song, Y., Zhang, C., Liu, Y., Wang, P., Lin, T., Deng, M., & Li, H. (2020). T-GCN: A Temporal Graph Convolutional Network for Traffic Prediction. *IEEE Transactions on Intelligent Transportation Systems, 21*(9), 3848-3858. https://doi.org/10.1109/TITS.2019.2935152

Zhao, Y., Shen, S., & Liu, H. X. (2021, 2021/07/01/). A hidden Markov model for the estimation of correlated queues in probe vehicle environments. *Transportation Research Part C: Emerging Technologies, 128*, 103128. https://doi.org/https://doi.org/10.1016/j.trc.2021.103128

Zhao, Y., Zheng, J., Wong, W., Wang, X., Meng, Y., & Liu, H. X. (2019, 2019/10/01/). Various methods for queue length and traffic volume estimation using probe vehicle trajectories. *Transportation Research Part C: Emerging Technologies, 107*, 70-91. https://doi.org/https://doi.org/10.1016/j.trc.2019.07.008

Zheng, W., Lee, D.-H., & Shi, Q. (2006, 2006/02/01). Short-Term Freeway Traffic Flow Prediction: Bayesian Combined Neural Network Approach. *Journal of Transportation Engineering, 132*(2), 114-121. https://doi.org/10.1061/(ASCE)0733-947X(2006)132:2(114)

Zheng, Z., Yang, Y., Liu, J., Dai, H., & Zhang, Y. (2019). Deep and Embedded Learning Approach for Traffic Flow Prediction in Urban Informatics. *IEEE Transactions on Intelligent Transportation Systems, 20*(10), 3927-3939. https://doi.org/10.1109/TITS.2019.2909904

Zhu, J. Z., Cao, J. X., & Zhu, Y. (2014, 2014/10/01/). Traffic volume forecasting based on radial basis function neural network with the consideration of traffic flows at the adjacent intersections. *Transportation Research Part C: Emerging Technologies, 47*, 139-154. https://doi.org/https://doi.org/10.1016/j.trc.2014.06.011

APPENDICIES

Appendix A

List of Notations

Notation	Description
L_Q	Actual queue length
p_{QV}	Position of the queued vehicle
p_{SD}	Position of the slowed-down vehicle
v_{QV}	Speed of the queued vehicle
v_{SD}	Speed of the slowing down vehicle
v_d	Desired speed (speed limit)
v_{SB}	Speed at the capacity state based on speed distribution
v_{CS}	Speed at the capacity state based on speed distribution
v_{EQV}	Estimated speed of the last queued vehicle
S	Space gap between the leading and the following vehicle
T	Time gap between the leading and the following vehicle
q_i	Flow rate during a period
n_i	Number of vehicles during a period
t_i	Time period
h_σ	Mean headway
v_σ	Mean speed
k_σ	Mean density
t_G	Time since green phase has started
t_i	Time of the initial move of the vehicle during green time phase
t_m	Time since the vehicle has been moving
t_{SD}	Time when the slowing down vehicle joined the moving queue

d_m	Distance the vehicle has moved after the full stop
d_{SB}	Distance from the vehicle to the stop bar
d_{QV}	Distance from the queued vehicle to the stop bar
d_{SD}	Distance to the stop bar when slowing down vehicle joined the moving queue
q	Traffic flow rate
L_E	Estimated queue length
t_w	Waiting time
q_E	Estimated traffic flow
V_E	Estimated traffic volume
C	Cycle length

Appendix B

The interface of WEKA

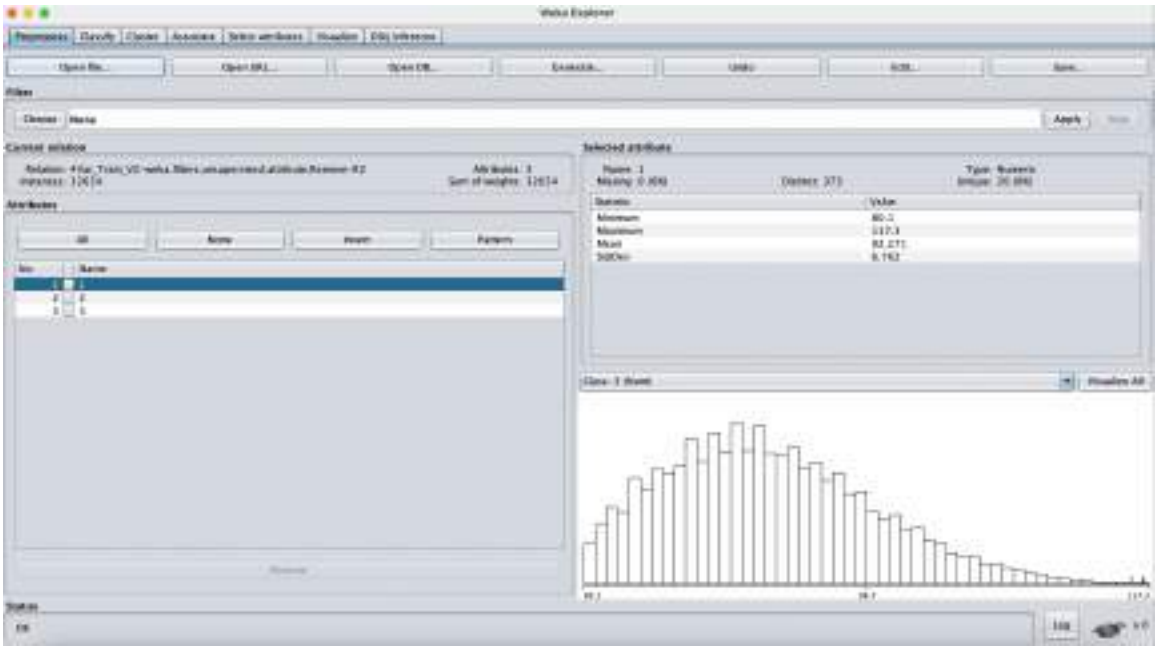

Appendix C (1 out of 4)

Multilayer Perceptron (MLP)

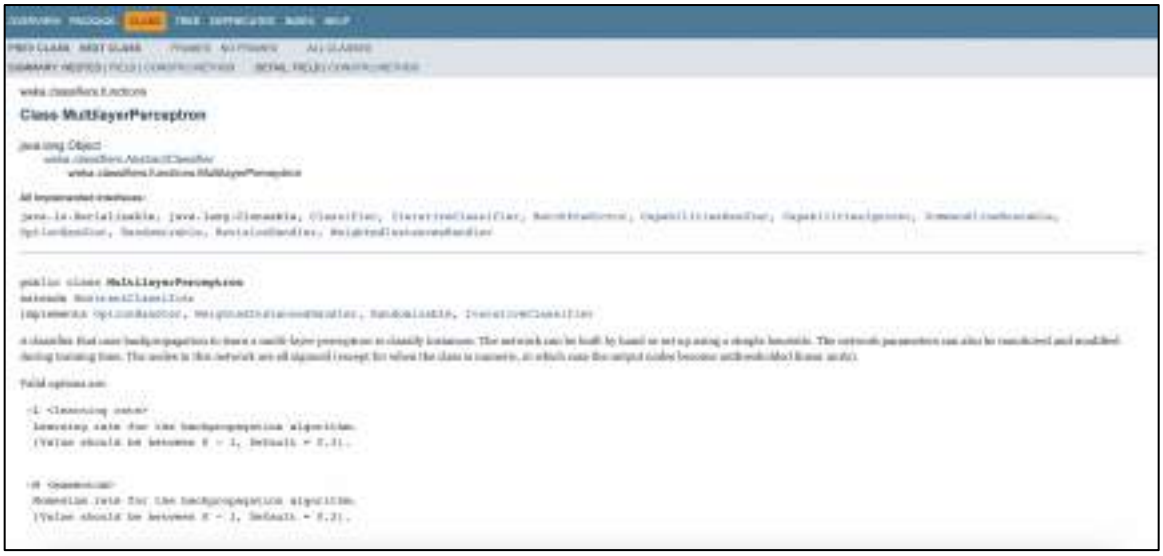

Appendix C (2 out of 4)

Multilayer Perceptron (MLP)

Appendix C (3 out of 4)

Multilayer Perceptron (MLP)

Appendix C (4 out of 4)

Multilayer Perceptron (MLP)

CURRICULUM VITA

Majeed Algomaiah

502-389-3563 | amalgo01@louisville.edu
W.S. Speed Bldg., Room LL06 Louisville, KY 40292

Education

University of Louisville — Louisville, KY
Ph.D. in Civil Engineering (Transportation) — Aug. 2017 – May 2022

Dissertation: Utilizing Shockwave Theory and Deep Learning to Estimate Intersection Traffic Flow and Queue Length Based on Connected Vehicles

University of Louisville — Louisville, KY
Master of Science in Civil Engineering (Transportation) — May 2015 – Jul. 2017

Dissertation: Smart Highway Work Zone Merge System Enabled by Connected Vehicles

Queensland University of Technology — Brisbane, Australia
Bachelor of Civil Engineering (Second Major: Transportation and Planning) — Feb. 2011 – Dec. 2014

Experience

Graduate Teaching Assistant — Louisville, KY
University of Louisville — Aug. 2017 – Present

- CEE 205 Mechanics I: Statics
- CEE 460 Transportation System Engineering
- CEE 470 Surface Water Hydrology
- CEE 560 Traffic Engineering
- CEE 663 Advanced Traffic Operations

Graduate Research Assistant — Louisville, KY
University of Louisville — Aug. 2017 – Present

- Connected and Autonomous Vehicle Empowered Next-Generation Interchange Control with Improved Operational Efficiency and Energy Consumption. Funded by: National Science Foundation (NSF), 2017-2019.
- Proactive Intersection Safety Assessment based Radar Sensor Data. Funded by: Federal Highway Administration (FHWA) through Kentucky Transportation Cabinet, 2019.

Awards and Honors

- American Society of Highway Engineers Scholarship. ASHE. 2021.
- Doctoral Dissertation Writing Award. Graduate School - University of Louisville. 2021.
- Master's Degree Scholarship, Saudi Arabian Cultural Mission (SACM). 2015 - 2017.
- Student Presentation Competition Award. The 58th Annual Meeting of the International Highway Engineering Exchange (IHEEP). 2016.
- Distinguished Future Engineers Scholarship, University of Kassel, Germany. 2013.
- Bachelor Degree Scholarship, Saudi Arabian Cultural Mission (SACM). 2011 - 2014.

Areas of Specialization

Connected and Autonomous Vehicles (CAV)

- V2V and V2I Communication
- Cooperative Driving Applications
- Advanced Driver-Assistance Systems (ADAS)
- Vehicle and Truck Platooning
- Autonomous Intersection/Interchange
- CAV in Mixed Traffic

Intelligent Transportation System (ITS)

- Traveler Information Systems (TIS)
- Traffic Signal Coordination
- Traffic Data Detectors
- Variable Speed Limits (VSL)
- Intelligent Public Transit System

Traffic Operations

- Traffic Flow Theory
- Traffic Simulation
- Traffic Signals and Traffic Control
- Innovative Intersections and Interchanges
- Freeway Operations

Data Science and Data Management in Transportation

- Big Data in Transportation
- Machine Learning & Deep Learning
- Geographic Information System (GIS)
- Spatial Analysis

Public Transportation

- Network-Level and Route-Level Planning
- Quality of Service and Ridership
- Integrated Transportation Systems
- O-D and Mode Choice
- Innovation in Public Transit Data Collection

Smart Mobility & Sustainable Cities

- Micromobility Studies
- First/Last Mile Solutions
- Smart City Applications
- Urban Sustainability

Projects

- Empirical Modelling of the Relationship between Speed and Bus Bunching Phenomenon. Queensland University of Technology. 2014.
  Role: Lead Researcher
- A Smart Highway Work Zone Merge System Enabled by Connected Vehicles. University of Louisville. 2016-2017.
  Role: Lead Researcher
- Connected and Autonomous Vehicle Empowered Next-Generation Interchange Control with Improved Operational Efficiency and Energy Consumption.Funded by: National Science Foundation (NSF). 2017-2019.
  Role: Acting Co-PI & Lead Researcher
- Developing a Machine Learning Model to Exploit Crowdscourcing Data in Predicting Traffic Volume. University of Louisville. 2018-2020.
  Role: Lead Researcher
- The Applications of Wi-Fi Detector in Improving the Traffic Operation in Urban Streets. University of Louisville. 2018-2019.
  Role: Lead Researcher
- Utilizing Wi-Fi Detector in Bus System to Automatically Capture Passenger Transfers and Construct Network O-D. University of Louisville. 2018-2019.
  Role: Lead Researcher
- Investigating the Trip Density and Other Related Characteristics of E-Scooters as an Emerging Shared Micromobility Mode. University of Louisville. 2019-2020.
  Role: Lead Researcher
- Proactive Intersection Safety Assessment based Radar Sensor Data. Funded by: Federal Highway Administration (FHWA) through Kentucky Transportation Cabinet, 2019.
  Role: Supportive Researcher.
- Developing an Estimation Algorithm Based on Shockwave Analysis and Deep Learning from Connected Vehicle Trajectory Data. University of Louisville. 2019-2021.
  Role: Lead Researcher

Publications

Journal Articles (Published)

- J1. Algomaiah, M., & Li, Z. (2019). Next-Generation Interchange Control Based on Centralized Management of Connected and Autonomous Vehicles. IEEE Access, 7, 82939-82955.
- J2. Algomaiah, M., & Li, Z. (2019). Utilizing Lane-Based Strategy to Incorporate Mixed Traffic in Interchange Control for Connected and Autonomous Vehicles. Transportation Research Record, 2673(5), 454-465.
- J3. Hosseinzadeh, A., Algomaiah, M., Kluger, R., & Li, Z. (2021). Spatial Analysis of Shared E-Scooter Trips. Journal of transport geography, 92, 103016.
- J4. Hosseinzadeh, A., Algomaiah, M., Kluger, R., & Li, Z. (2021). E-scooters and Sustainability: Investigating the Relationship Between the Density of E-scooter Trips and Characteristics of Sustainable Urban Development. Sustainable Cities and Society, 102624.
- J5. Algomaiah, M., & Li, Z. (2021). Exploring Work Zone Late Merge Strategies With and Without Enabling Connected Vehicles Technologies. Transportation Research Interdisciplinary Perspectives, 102624.

Projects

- Empirical Modelling of the Relationship between Speed and Bus Bunching Phenomenon. Queensland University of Technology. 2014.
  Role: Lead Researcher
- A Smart Highway Work Zone Merge System Enabled by Connected Vehicles. University of Louisville. 2016-2017.
  Role: Lead Researcher
- Connected and Autonomous Vehicle Empowered Next-Generation Interchange Control with Improved Operational Efficiency and Energy Consumption.Funded by: National Science Foundation (NSF), 2017-2019.
  Role: Acting Co-PI & Lead Researcher
- Developing a Machine Learning Model to Exploit Crowdscourcing Data in Predicting Traffic Volume. University of Louisville. 2018-2020.
  Role: Lead Researcher
- The Applications of Wi-Fi Detector in Improving the Traffic Operation in Urban Streets. University of Louisville. 2018-2019.
  Role: Lead Researcher
- Utilizing Wi-Fi Detector in Bus System to Automatically Capture Passenger Transfers and Construct Network O-D. University of Louisville. 2018-2019.
  Role: Lead Researcher
- Investigating the Trip Density and Other Related Characteristics of E-Scooters as an Emerging Shared Micromobility Mode. University of Louisville. 2019-2020.
  Role: Lead Researcher
- Proactive Intersection Safety Assessment based Radar Sensor Data. Funded by: Federal Highway Administration (FHWA) through Kentucky Transportation Cabinet, 2019.
  Role: Supportive Researcher.
- Developing an Estimation Algorithm Based on Shockwave Analysis and Deep Learning from Connected Vehicle Trajectory Data. University of Louisville. 2019-2021.
  Role: Lead Researcher

Publications

Journal Articles (Published)

- J1. Algomaiah, M., & Li, Z. (2019). Next-Generation Interchange Control Based on Centralized Management of Connected and Autonomous Vehicles. IEEE Access, 7, 82939-82955.
- J2. Algomaiah, M., & Li, Z. (2019). Utilizing Lane-Based Strategy to Incorporate Mixed Traffic in Interchange Control for Connected and Autonomous Vehicles. Transportation Research Record, 2673(5), 454-465.
- J3. Hosseinzadeh, A., Algomaiah, M., Kluger, R., & Li, Z. (2021). Spatial Analysis of Shared E-Scooter Trips. Journal of transport geography, 92, 103016.
- J4. Hosseinzadeh, A., Algomaiah, M., Kluger, R., & Li, Z. (2021). E-scooters and Sustainability: Investigating the Relationship Between the Density of E-scooter Trips and Characteristics of Sustainable Urban Development. Sustainable Cities and Society, 102624.
- J5. Algomaiah, M., & Li, Z. (2021). Exploring Work Zone Late Merge Strategies With and Without Enabling Connected Vehicles Technologies. Transportation Research Interdisciplinary Perspectives, 102624.

- P2. Improved Emission Estimation at Intersections – A Roundabout Study. Presented at Ohio Transportation Engineering Conference, Columbus, OH, October 2016.
- P3. Connected Vehicles in Mitigating Work Zone Operations. Presented at American Society of Civil Engineers, Kentucky Section Annual Meeting, Lexington, KY, October 2016.
- P4. Automated Extraction of Horizontal Curve Data From GIS Roadway Maps. Presented at Ohio Transportation Engineering Conference, Columbus, OH, October 2016.
- P5. Utilizing Lane-Based Strategy to Incorporate Mixed Traffic in Interchange Control for Connected and Autonomous Vehicles. Presented at Transportation Research Board 98th Annual Meeting Transportation Research Board, Washington, D.C., January 2019.
- P6. Next-Generation Interchange Control of Connected and Autonomous Vehicles. Presented at Transportation Research Board 98th Annual Meeting Transportation Research Board, Washington, D.C., January 2019.
- P7. Automated Capturing of Transit Passenger Transfers and Network O-D Using An Optimized Wi-Fi-Based Recognition Algorithm. Presented at Transportation Research Board 98th Annual Meeting Transportation Research Board, Washington, D.C., January 2021.

Research Grant Proposals

- Connected and Autonomous Vehicle Empowered Next-Generation Interchange Control with Improved Operational Efficiency and Energy Consumption
  Funding Agency: National Science Foundation (NSF)
  Amount and Duration: $46,345 for two years (2017 - 2019)
  Role: Wrote the Methodology
  Result: Awarded
- Automated System for Bus Ridership and Performance Data Collection, Analysis and Diagnosis Based on Big Data Analytics
  Funding Agency: Transit Cooperative Research Program (TCRP)
  Amount and Duration: $100,000 for one year (2019)
  Role: Wrote the Problem Statement and Methodology
  Result: Unfunded
- Proactive Intersection Safety Assessment based Radar Sensor Data
  Funding Agency: Federal Highway Administration (FHWA) through Kentucky Transportation Cabinet
  Amount and Duration: $39,316 for six months (2019)
  Role: Wrote the Background
  Result: Awarded
- Collecting Transit Passenger Origin-Destination and Capturing Transfer Information Based on Wi-Fi Sensor
  Funding Agency: Transit Cooperative Research Program (TCRP)
  Amount and Duration: $100,000 for one year (2020)
  Role: Wrote the Problem Statement and Methodology
  Result: Unfunded
- The Center for Automated-Vehicle-Accessible Mobility for People with Disabilities (CAMPD)
  Funding Agency: U.S. Department of Transportation (US DOT) for Tier 1 University Transportation Centers (UTCs)
  Amount and Duration: $1,000,000 for two years (2020 - 2022)
  Role: Wrote the Background
  Result: Unfunded

Teaching Experience

Graduate Teaching Assistant — Louisville, KY
University of Louisville — Aug. 2017 – Present

Courses:

- CEE 205 Mechanics I: Statics
  - Summer 2018, Summer 2019, Summer 2020, & Summer 2021
  - 3-Credit; Undergraduate Level
- CEE 460 Transportation System Engineering.
  - Spring 2018, Spring 2019 & Spring 2020.
  - 3-Credit; Undergraduate Level
- CEE 470 Surface Water Hydrology.
  - Fall 202
  - 3-Credit; Undergraduate Level
- CEE 660 Traffic Engineering
  - Fall 2017, Fall 2018 & Fall 2021
  - 3-Credit; Undergraduate Level/Graduate Level
- CEE 663 Advanced Traffic Operations
  - Fall 2019 & Fall 2021
  - 3-Credit; Graduate Level

Responsibilities:

- Assisted in developing the content and preparing materials and resources.
- Contributed in the content delivery by teaching some classes and holding help sessions for students.
- Reviewed the content and the assessments and to modify them based on ABET standards.
- Prepared assessments including assignments, exams, and projects.
- Handled the grading and the evaluation of the assessments submitted by students.

Teaching Interests

- Introduction to Transportation Engineering
- Traffic Engineering & Traffic Operations
- Highway Traffic Operations
- Intelligent Transportation Systems (ITS)
- Advanced Topics in Transportation
- GIS Applications in Civil & Environmental Engineering
- Public Transportation Systems
- Sustainability in Transportation System
- Computer and Simulation Methods in Transportation
- Big Data and Analysis of Transportation
- Mobility in Smart Cities

Academic Services

Committees

- Committee Member, The Affairs of International Students, Queensland University of Technology, 2014.
- Committee Member, Sustainability Council, University of Louisville, 2017 - 2020.
- Volunteer Member, TRB Committee ACP15: Standing Committee on Intelligent Transportation Systems, Washington, D.C., 2019.
- Volunteer Member, TRB Committee AKD10: Standing Committee on Performance Effects of Geometric Design, Washington, D.C., 2019.
- Volunteer Member, TRB Committee AP090: Standing Committee on Transit Data, Washington, D.C., 2021.

Paper Review

- Transportation Research Record: Journal of Transportation Research Board
- Journal of Transport Geography
- IEEE Access
- Journal of Transportation Engineering, Part A: Systems
- PLoS ONE
- Transportation Research Board 101st Annual Meeting Transportation Research Board
- Transportation Research Board 100th Annual Meeting Transportation Research Board
- Transportation Research Board 99th Annual Meeting Transportation Research Board
- The 19th COTA International Conference for Transportation Professionals
- The 20th COTA International Conference for Transportation Professionals

Professional Affiliation

- Member, American Society of Civil Engineers (ASCE), Since 2015
- Member, Engineers Australia, Since 2014

Professional Skills

Transportation Software

- Highway Capacity Software (HCS7), Traffic Operations
- VISSIM, VISSIM External Driver Model, & Visum, Traffic Simulation & Planning
- CORSIM, microscopic traffic simulation software
- ArcGIS, Geographic Information System.
- HCM – Highway Capacity Manual (TRB)
- HSM – Highway Safety Manual (AASHTO)
- MUTCD – Manual on Uniform Traffic Control Devices (FHWA)
- Traffic Signal Timing Manual (FHWA).
- Green Book – A Policy on Geometric Design of Highways and Streets (AASHTO)
- C++
- C#
- Visual Basic
- SQL
- MATLAB – A Numeric Computing Environment
- R – Software Environment for Statistical Computing and Graphics.
- Minitab – Data Analysis, Statistical & Process Improvement Tools.
- Weka 3 – Machine Learning software.

Volunteering

- International Student Supporting Program, Queensland University of Technology, 2011 - 2014
- Exchange Program Ambassador, Queensland University of Technology, 2013 - 2014
- Apartment Setup Coordinator, Kentucky Refugee Ministries (KRM), 2015 - 2017.
- International Students Support, University of Louisville, 2016 - 2018
- Civil Engineering Department Representative, University of Louisville, 2017 - 2019
- Improving African American Communities, Food-Sharing Program, 2016 - 2021